MOLECULAR ASPECTS OF ANTIESTROGEN RESISTANCE AND AUTOPHAGY IN BREAST CANCER CELLS

by

IRINA NAYVELT

A Dissertation submitted to the

Graduate School-New Brunswick

Rutgers, The State University of New Jersey

in partial fulfillment of the requirements

for the degree of

Doctor of Philosophy

Graduate Program in Nutritional Sciences

written under the direction of

Dr. T. J. Thomas

and approved by

_____

_____

_____

_____

_____

New Brunswick, New Jersey

[May, 2009]

ABSTRACT OF THE DISSERTATION

Molecular Aspects of Antiestrogen Resistance and Autophagy in Breast Cancer Cells

By

IRINA NAYVELT

Dissertation Director:

Dr. T. J. Thomas

The major objective of this thesis was to examine the molecular aspects of estrogenic growth and autophagy in estrogen receptor α (ERα)-positive breast cancer cells. We first examined the role of autophagy mediator, Beclin 1, in estrogenic signaling and antiestrogen resistance in Beclin 1-overexpressing MCF-7 cells. We found that a potential interaction between ERα and Beclin 1 rendered Beclin 1-transfected cells less sensitive to estradiol (E_2)-induced growth stimulation, and to antiestrogen-mediated growth inhibition. Thus, a novel function for Beclin 1 might involve down-regulation of the action of ERα, contributing to resistance of breast cancer cells to antiestrogens.

In an attempt to develop novel therapeutic agents for breast cancer, we explored the effect of the polyamine analogue, 1,15-bis(ethylamino)-4,8,12-triazapentadecane (BE-3-3-3-3), on MCF-7 cell growth in the presence and absence of E_2. BE-3-3-3-3 caused growth inhibition in the presence of E_2. However, it mimicked estradiol and stimulated cell growth in the absence of E_2, and induced growth response genes, such as c-fos, c-jun, and c-myc. This also induced autophagy, and increased levels of autophagy-related proteins, Beclin 1 and MAP LC3-II.

In another approach to introduce gene therapy for breast cancer treatment, we explored the physico-chemical aspects of DNA nanoparticle formation. In an effort to optimize gene delivery systems, we investigated DNA condensation to nanoparticles in the presence of α,α'-methylated spermine analogues, and characterized the size, shape and stability of the resultant nanoparticles. Although some analogues proved more efficacious DNA condensing agents than

spermine, hydrodynamic radii of nanoparticles produced by analogues were comparable to those produced by spermine.

We also compared the DNA condensing abilities of poly-L-lysine (PLL) and oligolysines, and characterized the physico-chemical properties of their condensates. PLL was a more effective condensing agent than oligolysines, and produced more stable nanoparticles. We conclude that PLL and oligolysines bind and condense DNA through different mechanisms.

In summary, our research provides new insights into the mechanism of antiestrogen resistance and autophagy in breast cancer. We also provide mechanistic insight into DNA nanoparticle formation in the presence of polyamine analogues and lysines.

DEDICATION

I dedicate this work to my late grandparents, Raisa and Anatoliy Yampolsky. I love you and miss you, and wish you were here to see the end.

ACKNOWLEDGEMENT

I would like to express my deepest gratitude to my advisor, Dr. T. J. Thomas. Thank you for your guidance along my erratic course to completion. Thank you for your understanding, and for helping me with my problems. I greatly appreciate that you were always available for meetings, and that your stories and examples made me think along more positive lines. I also express my gratitude to Dr. Thresia Thomas for her essential help at the moments of my greatest need.

I would like to thank the members of my proposal defense, as well as my thesis defense, committees, Dr. T. J. Thomas, Dr. Thresia Thomas, Dr. Judith Storch, Dr. Huixin He, Dr. Sue Shapses, Dr. Joseph Dixon, and Dr. Shridar Ganesan, for their insightful comments and critical analysis of my thesis work.

I am also extremely grateful to my long-suffering and surprisingly patient family. I thank my parents, Arnold and Anna Nayvelt for their unwavering support and loving encouragement. I thank my brother, Eugene Nayvelt, for his uplifting and informative conversations, and his sacrifice of time and sleep for my thesis defense. I thank my grandmother, Dolya Nayvelt, for her encouraging conversations. I thank my uncle and aunt, Ben and Laura Yampolsky, for their support and belief in me. I thank my cousins, Eugene, Ilya, Liz, Nicole, and Stella, for their sympathy and support.

Last but not least, I would like to express my deep gratitude and appreciation to my best friend, Natalya Verbitsky, for her unshakable confidence in my abilities, positive and insightful conversations, and support of my efforts.

TABLE OF CONTENTS

LIST OF TABLES

LIST OF FIGURES

GENERAL INTRODUCTION

Breast Cancer Statistics. Breast cancer is the second leading cause of death in women in the United States, after lung cancer. In 2008, more than 40,000 deaths occurred in the United States (Jemal et al., 2008). One out of eight women in the U. S. develops this cancer, and 182,460 invasive cases were expected in 2008. Breast cancer incidence is higher in developed countries, but less developed countries are slowly closing the incidence gap (Kurian et al. 2009, Love 2008). Findings of observational and migration studies have indicated that dietary, environmental and hormonal factors contribute to the development of breast cancer (Clemons et al. 2001, Rastogi et al. 2008, Forman et al. 2007).

Estrogen and Breast Cancer. Estrogens are synthesized from cholesterol precursors, and 17β-estradiol (E_2) is the principal circulating form of estrogen in the female body. Estrogen is produced primarily in the ovaries, but low levels of E_2 are also obtained from aromatization of adrenal and ovarian androgens in the adipose tissue, bone, vascular endothelium, aortic smooth muscle, and brain (Simpson et al. 2001, Ali et al 2002). These secondary sites become the major sources of estrogen synthesis in post-menopausal women, and play a role in breast cancer progression in this population (Clemons et al. 2001, Ali et al. 2002).

Evidence of estrogen involvement in breast cancer development derives from studies in which estrogens induced breast cancer cell proliferation in vitro, and promoted the mammary carcinogenesis in experimental animals (Lupulescu 1995, Yue et al. 2003). Also, inhibition of estrogen synthesis with aromatase inhibitors in aging Sprague-Dawley rats inhibited the development of spontaneous breast tumors (Gunson et al., 1995).

Development of Hormonal Therapy for Breast Cancer. More than a century ago, Beatson reported that removal of the ovaries resulted in breast cancer remission in pre-menopausal women, although only a fraction of patients benefited from this treatment (Beatson 1896, Boyd 1900). This finding was later explained by the discovery of the estrogen hormone (Allen and Doisy,1923). Estrogen's induction of mouse mammary carcinogenesis led Lacassagne to propose that breast cancer could be inhibited by the use of an estrogen antagonist (Lacassagne,

1936). In the late 1950s, Lerner discovered the first nonsteroidal antiestrogen, MER25, which proved to be highly toxic and not potent enough for clinical use (Lerner, 1958). Later, the discovery, purification, and cloning of the estrogen receptor (ER) led to the development of assays that predicted response to hormonal therapy, promoted the identification and design of antiestrogenic ligands, and advanced our understanding of estrogen receptor-mediated gene regulation.

Tamoxifen (TAM) was initially designed as a contraceptive. However, its anti-estrogenic properties were noted by Jordan, who utilized it to prevent mammary carcinogenesis in rats (Jordan, 1976). Successful animal studies led to clinical trials that resulted in the 1977 FDA approval of TAM for the treatment of metastatic breast cancer in postmenopausal women (Jordan, 2009). Further clinical studies led to the use of TAM as breast cancer prevention therapy in high-risk pre- and post-menopausal women, and established it as the "gold standard" for treatment of all stages of hormone-sensitive breast cancer (Jordan, 2008). TAM demonstrated a 70% response rate in ER-positive breast cancer patients, reduced the risk of contralateral breast cancer by 50%, and had positive effects on bone and cardiovascular health (Fisher et al., 1998). However, this antiestrogen significantly raised the risk of endometrial cancer and blood clots in post-menopausal women (Fisher et al., 1998). The negative side effects of TAM prompted the search for other selective estrogen receptor modulators (SERM) that would show antagonistic activity in the breast, and retain the protective agonistic activity on the bone and cardiovascular system. Raloxifene (EVISTA), a second generation SERM, was recently compared to TAM in a clinical setting (STAR trial) (Vogel et al., 2006). Raloxifene was found to be equally effective in preventing invasive breast cancer and protecting against osteoporosis, without increasing the risk of uterine cancer like TAM (Vogel et al., 2006). Thus, raloxifene is an antiestrogen in the breast epithelial cells, but acts as an estrogen in bone cells.

Pure estrogen antagonists, those compounds without estrogenic activity in some cells, represent another potent form of breast cancer treatment that proves effective when TAM fails (Howell, 2006). Pure antiestrogens completely abolish ER signaling, accelerate ER degradation, and do not exhibit agonistic activity in any tissues (Osborne et al., 2004). ICI 182,780 or

fulvestrant (Faslodex) was approved for the treatment of advanced breast cancer in post-menopausal women (Howell et al. 2006, Wardley et al. 2002). However, the abrogation of estrogenic effects induced by this drug has a negative effect on bone density and cardiovascular health in this cohort of women.

Aromatase inhibitors are an alternative breast cancer therapy based on the inhibition of production of estrogens from androgens in the peripheral tissues (i.e. breast, liver, adipose tissue) (Ali et al., 2002). Specifically, these inhibitors act on the aromatase enzyme CYP19, whose levels are often elevated in breast tumors (Ali et al. 2002, Castagnetta et al., 1996). Third generation aromatase inhibitors (i.e.anastrazole, letrozole) have recently undergone clinical testing and proved more efficacious than TAM in treating advanced breast cancer in ER-positive, post-menopausal women (Baum et al. 2002, Howell et al. 2005, Thurlimann et al. 2005). These inhibitors are also superior to TAM due to the lack of agonistic side effects that are observed with TAM treatment (Howell et al., 2005). The disadvantages of estrogen ablation with aromatase inhibitors include a high rate of osteoporosis and elevated serum cholesterol levels (Patel et al., 2007).

Estrogen Action is Mediated by the ERs. In mammalian cells, estrogen action is mediated via the estrogen receptor (ER). Estrogen receptor was discovered by Jenson and Jacobson in the early 1960s as an E_2 binding protein of high affinity found in the uterine tissues (Jensen and Jacobson, 1962). ER is a member of the nuclear receptor superfamily of transcription factors, which also include vitamin D receptor (VDR), glucocorticoid receptor (GR), thyroid receptor (TR), androgen receptor (AR), progesterone receptor (PR), and the retinoic acid receptors (RAR and RXR) (McEwan, 2009). In 1985, ER was isolated from MCF-7 cells and the gene was identified and cloned. This receptor later became known as ERα, when a second receptor, ERβ, was discovered (Walter et al. 1985, Green et al. 1986). Although alternately spliced variants of this protein have also been described, their exact function is unknown (Poola et al., 2000). ERα is a 66 kDa, 595 amino acid-containing protein. In 1995, another estrogen receptor was cloned from the rat prostate cDNA library, and was called ERβ (Kuiper et al., 1997). Although this receptor shared homology with ERα, it was a product of a different gene (Enmark et al., 1997). Since

then, ERβ was isolated from mice and humans, and the full-length form of this receptor contains 530 amino acids (Lewandowski et al., 2002).

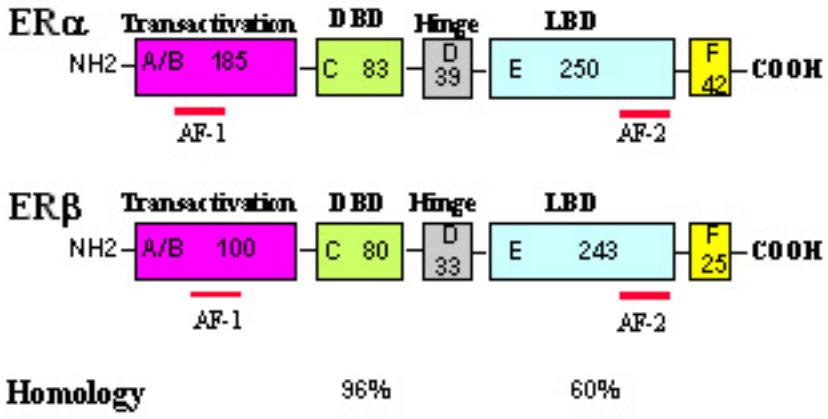

Figure 1: Structural domains of ERα and ERβ. The N-terminus is represented on the left, and the C-terminus on the right. The names of the domains and the number of amino acids they contain are indicated inside the box diagrams. The regions of the receptors responsible for specific functions are indicated above and below the box diagram representations (DBD, DNA binding domain; LBD, ligand-binding domain; AF-1, Activation function 1, AF-2, Activation function 2).

The estrogen receptors are comprised of distinct domains, which are responsible for various receptor functions. The N-terminal A/B domain contains the constitutive, ligand-independent activation function 1 (AF-1). This domain does not demonstrate high homology between the receptor subtypes (30%). The C domain corresponds to the DNA binding domain, and is the most highly conserved region between the ERs (96%). The D domain, which includes the hinge and the nuclear localization signal (NLS), is only 30% homologous between ERα and ERβ. The C-terminal E/F domain contains the ligand binding (LBD) and dimerization domains, a second NLS, ligand-dependent activation function 2 (AF2), and a co-regulator binding surface. The receptors share significant homology in the E/F region (about 53%) (Pearce et al., 2004).

ERα and ERβ have similar E_2 binding affinity, but exhibit different affinities for antiestrogens and various SERMs (Kuiper et al., 1997). Tissue distribution analysis of ERα and ERβ mRNA showed some overlapping, but also distinct differences in the pattern of expression. In the rat, ERα expression is moderate to high in the uterus, ovary, testis, pituitary, kidney, and

adrenal, whereas ERβ expression is moderate to high in the prostate, ovary, lung, bladder, brain, and testis (Kuiper et al., 1997). Receptor knockout studies in mice demonstrated that ERα, but not ERβ, is necessary for the full development of the mammary glands (Bocchinfuso et al., 1997). In tissues expressing both ERα and ERβ, it is important to consider possible interactions between receptor subtypes, which depend in part on tissue type, receptor abundance, and ligand affinity. For example, ERβ repressed ERα-mediated transcription at subsaturating concentrations of E_2 (Hall et al., 1999). There is evidence that ERα/ ERβ expression may be altered in carcinogenesis. The ratio of ERα to ERβ was significantly higher in breast tumors than that in adjacent normal tissue (Leygue et al., 1998). This finding, taken together with the results of ERα/ERβ transfection studies, indicates that ERα has a tumor-promoting role, whereas ERβ may act as a tumor suppressor in certain circumstances. Both ER subtypes have been identified in the mitochondria of multiple cell types, and E_2 can stimulate transcription of mitochondrial genes. (Chen et al. 2004, Demonacos et al. 1996)

The classic mode of ER action involves E_2 binding to the nuclear receptor, dimerization, and subsequent binding to the estrogen response element (ERE) in the promoter of E_2-responsive genes. In addition, ER can also stimulate transcription indirectly through protein-protein interactions with other transcription factors such as the activating protein 1 (AP-1) and the stimulating protein 1 (SP-1). Transcriptional regulation by ER requires the recruitment of multiple proteins, including co-activators, co-repressors, histone acetyl transferases (HAT), histone deacetylase complexes (HDAC), and general transcriptional machinery.

In addition to its function as a transcription factor, ERs can mediate a fast, non-genomic response to hormone or growth factor signaling, which can be mobilized within a few minutes. The non-genomic signalling is initiated by the cellular membrane-associated ERs that may interact with G-proteins or other cell membrane growth receptors (EGFR, IGF, etc.), and is followed by events such as calcium flux, phospholipase C activation, production of cAMP and of inositol triphosphate (IP_3) (Levin et al., 2001). The aforementioned second messengers stimulate kinase cascades, which produce a rapid physiological response. Kinase cascades can also lead

to transcriptional activation, denoting cross-talk between the genomic and non-genomic modes of ER action (Levin et al. 2002, Yager et al. 2006).

ER Transactivation in the Presence of Estrogens/Antiestrogens. X-ray crystallographic investigations showed that the C-terminal domain of ER contains a ligand binding pocket formed by several α-helices (Brzozowki et al., 1997). E_2 binding to the ligand pocket induces a conformational change, in which Helix 12 is positioned over the pocket in such a manner as to facilitate co-activator recruitment (Pike et al. 2000, Pearce et al. 2004). These co-activators interact with transcriptional machinery and stimulate transcription, as well as participate in chromatin remodeling due to intrinsic HAT activity (Glass et al., 2000). When SERMs such as TAM and Raloxifene bind to the ligand-binding pocket, Helix 12 is positioned in such a way as to block co-activator association and to favor the interaction with co-repressors (Pearce et al. 2004, Shiau et al. 1998). This, in turn, leads to the inhibition of the AF2 transactivation function and repression of transcription. While SERMs, such as TAM, inactivate the AF2-mediated transcription, they do not suppress AF1 activity. Thus, it is believed that TAM's agonistic activity in certain tissues is mediated by the AF1 (Tzukerman et al., 1994). Pure antiestrogens, such as ICI 164,384 and ICI 182,780, repress both AF1 and AF2 transactivation functions of the ER, thereby completely abolishing ER agonistic activity. ICI 164,384 binding to the ligand pocket of the ER promotes co-repressor recruitment, and results in transcriptional inactivation of AF2 (Webb et al., 1998). Pure antiestrogens also prevent receptor dimerization, nuclear receptor localization, and promote ER degradation via the proteosomal pathway (Fawell et al. 1990, Wijayratne et al. 1999, Howell et al. 2006).

Antiestrogen Resistance. Thirty percent of breast cancers fail to respond to initial TAM treatment, demonstrating de novo resistance to hormonal therapy (Riggins et al., 2007). In clinical studies, such resistance strongly correlates with the absence of the ER, amplification of human epidermal growth factor receptor 2 (HER2/neu), and the lack of progesterone receptor (PR) (Milano et al. 2006, Harris et al. 1989). Therefore, presence of the ER is used to classify breast cancer patients, and to select those with a better chance for successful TAM therapy.

Among the ER-positive patients, even short-term (1-3 years) TAM therapy can lead to the development of acquired resistance, which manifests as tumor growth despite TAM treatment (Jordan et al., 2009). Acquired resistance also develops with other SERMs, and pure antiestrogens (O'Regan et al. 2006, Brunner et al. 1997). Laboratory models of acquired antiestrogen resistance show that the evolution of this resistance is a complex process that may involve multiple mechanisms, which have not been completely elucidated to date. Since ER mediates the action of antiestrogens, many proposed mechanisms of antiestrogen resistance involve the ER. Table 1 shows an array of potential pathways of antiestrogen resistance based on the evidence obtained from, either, in vitro investigations or clinical studies.

Table 1. Proposed mechanisms for the development of antiestrogen resistance.

	Mechanisms of Antiestrogen Resistance
1	**Loss/downregulation of ER**
2	**ER mutation**
3	**Growth factor receptor signaling**
4	**ER phosphorylation**
5	**Overexpression of co-activators**
6	**Overexpression/downregulation of cell cycle mediators**
7	**Autophagy**

Loss of ER. The absence of ER in ER-negative tumors is believed to be responsible for their de novo antiestrogen resistance. Although a loss of ERα has been observed in an in vitro model of antiestrogen resistance (van den Berg et al. 1989), it is rarely observed in vivo, and is not considered as a major mechanism of acquired resistance (Clarke et al. 2001, Riggins et al. 2007).

ER Mutation. Several ER mutations have been identified in breast tumors that lead to altered ER phenotypes and may mediate resistance to hormonal therapy. For example, a tyrosine 537 substitution for asparagine in the LBD resulted in a constitutively transcriptionally active ER phenotype that functioned as well in the absence of ligand as in the presence of E_2 or TAM (Zhang et al., 1997). Another substitution mutation, lysine-to-arginine at position 303 rendered the receptor hypersensitive to minute concentration of E_2. This mutation may play a role in resistance to estrogen ablation therapy (Ali et al., 2002). ER mutations are thought to play a minor role in endocrine-therapy resistance due to clinical observations of their presence in only 1% of primary breast tumors (Roodi et al., 1995).

Growth Factor Receptors. Increased activation of growth receptor signaling pathways can bypass the need for ER-stimulated transcription of genes involved in cell proliferation and/or survival and lead to antiestrogen resistance (Riggins et al., 2007). Clinical data indicates that the HER2 gene is amplified in 20-30% of breast tumors overexpressing HER2/neu (Ignatiadis et al., 2009). Overexpression of HER2/neu in vitro has been shown to produce antiestrogen resistance in previously sensitive ER-positive breast cancer cells (Kurokawa et al. 2000, Knowlden et al. 2003, McClelland et al. 2001). This acquired resistance was associated with increased activation of second messenger molecules such as ERK1/2, PI3K, and Akt, which are known promoters of cell survival and proliferation (Knowlden et al. 2003, McClelland et al. 2001). HER2 signaling has also been implicated in downregulation of ERα levels in vitro (Holloway et al., 2004). Resistance to fulvestrant frequently correlates with an enhanced EFGR-mediated signaling, and can be reduced by EFGR-tyrosine kinase inhibitors such as “Iressa” (McClelland et al. 2001, Okubo et al., 2004). Growth factor receptors can also modulate ER activity through phosphorylation of the receptor and its co-regulators (Riggins et al., 2007).

ER Phosphorylation. Phosphorylation of the ERα at serine/threonine and tyrosine residues is the basis for its ligand-independent activity, and most often occurs in the AF1 region of the receptor. Ser-167 is the major target of ERK and Akt kinases. Increased phosphorylation of this amino acid leads to reduced tamoxifen sensitivity and promotes ER-DNA binding and coactivator interactions (Glaros et al. 2006, Likhite et. al. 2006). Ser-118 phosphorylation at AF1 by ERK1/2

kinases results in ligand-independent transactivation of the ER (Bunone et al., 1996). Cell culture models of tamoxifen resistance demonstrated increased basal phosphorylation of Ser-118 (Likhite et al. 2006, Britton et al. 2006).

Cell Cycle Regulators. Since antiestrogen action involves the induction of cell cycle arrest, deregulation of cell cycle mediators can result in antiestrogen resistance. Cyclin D1 is an essential regulator of G1 progression, and is overexpressed in 50% of breast cancers (Riggins et al., 2007). Studies have demonstrated that overexpression of cyclin D1 can produce TAM and fulvestrant resistance in vitro (Hui et al., 2002). p21 and p27 function as CDK inhibitors and negatively regulate of cell cycle progression. Studies have shown them to be essential mediators of breast cancer cell growth arrest by antiestrogens such as TAM, and their downregulation prevented antiestrogen-induced growth inhibition (Cariou et al., 2000).

Coactivator Overexpression. Since SERMs can act as agonists or antagonists, nuclear concentrations of co-regulators have a critical impact on their ER-mediated transcriptional activity. Co-activator overexpression and co-repressor downregulation can result in agonistic ER activity in the presence of previously inhibitory concentrations of SERMs (Takimoto et al. 1999, Schiff et al. 2005). Clinical analysis showed that coactivator AIB1 was amplified in 5-10% of breast cancers, most of which were ER-positive (Bautista et al., 1998). Overexpression of nuclear coactivator 1 (NCOA1) enhanced ER's agonist activity in vitro, which may promote resistance to antiestrogen therapy (Webb et al., 1998).

Taken together, the aforementioned and other studies have shown that the development of antiestrogen resistance is a complex process that involves multiple factors and pathways. Therefore, multiple mechanisms may contribute to antiestrogen resistance and are currently under investigation. Our aim was to explore a novel resistance mechanism that involves the mammalian autophagy mediator protein Beclin 1.

Autophagy. Normal cell proliferation and development requires a tightly controlled homeostasis between protein and organelle biosynthesis and their degradation and/or turnover (Klionsky et al., 2000). The two major degradative pathways are the proteasome-mediated destruction of short-lived and/or misfolded proteins, and the autophagic degradation of long-lived proteins and

organelles. In autophagy, cellular components are enclosed into double-membrane vesicles, termed autophagic vacuoles or autophagosomes, and delivered to the lysosome for degradation and recycling. Autophagy can be activated in the course of normal cell/tissue development or in conditions of stress, such as nutrient or growth factor deprivation (Rubinztein et al., 2007). In such context, autophagy provides cells with energy obtained from the recycling of non-essential cellular components, thereby promoting cell survival. Activation of autophagy can also result in Active cell death II (ACDII), characterized by the presence of autophagic vacuoles in the cytoplasm (Gewirtz et al., 2007). Thus, autophagy plays a role in both, cell survival and cell death. Table 2 lists the major differences between autophagy and apoptosis (Bursch et al. 2000, Levine et al. 2005).

Table 2. A comparison of characteristics of autophagy and apoptosis.

Characteristics	Autophagy	Apoptosis
Reversible	**Yes**	**No**
Autophagic Vacuoles	**Yes**	**No**
Organelle Degradation	**Early**	**Late**
Caspase Activation	**No**	**Yes**
Nucleosomal Cleavage	**Late (if at all)**	**Early**
Cytoskeleton Collapse	**Late**	**Early**
Cytoplasm Condensation	**No**	**Yes**
Nuclear Protein Breakdown	**No**	**Yes**

Beclin 1 is a Mediator of Autophagy. Beclin 1 is a homologue of yeast Apg6/Vps30p gene, and is essential for autophagy in mammals (Liang et al., 1999). It is a part of the phosphotidyl inositol kinase III (PI3K) complex, and plays a key role in autophagosome formation. Beclin 1 is a 60-kDa protein with an N-terminal Bcl-2 binding domain, a coiled-coil central domain, and a C-terminal domain that promotes association with intracellular membranes (Aita et al., 1999). The

protein does not share any significant homology with any other proteins of known function (Liang et al., 2001). The exact mechanism of autophagy stimulation by Beclin 1 has not been elucidated to date. However, the identification of a nuclear export signal (NES), and the demonstration that NES mutation blocked Beclin 1-induced autophagy, suggest that nuclear-cytoplasmic shuttling may play a role in the regulation of autophagy (Liang et al., 2001).

Beclin 1 gene functions as a tumor suppressor. It is monoallelically deleted in 50% of human breast cancers (Futreal et al. 1992, Saito et al. 1993). Heterozygous disruption of the Beclin 1 gene increased tumor incidence and induced preneoplastic transformation of the breast tissue in mice (Qu et al., 2003).

Beclin 1 was discovered in a yeast two-hybrid assay that searched for the apoptosis inhibitor Bcl-2 interacting proteins (Liang et al., 1998). It was demonstrated to bind to other anti-apoptotic proteins such as Bcl-x_L, and Bcl-w, but not to the pro-apoptotic members of the Bcl-2 family (i.e. Bax). (Erlich et al. 2007, Feng et al. 2007, Oberstein et al. 2007, Maiuri et al. 2007). Structural modeling suggests that Beclin has a BH3-like domain that may promote its interactions with anti-apoptotic members of the Bcl-2 family (Erlich et al., 2007). Bcl-2 binding to Beclin 1 leads to negative regulation of autophagy by this anti-apoptotic protein (Mauri et al. 2007, Pattingre et al. 2005). These findings indicate the existence of a cross-talk between autophagy and apoptosis within cells, and suggest a mechanism by which autophagy may promote cell death under certain conditions (Maiuri et al., 2007).

Recent studies have identified additional Beclin 1-interacting proteins, such as UV radiation resistance-associated gene (UVRAG), Ambra1, yeast Atg14-like (Atg14L), and Rubicon (Run domain and cystein-rich domain containing, Beclin 1 interacting protein) (Liang et al. 2006, Maria Fimia et al. 2007, Zhong et al. 2009). UVRAG, Atg14L, and Rubicon have been shown to associate with both Beclin 1 and Vp34/PIK3 (Liang et al. 2006, Zhong et al. 2009). UVRAG, Atg14L, and Ambra1 are positive regulators of autophagy, whereas Rubicon is a negative modulator of this process (Liang et al. 2006, Maria Fimia et al. 2007, Zhong et al. 2009).

Antiestrogens Can Induce Autophagy. A key study by Bursch demonstrated that while antiestrogens (TAM, OHT, ICI 164,384) induced apoptosis at high concentrations (10^{-5} M), at low

concentration (10^{-6} M) they induced autophagy, which could be rescued by E_2 (Bursch et al., 1996). 4-Hydroxytamoxifen (OHT) is the active metabolite of tamoxifen (Jordan et al., 2008). This finding prompted a question of whether autophagy, as a survival mechanism, can lead to drug resistance. A recent study demonstrated inhibition of autophagy in a tamoxifen-resistant cell line sensitized these cells to TAM's antiestrogenic effects, demonstrating that autophagy may play a role in antiestrogen-resistance (Quadir et al., 2008). Another study also demonstrated that autophagy plays a survival role in breast cancer cells and mediates resistance to OHT. This study indicated that autophagy was not necessarily a precursor of ACD II, which may become important if apoptosis is compromised in cancer cells (Samaddar et al., 2008). Based on these finding, we decided to investigate the role of the autophagy mediator, Beclin 1, in estrogenic signaling and antiestrogen resistance. The results of our study are presented in Chapter 1.

We found that Beclin 1 overexpressing cells had reduced proliferative response to E_2, and that the expression of E_2-responsive genes was down-regulated. E_2 caused a decrease in Akt phosphorylation in Beclin 1 transfected cells. Growth inhibitory responses of antiestrogens, raloxifene and 4-hydroxytamoxifen were also limited by Beclin 1 transfection. Confocal microscopic studies demonstrated co-localization of ERα and Beclin 1 in the presence of E_2 in MCF-7.beclin cells. An interaction between Beclin 1 and ERα was also evident from the results of co-immunoprecipitation experiments. ChIP assay results suggest that interaction of ERα and Beclin 1 in the presence of antiestrogens leads to decreased promoter occupancy of E_2-regulated genes. Our results show that Beclin 1 can downregulate estrogen-induced signaling events and cell growth in ERα-positive breast cancer cells. Our results further suggest that Beclin 1 may alter sensitivity of antiestrogens to breast cancer cells.

Apoptosis. Apoptosis, or Type I Programmed Cell Death, is an important regulatory mechanism in embryonic development and carcinogenesis. It is activated or inhibited by a variety of intrinsic or environmental signals, and functions to eliminate excessive cells during an organism's development as well as to remove diseased or damaged cells (Bursch et al., 2000). Apoptotic cells are classified on the basis of specific morphological changes, such as cytoplasmic

shrinkage, chromatin condensation and fragmentation, and, finally, cell fragmentation into apoptotic bodies that are phagocytosed by neighboring cells (Bursch et al., 2000).

Antiestrogens Can Induce Apoptosis. Antiestrogenic action of TAM in breast cancer has been shown to cause cell cycle arrest and induce apoptosis both in vitro and in vivo in a concentration-dependent manner (Perry et al.1995, Martin et al. 1996, Cameron et al. 2000). At low concentrations (nM), TAM induced cell cycle arrest (cytostasis), wheras at high concentrations (μM), apoptotic (cytotoxic) response was observed in vitro. Clinical and animal studies also indicated that TAM's antagonistic activity in breast cancer resulted from the stimulation of apoptosis, as reduced cell proliferation, increased apoptosis, and tumor regression were observed with TAM treatment (Cameron et al. 2000, Keen et al. 1997).

In ER positive cells, induction of apoptosis by TAM is thought to occur via an ER-mediated (genomic) pathway, and result from transcriptional activation and/or repression of key cell cycle and apoptotic genes. However, TAM and its metabolite (i.e. OHT) can induce apoptosis in ER negative cells at much higher concentrations than those used in ER-positive cells, and this is believed to involve non-genomic signaling pathways (Mandlekar et al., 2000). The non-genomic mechanism(s) of apoptosis induction are unclear at present, but may involve TAM modulation of PKC, calmodulin, c-myc, MAP kinases, and caspases (Mandlekar et al., 2000).

Polyamines. Natural polyamines, putrescine ($H_2N(CH_2)_4NH_2$), spermidine ($H_2N(CH_2)_3NH(CH_2)_4NH_2$) and spermine ($H_2N(CH_2)_3NH(CH_2)_4NH(CH_2)_3NH_2$), are polycations found in all eukaryotic cells and are obtained from dietary sources in addition to biosynthesis (Thomas et al, 2002.). Polyamines are necessary for normal cell growth and differentiation, and are involved in a variety of processes including DNA packaging, replication, transcription and translation (Casero et al. 2007, Gerner et al. 2004). Polyamines have a net positive charge at physiological pH, and form complexes with nucleic acids and proteins through ionic interactions (Thomas et al., 2002). Polyamine homeostasis is carefully maintained within cells, as de-regulation of this homeostasis can have deleterious consequences. Polyamine balance is controlled by the biosynthetic enzymes, ornithine decarboxylase (ODC) and S-adenosyl

methionine decarboxylase (SAMDC), the catabolic enzymes, spermidine/spermine N^1-acetyltransferase (SSAT) and polyamine oxidases (PAO), and cellular transport pathways (Thomas et al. 2003, Casero et al., 2007).

Several lines of evidence link polyamines and cancer development/progression. ODC overexpression led to neoplastic transformation of cells and the development of tumors in nude mice (Moshier et al. 1993, Auvinen et al. 1997). Difluoromethylornithine (DFMO), an irreversible inhibitor of ODC, suppressed cancer development in animal models (Gerner et al. 2004, Meyskens et al. 1999). Polyamine involvement in breast cancer is supported by the following findings. Polyamine levels and their biosynthetic enzymes are significantly higher in breast tumors compared to normal tissue (Canizares et al. 1999, Leveque et al. 2000a, Leveque et al. 2000b). Elevated polyamine levels promote the interaction of ER with its response element, and lead to overexpression of ER-responsive genes in breast cancer cells (Shah et al., 2001).

Polyamine Analogues Induce Cell Death. Since polyamine overabundance has been linked to cancer development/progression, a therapeutic effort has been made to deplete polyamine levels. The use of biosynthetic enzyme inhibitors had limited results due to the existence of compensatory mechanisms, such as increased polyamine uptake and target gene upregulation, and harmful side effects of these agents (Casero et al. 2007, Thomas et al. 2002). Polyamine analogues were developed in order to circumvent these problems.

Bergeron and colleagues, synthesized bis(ethyl)polyamines, in which the primary amines were modified by the addition of alkyl groups, thereby protecting these analogues against degradation by PAO (Bergeron et. al., 1988). Bis(ethyl)polyamines are readily transported into cells and cause growth inhibition and depletion of polyamine levels, but they cannot substitute for the functions of natural polyamines. Spermine analogues were shown to be more effective growth inhibitory agents than either spermidine or putrescine analogues (Porter et al., 1987). Bis(ethyl) analogues' cytotoxic action occurs through modulation of growth stimulatory and anti-apoptotic genes and induction of apoptosis (Faaland et al. 2000, Thomas et al. 2002). The exact mechanism of apoptosis induction by polyamines has not been elucidated due to the complexity of their effects on target cells. However, a part of the mechanism is believed to be the generation

of cell-damaging reactive oxygen species through the induction of SSAT (Chen et al.). Polyamine analogue 1,15-bis(ethylamino)-4,8,12-triazapentadecane (BE-3-3-3-3) stimulated apoptosis in MCF-7 cells, and induced the activity of SSAT (Faaland et al., 2000). In addition, BE-3-3-3-3 was more effective than the commonly used compound, bis(ethyl)norspermine (BE-3-3-3), in inhibiting tumor growth in a transgenic mouse model of breast cancer (Shah et al., 1999).

Bis(ethyl) analogues did not prove to be safe for clinical use due to adverse side effects. For instance, BE-3-3-3 has been tested in Phase I and II clinical trials, and demonstrated unacceptable neurotoxicity as well as a lack of therapeutic effect (Creaven et al. 1997, Streiff et al. 2001, Wolff et al. 2003). Thus, the need exists for the development of new polyamine analogues with an improved clinical potential.

BE-3-3-3-3 as an Estrogenic Compound. Synthetic environmental compounds such as dioxins, polychlorobiphenyls (PCBs), Dichlorodiphenyltrichloroethane (DDT) and derivatives, and phthalases have been implicated in the interference of endocrine system function, and are know as endocrine disruptors (ED) (Witorsch, 2002). These compounds are found in a variety of commonly used products such a plastics, food packaging, pesticides, petroleum, etc. Some of these chemicals (i.e. selected PCBs, Bisphenol-A, Alkyphenols) can bind to the ER and mimic estrogen activity in laboratory studies (Witorsch 2002, Le 2008). A recent report demonstrated that BE-3-3-3 promoted cell proliferation at low concentrations (up to 10 μM) in melanoma cells (Minchin et al., 2006). This finding prompted us to examine whether a related polyamine analogue, BE-3-3-3-3, can also exert an estrogenic, growth-promoting effect on breast cancer cells.

Our laboratory recently demonstrated that some compounds (i.e. 2-methoxyestradiol) can exert differential effects on breast cancer cells in the presence and absence of E_2 (Vijayanathan et al., 2006).

We, therefore, examined the effect of BE-3-3-3-3 on MCF-7 cells in the presence and absence of E_2. In the presence of E_2, there was a concentration-dependent decrease of cell growth, as measured by [^{3}H]-thymidine incorporation. In the absence of E_2, low concentrations (1.25 to 10 μM) of BE-3-3-3-3 increased [^{3}H]-thymidine incorporation at 24 and 48 h of treatment.

However, growth inhibition was observed by 96 h of treatment. During the growth-stimulatory phase in the absence of E_2, BE-3-3-3-3 induced Akt phosphorylation, indicating the involvement of non-genomic cell signaling. Delayed growth inhibition in the absence of E_2 was associated with the induction of autophagy, demonstrated by elevated levels of autophagy-related proteins, Beclin 1 and MAP LC3 II. Electron microscopic studies confirm the induction of autophagy in the presence of BE-3-3-3-3. Confocal microscopy also demonstrated higher levels of Beclin 1 in BE-3-3-3-3-treated cells, and showed Beclin 1 accumulation around the nucleus. These results provide a novel mechanistic pathway for the action of polyamine analogues on breast cancer cell growth. Therapeutic agents specifically targeted for modulating autophagy might be useful in combination with polyamine analogues in breast cancer.

The results of this investigation are presented in Chapter 2.

Gene Delivery is a Prerequisite of Gene Therapy. The need for treatments of inherited or acquired genetic disorders led to research and development of gene therapy, where a therapeutic gene is delivered into target cells in order to either express a therapeutic protein or to regulate existing proteins (Garnett 1999, Wagner 1998, Merdan et.al. 2002, Nishikawa et al. 2001). The ideal delivery systems should be stable to serum inactivation, protective against DNA degradation, nontoxic, and biodegradable. In addition, they should mediate efficient uptake by target cells (Vijayanathan et al., 2002). Many gene delivery agents, such as liposomes and cationic polymers, have been investigated and showed either high cytotoxicity or low uptake rates.

DNA compaction is a necessary step for successful gene delivery. DNA condensation in a single state, coil-globule transition, in which the positively charge condensing agents associate with negatively charged DNA molecule via ionic interaction, and lead to DNA compaction when 89-90% of the charges are neutralized (Bloomfield 1997). In order to enter target cells, condensed particles must interact with the anionic proteoglycans at the cell surface and be sufficiently small in size to undergo endocytosis. (Wagner et al. 1998, Merdan et al. 2002, Nishikawa et al. 2001, Vijayanathan et al. 2002). Therefore, nanoparticles need to have sufficient positive charge and optimum size distribution for efficient internalization.

Methylated Spermine Analogues as Gene Delivery Vehicles. The need for clinically safe and effective polyamine analogues lead to the design of a novel class of analogues in which the alkyl(s) are attached to backbone carbon atom. The placement of the methyl group at the α-position interferes with acetylation of the primary amino group by SSAT, and ensures analogue stability by preventing degradation (Jarvinen et al., 2006). Methylated analogues such as α-methylspermine (α-MeSpm) and bis-α,α'methylspermine (α,α'-Me_2Spm) retain some characteristics of natural polyamines, such as the ability to transform B-DNA to Z-DNA, and α-MeSpm's can serve as substrate for deoxyhypusine synthase, an enzyme involved in the modification of initiation factor 5A (Varnado et al. 2000, Byers et al. 1994). Administration of 1-methylspermidine resulted in a stable accumulation of this polyamine analogue in the pancreas, and successfully treated severe pancreatitis caused by pancreatic polyamine depletion (Rasanen et al. 2002). These findings indicate that methylated polyamine analogues were successfully internalized by pancreatic cells, were stable against degradation, and were able to substitute for the functions of natural polyamines, such as cell proliferation (Rasanen et al. 2002). Methylated analogues' abilities to substitute for the function of natural polyamines probably derive from the fact that their amino groups are not disturbed by the modification, and, as a result, are able to mediate charge-dependent interactions (Keinanen et al. 2007).

The lack of cytotoxicity of methylated analogues in vivo (Rasanen et al. 2002, Jarvinen et al., 2006), their easy internalization and stability (Jarvinen et al., 2006), prompted us to investigate their possible use as gene delivery agents. We investigated the binding of α-methyl polyamines using physical-chemical studies, such as total intensity light scattering, dynamic light scattering, and melting temperature (Tm) determination. Total intensity light scattering results demonstrated that 3 out of 4 stereoisomers (RR-, RS-, and Rac-Me_2Spm) were significantly more effective DNA condensing agents than spermine. Nanoparticle sizes did not correlate with condensing efficiency, however, and both RR-, and SS-Me_2Spm produced larger condensates than spermine. Electron microscopy analysis showed that condensed structures possessed spheroidal or toroidal morphology.

Our findings are presented in Chapter 3. They indicate that in addition to ionic charge, polyamine's structure/spatial arrangement plays an important role in its biophysical properties. Our overall conclusion is that Me_2Spm isomers are efficient DNA packaging agents, and may be considered as possible gene delivery vehicles.

Lysines as Gene Delivery Vehicles. Among the cationic polymer gene delivery agents, by far the most attention has been devoted to poly-L-lysine (PLL). DNA collapse by PLL leads to structures of various shapes (i.e. toroids, spheroids or rods) and sizes, depending on its ratio to DNA, ionic environment and mixing conditions (Hansma et.al. 1998, Kwoh, et.al. 1999, Tang et.al. 1997, Wolfert et.al. 1996). PLL can bind DNA cooperatively or non-cooperatively, producing unimolecular complexes or multimolecular aggregates, respectively (Liu et al. 2001, Perales et al. 1997). PLL is a biodegradable polymer, a desirable characteristic for in vivo use. Like most other cationic polymers it has a high positive ζ potential that, on one hand, may facilitate the interactions of its complexes with negatively charged cell surface, but, on the other hand, makes these nanostructures susceptible to complex activation and eventual destruction by the immune system (Plank et.al. 1999, Tang et.al. 1997, Vijayanathan et.al. 2002).

The polypeptide demonstrated modest to high toxicity during transfection studies, where lower toxicity generally correlated with lower charge density and ζ potential (Plank et al. 1999, Wolfert et al. 1996). PLL's transfection efficiency is several orders of magnitude lower than that of polyethylenimine (PEI), another widely used cationic polymer (Garnett, 1999). A major advantage of PLL is its amenability to chemical alteration, which can result in significantly higher transfection efficiency. The polymer can be modified with a variety of ligands to achieve receptor-specific uptake, intracellular release, and/or nuclear translocation for gene delivery applications (Garnett 1999, Wagner 1998, Kwoh et.al. 1999, Perales et.al. 1997, Vijayanathan et.al. 2002).

We investigated the use of oligolysines and PLL as gene delivery vehicles using physical-chemical methods to examine DNA condensation in the presence of these cations, and to determine the size, shape, and stability of the resultant nanoparticles. Total intensity light scattering investigation demonstrated PLL's superior DNA-condensing ability and DNA-stabilization in high salt conditions compared to oligolysines, Lys_5 and Lys_4. In addition, dynamic

light scattering studies showed that PLL-DNA nanoparticles remained stable in size in the presence of increasing salt concentration or temperature, whereas oligolysine particle sizes increased dramatically. Melting temperature studies demonstrated concentration-dependent DNA stabilization by oligolysines, but no detectable stabilization by PLL. These results indicate distinct differences in the mechanism(s) by which oligolysines and PLL provoke DNA condensation to nanoparticles. They also underscore the role of cationic polymer structure and charge distribution on nanoparticle formation, and may help contribute to optimization of gene delivery agents. The aforementioned findings comprise Chapter 4 of this thesis.

The following are brief rationales for developing hypotheses and specific aims involved in this thesis.

Our hypothesis in the first chapter is that Beclin 1 interacts with ERα and limits estrogenic signaling, leading to antiestrogen resistance. The hypothesis is based on the general observation that functions of ERα as a transcription factor is dependent on accessory proteins and co-regulators. Furthermore, it was reported by Liang et al. (1999) that Beclin 1 overexpression inhibited E_2-dependent growth of MCF-7 cells in immunodeficient mice. Our specific aim was to determine the mechanisms by which Beclin 1 modulates estrogenic function and contributes to antiestrogen resistance.

Our hypothesis in the second chapter is that BE-3-3-3-3 exerts differential effects on cell growth in the presence and absence of E_2, and induces autophagy in ER-positive, MCF-7 cells. This hypothesis was based on previous studies from our laboratory demonstrating differential responses to therapeutic agents tested in breast cancer cells in the presence and absence of E_2. Additionally, Minchin et al. (2006) reported that a polyamine analogue that had reached phase II clinical trials exerted a growth-stimulatory effect at low concentrations. Our specific aim has been to determine the growth-inhibitory responses of BE-3-3-3-3 in breast cancer cells in the presence and absence of E_2, and understand the role of autophagy in the differential responses involved.

In the third chapter, our hypothesis is that the structural features of spermine's α,α'-dimethylated stereoisomers significantly impact their ability to condense DNA, and affect the properties of the resultant nanoparticles. This hypothesis is based on a series of studies from our

laboratory that featured structural specificity of polyamine analogues in DNA condensation, conformational transitions, and DNA-protein interactions. Our specific aim was to evaluate and compare the abilities of different stereoisomers in DNA condensation, and to analyze the properties of the nanoparticles in terms of size, stability, and structural morphology. These parameters are important in their ultimate utilization in gene therapy.

In the fourth chapter, our hypothesis is that PLL is more effective than in DNA condensation and stabilization than oligolysines (trilysine, tetralysine, pentalysine). This hypothesis is based on the polyelectrolyte theories and the observations that longer chain alkylated lysines condense DNA at lower concentrations and produced smaller nanoparticles than shorter chain lysines (Wadhwa et al., 1997). Our specific aim has been to determine the comparative DNA condensing and duplex stabilizing capabilities of oligo- and poly-L-lysine, and determine the stability of the resultant nanoparticles at different ionic and temperature conditions. Optimization of these properties is necessary for the development of these compounds as gene delivery vehicles. Overall, these molecular aspects of antiestrogen resistance and the exploration of gene delivery agents advance the development of novel breast cancer therapies.

REFERENCES

Aita, V. M., Liang, X. H., Murty, V. V, Pincus, D. L., Yu, W., Cayanis, E., Kalachikov, S., Gilliam, C., Levine, B. (1999) Cloning and genomic organization of Beclin 1, a candidate tumor suppressor gene on chromosome 17q21. Genomics **59**:59-65.

Ali, S., Coombes, R. C. (2002) Endocrine-responsive breast cancer and strategies for combating resistance. Nat. Rev. Cancer **2**:101-115.

Allen, E., Doisy, E. A. (1923) An ovarian hormone: preliminary reports on its localization, extraction and partial purification and action in test animals. JAMA **81**:810-21.

Auvinen, M., Laine, A., Paasinen-Sohns, A., Kangas, A., Kangas, L., Saksela, O., Andersson, L. C., Holtta, E. (1997) Human ornithine decarboxylase-overproducing NIH3T3 cells induce rapidly growing, highly vascularized tumors in nude mice. Cancer Res. **57**:3016-3025.

Baum, M., Budzar, A. U., Cuzick, J. et al. (2002) Anastrozole alone or in combination with tamoxifen versus tamoxifen alone for adjuvant treatment of postmenopausal women with early breast cancer: first results of the ATAC randomized trial. Lancet **359**:2131-2139.

Bautista, S., Vallès, H., Walker, R. L., Anzick, S., Zeillinger, R., Meltzer, P., Theillet, C. (1998) In breast cancer, amplification of the steroid receptor coactivator gene AIB1 is correlated with estrogen and progesterone receptor positivity. Clin. Cancer Res. **4**:2925-2929.

Beatson, G. T. (1896) On the treatment of inoperable cases of carcinoma of the mammary. Suggestions for a new method of treatment with illustrative cases. Lancet **2**: 162-165.

Bergeron, R. J. Neims, A. H., McManis, J. S., Hawthorne, T. R., Vinson, J. R., Bortell, R., Ingeno, M. J. (1988) Synthetic polyamine analogues as antineoplastics. J. Med. Chem. **31**:1183-1190.

Bloomfield, V. A. (1997) DNA condensation by multivalent cations. Biopolymers **44:**269-82.

Bocchinfuso, W. P., Korach, K. S. (1997) Mammary gland development and tumorigenesis in estrogen receptor knockout mice. J. Mammary Gland Biol. Neoplasia **2**:323-334.

Boyd, S. (1900) On oophorectomy in cancer of the breast. BMJ **ii**:161-167.

Britton, D. J., Hutcheson, I. R., Knowlden, J. M., Barrow, D., Giles, M., McClelland, R. A., Gee, J. M., Nicholson, R. I. (2006) Bidirectinal cross talk between ER alpha and EGFR signaling pathways regulates tamoxifen-resistant growth. Breast Cancer Res. Treat. **96**:131-146.

Brunner, N., Boysen, B., Jirus, S., Skaar, T. C., Holst-Hansen, C., Lippman, J., Frandsen, T., Spang-Thomsen, M., Fuqua, S. A., Clarke, R. (1997) MCF7/LCC9: an antiestrogen-resistant MCF-7 variant in which acquired resistance to the steroidal antiestrogen ICI 182,780 confers and early cross-resistance to the nonsteroidal antiestrogen tamoxifen. Cancer Res. 57:3486-3493.

Brzozowski, A. M., Pike, A. C., Dauter, Z., Hubbard RE, Bonn T, Engström O, Ohman L, Greene GL, Gustafsson JA, Carlquist M. (1997) Molecular basis of agonism and antagonism in the oestrogen receptor. Nature **389**:753-758.

Bunone, G., Briand, P. A., Miksicek, R. J., Picard, D. (1996) Activation of the unliganded estrogen receptor by EGF involves the MAP kinase pathway and direct phosphorylation. EMBO J. **15**:2174-2183.

Bursch, W., Ellinger, A., Gerner, C. Frohwein, U., Schulte-Hermann, R. (2000) Programmed Cell Death (PCD). Apoptosis, autophagic PCD, or others? Ann. N Y Acad. Sci. **926**:1-12.

Bursch, W., Ellinger, A., Kienzl, H., Torok, L., Pandey, S., Sikorska, M., Walker, R., Hermann, R. S. (1996) Active cell death induced by the anti-estrogens tamoxifen and ICI 164 384 in human mammary carcinoma cells (MCF-7) in culture: the role of autophagy. Carcinogenesis **17**:1595-1607.

Byers, T. L., Lakanen, J. R., Coward, J. K., Pegg, A. E. (1994) The role of hypusine depletion in cytostasis induced by S-adenosyl-L-methionine decarboxylase inhibition: New evidence provided by 1-methylspermidine and 1,12-dimethylspermine. Biochem. J. **303**:363-368.

Cameron, D. A., Keen, J. C., Dixon, J. M., (2000) Effective tamoxifen therapy of breast cancer involves both antiproliferative and pro-apoptotic changes. Eur. J. Cancer **36**:845-851.

Cameron, D. A., Ritchie, A. A., Langdon, S., Anderson, T. J., Miller, W. R. (1997) Tamoxifen induced apoptosis in ZR-75 breast cancer xenografts antedates tumor regression. Breast Cancer Res. Treat. **45**:99-107.

Canizares, F., Salinas, J., De Las Heras, M., Diaz, J., Tovar, I., Martinez, P., Penafiel, R. (1999) Prognostic valued of ornithine decarboxylase and polyamines in human breast cancer: Correlation with clinicopathologic parameters. Clin Cancer Res. **5**:2035-41.

Cariou, S., Donovan, J. C., Flanagan, W. M., Milic, A., Bhattacharya, N., Slengerland, J. M. (2000) Down-regulation of $p21^{WAF1/CIP1}$ or $p27^{Kip1}$ abrogates antiestrogen-mediated cell cycle arrest in human breast cancer cells. Proc. Natl. Acad. Sci. USA **97**:9042-9046.

Casero, R. A., Marton, L. J. (2007) Targeting polyamine metabolism and function in cancer and other hyperproliferative diseases. Nat. Rev. Drug Discov. **6**:373-390.

Castagnetta, L. A., Lo Casto, M., Granata, O. M., Polito, L., Calabrò, M., Lo Bue, A., Bellavia, V., Carruba, G. (1996) Estrogen content and metabolism in human breast tumor tissues and cells. Ann. NY Acad. Sci. **784**:314-324.

Chen, J. Q., Delannoy, M., Cooke, C., Yager, J. D. (2004) Mitochondrial localization of ERalpha and ERbeta in human MCF-7 cells. Am. J. Physiol. Endocrinol. Metab. **286**:E1011-E1022.

Chen, Y., Kramer, D. L., Diegelman, P., Vujcic, S., Proter, C. W. (2001) Apoptotic signaling in polyamine analogue-treated SK-MEL-28 human melanoma cells. Cancer Res. **61**:6437-6444.

Clarke, R., Skaar, T. C., Bouker, K. B., Davis, N., Lee, Y. R., Welch, J. N., Leonessa, F. (2001) Molecular and pharmacological aspects of antiestrogen resistance. J. Steroid Biochem. Mol. Biol. **76**:71-84.

Clemons, M., Goss, P. (2001) Estrogen and the risk of breast cancer. N. Engl. J. Med. **344**:276-85.

Creaven, P. J., Perez, R., Pendyala, L., Meropol, N. J., Loewen, G., Levine, E., Berghorn, E., Raghavan, D. (1997) Unusual central nervous system toxicity in a Phase I study of N^1N^{11} diethylnorspemine in patients with advanced malignancy. Invest. New Drugs **15**:227-234.

Demonacos, C. V., Karayanni, N., Hatzoglou, E., Tsiriyiotis, C., Sandidos, D. A., Sekeris, C. E. (1996) Mitochondrial genes as sites of primary action of steroid hormones. Steroids **61**:226-232.

Enmark, E., Pelto-Huikko, M., Grandien, K., Lagercrantz, S., Lagercrantz, J., Fried, G., Nordenskjöld, M., Gustafsson, J. A. (1997) Human estrogen receptor beta-gene structure, chromosomal localization, and expression pattern. J. Clin. Endocrinol. Metab. **82**:4258-4265.

Erlich, S., Mizrachy, L., Segev, O., Lindenboim, L., Zmira, O., Adi-Harel, S., Hirsch, J. A., Stein, R., Pinkas-Kramarski, R. (2007) Differential interactions between Beclin 1 and Bcl-2 family members. Autophagy **3**:561-8.

Faaland, C. A., Thomas, T. J., Balabhadrapathruni, S., Langer, T., Mian, S., Shirahata, A., Gallo, M. A., Thomas, T. (2000) Molecular correlates of the action of bis(ethyl)polyamines in breast cancer cell growth inhibition and apoptosis. Biochem. Cell Biol. **78**:415-426.

Fawell, S. E. White, R., Hoare, S., Sydenham, M., Page, M. Parker, M. G. (1990) Inhibition of estrogen receptor-DNA binding by the “pure” antiestrogen ICI 164,384 appears to be mediated by impaired receptor dimerization. Proc. Natl. Acad. Sci. USA **87**:6883-6887.

Feng W, Huang S, Wu H, Zhang M. (2007) Molecular basis of Bcl-xL's target recognition versatility revealed by the structure of Bcl-xL in complex with BH3 domain of Beclin-1. J.Mol. Biol.**372**:223-35.

Fisher, B., Constantino, J. P., Wickerham, D. L., Redmond, C. K., Kavanah M., Cronin, W. M., Vogel, V., Robidoux, A., Dimitrov, N., Atkins, J., Daly, Ml, Wieand, S., Tan-Chiu, E., Ford, L., Wolmark, N. (1998) Tamoxifen for prevention of breast cancer: report of the national surgical adjuvant breast and bowel project P-1 study. J. Natl. Cancer Inst. **90**:1371-1388.

Forman, M. R. (2007) Changes in dietary fat and fiber and serum hormone concentrations: nutritional strategies for breast cancer prevention over the life course. J. Nutr. 137:170S-174S.

Furuya, N., Liang, X. H., Levine, B. Autophagy and Cancer. In Autophagy, Editor Klionsky, D. J. (2003) Landes Bioscience, Georgetown, Texas, USA:244-253.

Futreal, P. A., Soderkvist, P., Marks, J. R., Iglehart, J. D., Cochran, C., Barrett, J. C., Wiseman, R. W. (1992) Detection of frequent allelic loss on proximal chromosome 17q in sporadic breast carcinoma using microsatellite length polymorphisms. Cancer Res. **52**:2624-2627.

Garnett, M.C. (1999) Gene-delivery systems using cationic polymers. Crit. Rev. Ther. Drug Carrier Syst. **16:**147-207.

Gerner, E. W., Meyskens, F. L. (2004) Polyamines and cancer: old molecules, new understanding. Nat. Rev. Cancer **4**:781-792.

Gewirtz D. (2007) Autophagy as a mechanism of radiation senstization in breast cancer cells. Autophagy **3**:249-252.

Glaros, S., Atanaskova, N., Zhao, C., Skafar, D. F., Reddy, K. B. (2006) Activation function-1 domain of estrogen receptor regulates the agonistic and antagonistic actions of tamoxifen. Mol. Endocrinol. **20**: 996-1008.

Glass, C. K., Rosenfeld, M. G. (2000) The coregulator exchange in transcriptional functions of nuclear receptors. Genes Dev. **14**:121-141.

Greene, G. L., Gilna, P., Waterfield, M., Baker, A., Hort, Y., Shine, J. (1986) Sequence and expression of human estrogen receptor complementary DNA. Science **231**:1150-1154.

Gunson, D. E., Steele, R. E., Chau, R. Y. (1995) Prevention of spontaneous tumors in female rats by fadrozole hydrochloride, an aromatase inhibitor. Br. J. Cancer **72**:72-75.

Hall, J. M., McDonnell, D. P. (1999) The estrogen receptor β–isoform (ERβ) of the human estrogen receptor modulates ERα transcriptional activiety and is a key regulator of the cellular response to estrogens and antiestrogens. Endocrinology **140**:5566-5578.

Hansma, H.G., Golan, R., Hsieh, W., Lollo, C.P., Mullen-Ley, P., Kwoh, D. (1998) DNA condensation for gene therapy as monitored by atomic force microscopy. Nucleic Acids Res. **26:**2481-2487.

Harris, A., Nicholson, S., Sainsburry, J. R. (1989) Epidermal growth factor receptors in breast cancer: association with early relapse and death, poor response to hormones and interaction with neu. J. Steroid Biochem**. 34**:123-131.

Holloway, J. N., Murthy, S., El-Ashry, D. (2004) A cytoplasmic substrate of mitogen-activated protein kinase is responsible for estrogen receptor-alpha down-regulation in breast cancer cells: the role of nuclear factor-kappa B. Mol. Endocrinol. **18**:1396-1410.

Howell, A. (2006) Pure oestrogen antagonists for the treatment of advanced breast cancer. Endocr. Relat. Cancer **13**:689-706.

Howell, A., Cuzick, J., Baum, M., Buzdar, A., Dowsett, M., Forbes, J. F., Hoctin-Boes, G., Houghton, J., Locker, G. Y, Tobias, J. S.; ATAC Trialists' Group. (2005) Results of the ATAC (Arimidex, Tamoxifen, Alone or in Combination) trial after completion of 5 years' adjuvant treatment for breast cancer. Lancet **365**:60-62.

Hui, R., Finney, G. L., Carroll, J. S., Lee, C. S., Musgrove, E. A., Sutherland, R. L. (2002) Constitutive overexpression of cyclin D1 but not cyclin E confers acute resistance to antiestrogens in T-47D breast cancer cells. Cancer Res. **62**:6916-6923.

Ignatiadis, M., Desmedt, C., Sotiriou, C., Azambuja, E., Piccart, M. (2009) HER-2 as a target for breast cancer therapy. Clin.Cancer Res.**15**:1848-1852.

Jarvinen, A., Cerrada-Gimenez, M., Grigorenko, N. A., Khomutov, A. R., Vepsalainen, J., Sinervirta, R. M., Keinanen, T. A., Alhonen, L I., Janne, J. (2006) α-Methyl polyamines: efficient synthesis and tolerance studies in vivo and in vitro. First evidence for dormant stereospecificity of polyamine oxidase J. Med. Chem. **49**:399-406.

Jemal, A., Siegel, R., Ward, E., Hao, Y., Xu, J., Murray, T., Thun, M. J. (2008) Cancer Statistics, 2008. CA Cancer J. Clin. **58**:71-96.

Jensen, E. V., Jacobson, H. I. (1962) Basic guides to the mechanism of estrogen action. Recent Prog. Hormone Res. **18**:387-414.

Jordan, V. C. (1976) Effect of tamoxifen ICI 46,474 on the initiation and growth of DMBA-induced rat mammary carcinoma. Eur. J. Cancer **12**:419-424.

Jordan V. C. (2004) Selective estrogen receptor modulation: Concept and consequences in cancer. Cancer Cell **5**:207-213.

Jordan, V. C. (2008) Tamoxifen: Catalyst for the change to targeted therapy. Eur. J. Cancer **44**:30-38.

Jordan, V. C. (2009) A century of deciphering the control mechanisms of sex steroid action in breast and prostate cancer: the origins of targeted therapy and chemoprevention. Cancer Res. **69**:1243-1254.

Keen, J. C., Dixon, J. M., Miller, E. P., Cameron, D. A., Chetty, U., Hanby, A., Bellamy, C., Miller, W. R. (1997) The expression of Ki-S1 and BCL-2 and the response to primary tamoxifen therapy in elderly patients with breast cancer. Breast Cancer Res. Treat. **44**:123-133.

Keinanen, T. A.; Jarvinen, A.; Uimari, A.; Vepsalainen, J.; Khomutov, A. R.; Grigorenko, N. A.; Hyvonen, M. T.; Cerrada-Gimenez, M.; Alhonen, L.; Janne, J. (2007) α-Methylated polyamines as potential drugs and experimental tools in enzymology. Mini Rev. Med. Chem. **7**: 813-820.

Klionsky, D. J., Emr, S. D. (2000) Autophagy as a regulated pathway of cellular degradation. Science **290**:1717-1721.

Knowlden, J. M., Hutcheson, I. R., Jones, H. E., Madden, T., Gee, J. M., Harper, M. E., Barrow, D., Wakeling, A. E., Nicholson, R. I. (2003) Elevated levels of epidermal growth factor receptor/c-Erb2 heterodimers mediate an autocrine growth regulatory pathway in tamoxifen-resistant MCF-7 cells. Endocrinology **144**:1032-1044.

Kuiper, G.G., Carlsson, B., Grandien, K., Enmark, E., Haggblad, J., Nilsson, S., Gustafsson, J. (1997) Comparison of the ligand binding specificity and transcript tissue distribution of estrogen receptors α and β. Endocrinology **138**:863-870.

Kuiper, G. G., Gustafsson, J. (1997) The novel estrogen receptor-β subtype: potential role in the cell- and promoter-specific actions of estrogens and anti-estrogens. FEBS Lett. **410**:87-90.

Kurian, A. W., Clarke, C. A., Carlson, R. W. (2009) The decline in breast cancer: real or imaginary. Curr. Oncol. Rep.**11**:21-28.

Kurokawa, H., Lenferink, A. E., Simpson, J. F., Pisacane, P. I., Sliwkowski, M. X., Forbes, J. T., Arteaga, C. L. (2000) Inhibition of HER2/new (Erb-2) and mitogen-activated protein kinases enhances tamoxifen action against HER2-overexpressing, tamoxifen-resistant breast cancer cells. Cancer Res. **60**:5887-5894.

Kwoh, D.Y., Coffin, C.C., Lollo, C.P., Jovenal, J., Banaszczyk M.G., Mullen, P., Phillips, A, Amini, A., Fabrycki, J., Bartholomew, R.M., Brostoff, S.W., Carlo, D.J. (1999) Stabilization of poly-L-lysine/DNA polyplexes for in vivo gene delivery to the liver. Biochim. Biophys. Acta **1444:**171-190.

Lacassagne, A. (1936) Hormonal pathogenesis of adenocarcinoma of the breast. Am. J. Cancer **27**:217-225.

Le, H. H., Carlson, E. M., Chua, J. P., Belcher, S. M. (2008) Bisphenol A is released from polycarbonate drinking bottles and mimics the neurotoxic actions of estrogen in developing cerebellar neurons. Toxicol. Lett. **176**:149-156.

Lerner, L. J., Holthaus, J. F., Thompson, C. R. (1958) A non-steroidal estrogen antagonist 1-(p-2-diethylaminoethoxyphenyl)-1-phenyl-2-p-methoxyphenylethanol. Endocrinology **63**:295-318.

Leveque J., Foucher, F., Bansard, J. Y., Havouis, R., Grall, J. Y., Moulinoux, J. P. (2000) Polyamine profiles in tumor, normal tissue of the homologous breast, blood, and urine of breast cancer sufferers. Breast Cancer Res. Treat. **60**:99-105.

Leveque J., Foucher, F., Havouis, R., Desury, D., Grall, J. Y., Moulinoux, J. P. (2000) Benefits of complete polyamine deprivation in hormone responsive and hormone resistant MCF-7 human breast adenocarcinoma in vivo. Anticancer Res. **20**:97-101.

Levin, E. R. (2001) Cell localization, physiology, and nongenomic actions of estrogen receptors. J. Appl. Physiol. **91**:1860-67.

Levin, E. R. (2002) Cellular functions of plasma membrane estrogen receptors. Steroids **67**:471-475.

Levine, B., Yuan, J. (2005) Autophagy in cell death: an innocent convict? J. Clin. Invest. **115**:2679-2688.

Lewandowski, S., Kalita, K., Kaczmarek, L. (2002) Estrogen receptor beta. Potential functional significance of a variety of mRNA isoforms. FEBS Lett. **524**:1-5.

Leygue, E., Dotzlaw, H., Watson, P. H., Murphy, L. C. (1998) Altered Estrogen Receptor Messenger RNA Expression during Human Breast Tumorigenesis. Cancer Res. **58**:3197-3201.

Liang, C., Ku, B., Dotan, I., Canaani, D., Oh, B., Jung, J. U. (2006) Autophagic and tumor suppressor activity of a novel Beclin1-binding protein UVRAG. Nat. Cell Biol. **8**:688-99.

Liang, X. H., Jackson S, Seaman M, Brown, K., Kempkes, B., Hibshoosh, H., Levine, B. (1999) Induction of autophagy and inhibition of tumorigenesis by beclin 1. Nature **402**:672-76.

Liang, X. H., Kleeman, L. K., Jiang, H. H., Gordon, G., Goldman, J. E., Berry, G., Herman, B., Levine, B. (1998) Protection against fatal Sindbis virus encephalitis by Beclin, a novel Bcl-2 interacting protein. J. Virol. **72**:8586-8596.

Liang, X. H., Yu, J., Brown, K., Levine, B. (2001) Beclin 1 contains a leucine-rich nuclear export signal that is required for its autophagy and tumor suppressor function. Cancer Res. **61**:3443-49.

Likhite, V. S., Stossi, F., Kim, K., Katzenellenbogen, B. S., Katzenellenbogen, J. A. (2006) Kinase-specific phosphorylation of the estrogen receptor changes receptor interactions with ligand, deoxyribonucleic acid, and coregulators associated with alterations in estrogen and tamoxifen activity. Mol. Endocrinol. **20**:3120-3132.

Liu, G., Molas, M., Grossmann, G.A., Pasumarthy, M., Perales, J.C., Cooper, M.J., Hanson, R.W. (2001) Biological properties of poly-L-lysine-DNA complexes generated by cooperative binding of the polycation. J. Biol. Chem. **275:**34379-34387.

Love, R. R. (2008) Defining a global research agenda for breast cancer. Cancer **113**:2366-2371.

Lupulescu, A. (1995) Estrogen use and cancer incidence: a review. Cancer Invest. **13**:287-95.

McEwan, I. J. (2009) Nuclear receptors: one big family. Methods Mol. Biol. **505**:3-18.

McClelland, R. A., Barrow, D., Madden, T. A., Dutkowski, C. M. (2001) Enhanced epidermalgrowth factor receptor signaling in MCF-7 breast cancer cells after long-term culture in the presence of the pure antiestrogen ICI 182,780 (Faslodex). Endocrinology **142**:2776-2788.

Maiuri, M. C., Zalckvar, E., Kimchi, A., Kroemer, G. (2007) Self-eating and self-killing: crosstalk between autophagy and apoptosis. Nat. Rev. Mol. Cell Biol. **8**:741-52.

Maria Fimia, G., Stoykova, A., Romagnoli, A., Giiunta, L., Di Bartolomeo, S., Nardacci, R., Corazzari, M., Fuoco, C., Ucar, A., Schwartz, P., Gruss, P., Piacentini, M., Chowdhury, K., Cecconi, F. (2007) Ambra1 regulates autophagy and development of the nervous system. Nat. Cell Biol. **447**:1121-1125.

Mandlekar, S., Yu, R., Tan, T. H., Kong, A. N. (2000) Activation of caspase-3 and c-Jun NH2-terminal kinase-1 signaling pathways in tamoxifen-induced apoptosis of human breast cancer cells. Cancer Res**. 60**:5995-6000.

Martin, G., Melito, G., Rivera, E. (1996) Effect of tamoxifen on intraperitoneal N-nitroso-N-methylurea induced tumors. Cancer Lett **100**:227-234.

Merdan, T., Kopecek, J., Kissel, T. (2002) Prospects for cationic polymers in gene and oligonucleotide therapy against cancer. Adv. Drug Deliv. Rev. **54:**715-758.

Meyskens, F. L., Gerner, E. W. (1999) Development of difluoromethylornithine (DFMO) as a chemoprevention agent. Clin. Cancer Res. **5**:945-951.

Milano, A., Lago, L. D., Sotiriou, C., Piccart, M., Cardoso, F. (2006) What clinicians need to know about antiestrogen resistance in breast cancer therapy. Eur. J. Cancer **42**:2692-2705.

Minchin, R. F., Knight, S., Arulpragasam, A., Fogel-Petrovic, M. (2006) Concentration-dependent effects of N^1, N^{11}-diethylnorspermine on melanoma cell proliferation. Int. J. Cancer **118**:509-512.

Moshier, J. A., Dosescu, J., Skunca, M., Luk, G. D. (1993) Transformation of NIH/3T3 cells by ornithine decarboxylase overexpression. Cancer Res. **53**:2618-2622.

Nishiskawa, M., Huang, L. (2001) Nonviral vectors in the new millennium: delivery barriers in gene transfer. Hum. Gene Ther. **12:**861-870.

O'Regan, R. M., Osipo, C., Ariazi, E., Lee, E. S., Meeke, K., Morris, C., Bertucci, A., Sarker, M. A., Grigg, R., Jordan, V. C. (2006) Development and therapeutic options for the treatment of Raloxifene-stimulated breast cancer. Clin. Cancer Res. **12**:2255-2263.

Oberstein A, Jeffrey PD, Shi Y. (2007) Crystal structure of the Bcl-XL-Beclin 1 peptide complex: Beclin 1 is a novel BH3-only protein. J Biol Chem **282**:13123-13132.

Okubo, S., Kurebayashi, J., Otsuki, T., Yamamoto, Y. (2004) Additive antitumour effect of the epidermal growth factor receptor tyrosine kinase ihibitor gefitinib (Iressa, AD 1839) and the antiestrogen fulvestrant (faslodex, ICI 182,780) in breast cancer cells. Br. J. Cancer **90**:236-244.

Osborne, C. K., Wakeling, A., Nicholson, R. I. (2004) Fulvestrant: an estrogen receptor antagonist with a novel mechanism of action. Br. J. Cancer **90**:S2-S6.

Patel, R. R., Sharma, C. G., Jordan, V. C. (2007) Optimizing the antihormonal treatment and prevention of breast cancer. Breast Cancer **14**:113-122.

Pattingre S, Tassa A, Qu X, Garuti, R., Liang, X. H., Mizushima, N., Packer, M., Schneider, M. D., Levine, B. (2005) Bcl-2 antiapoptotic proteins inhibit Beclin 1-dependent autophagy. Cell **122**:927-39.

Pearce, S. T., Jordan, V. C. (2004) The biological role of estrogen receptors α and β in cancer. Crit. Rev. Oncol. Hematol. **50**:3-22.

Perales, J.C., Grossmann, G.A., Molas, M., Liu, G., Ferkol, T., Harpst, J., Oda, H., Hanson, R. (1997) Biochemical and Functional Characterization of DNA Complexes Capable of Targeting Genes to Hepatocytes via the Asialoglycoprotein Receptor. J. Biol. Chem. **272:**7398-7407.

Perry, R. R., Kang, Y., Greaves, B. (1995) Effects of tamoxifen on growth and apoptosis of estrogen-dependent and –independent human breast cancer cells. Ann. Surg. Oncol. **2**:238-245.

Pike, A. C., Brzozowski, A. M., Hubbard, R. E. (2000) A structural biologist's view of the estrogen receptor. J. Steroid Biochem. Mol. Biol. **74**:261-268.

Plank, C., Tang, M.X., Wolfe, A.R., Szoka, F.C. (1999) Branched cationic peptides for gene delivery: role of type and number of cationic residues in formation and in vitro activity of DNA polyplexes. Hum. Gene Ther. **10:**319-332.

Poola, I., Koduri, S., Chatra, S., Clarke, R. (2000) Identification of twenty alternately spliced estrogen receptor alpha mRNAs in breast cancer cell lines and tumors using splice targeted primer approach. J. Steroid Biochem. Mol. Biol. **72**:249-58.

Porter, C. W., McManis, J., Casero, R. A., Bergeron, R. J. (1987) Relative abilities of bis(ethyl) derivatives of putrescine, spermidine, and spermine to regulate polyamine biosynthesis and inhibit L1210 leukemia cell growth. Cancer Res. 47:2821-2825.

Qu, X., Yu, J., Bhagat, G., Furuya, N., Hibshoosh, H., Troxel, A., Rosen, J., Eskelinen, E., Mizushima, N., Ohsumi, Y., Cattoretti, G., Levine, B. (2003) Promotion of tumorigenesis by heterozygous disruption of the Beclin 1 autophagy gene. J. Clin. Invest. **112**:1809-1820.

Qadir, M. A., Kwok, B., Dragowska, W. H., To, K. H., Le, D., Bally, M. B., Gorski, S. M. (2008) Macroautophagy inhibition sensitizes tamoxifen-resistant breast cancer cells and enhances mitochondrial depolarization. Breast Cancer Res. Treat. **112**:289-403.

Rasanen, T. L., Alhonen, L., Sinervirta, R., Keinanen, T,; Herzig, K.H., Suppola, S., Khomutov, A.R., Vepsalainen, J., Janne J. (2002) A polyamine analogue prevents acute pancreatitis and restores early liver regeneration in transgenic rats with activated polyamine catabolism. J. Biol. Chem. **277**:39867-39872.

Rastogi, T., Devesa, S., Mangtani, P., Mathew, A., Cooper, N., Kao, R., Sinha, R. (2008) Cancer incidence rates among South Asians in four different regions: India, Singapore, UK and US. Int. J. Epidemiol. **37**:147-60.

Riggins, R., Schrecengost, R. S., Guerrero, M. S., Bouton, A. H. (2007) Pathways to tamoxifen resistance. Cancer Lett. **256**:1-24.

Roodi, N., Bailey, L. R., Kao, W. Y., Verrier, C. S., Yee, C. J., Dupont, W. D., Parl, F. F. 1995) Estrogen receptor gene analysis in estrogen receptor-positive and receptor-negative primary breast cancer. J. Natl. Cancer Inst. **8**7:446-451.

Rubinsztein, D. C., Gestwicki, J. E., Murphy, L. O., Klionsky, D. J. (2007) Potential therapeutic applications of autophagy. Nat. Rev. Drug Discov. **6**:304-12.

Saito, H., Inazawa, J., Saito, S., Kasumi, F., Koi, S., Sagae, S., Kudo, R., Saito, J., Noda, K., Nakamura, Y. (1993) Detailed deletion mapping of chromosome 17q in ovarian and breast cancers: 2 cM region on 17q21.3 often and commonly deleted in tumors. Cancer Res. **53**:3382-3385.

Samaddar, J. S., Gaddy, V. T., Duplantier, J., Thandavan, S. P., Shah, M., Smith, M. J., Browning, D., Rawson, J., Smith, S. B., Barrett, J. T., Schoenlein, P. V. (2008) A role for macroautophagy in protection against 4-hydroxytamoxifen-induced cell death and the development of antiestrogen resistance. Mol. Cancer Ther. **7**:2977-2987.

Schiff, R., Massarweh, S. A., Shou, J., Bharwani, L., Arpino, G., Rimawi, M., Osborne, C. K. (2005) Advanced concepts in estrogen receptor biology and breast cancer endocrine resistance: implicated role of growth factor signaling and estrogen receptor coregulators. Cancer Chemother. Pharmacol. **56(Suppl. 1)**:s10-s20.

Shah, N., Antony, T., Haddad, S., Amenta, P., Shirahata, A.,Thomas, T. J., Thomas, T. (1999) Antitumor effects of bis(ethyl)polyamine analogs on mammary tumor development in FVB/NTgN (MMTVneu) transgenic mice. Cancer Lett. **146**: 15-23.

Shah, N., Thomas, T. J., Lewis, J. S., Klinge, C. M., Gelinas, C., Thomas, T. (2001) Regulation of estrogenic and nuclear factor κB function by polyamines and their role in polyamine analog-induced apoptosis of breast cancer cells. Oncogene **20**:1715-1729.

Shiau, A. K., Barstad, D., Loria, P. M., Cheng, L., Kushner, P. J., Agard, D. A., Greene, G. L. (1998) The structural basis of estrogen receptor/coactivator recognition and the antagonism of this interaction by tamoxifen. Cell **95**:927-937.

Simpson, E. R., Davis, S. R. (2001) Minireview: aromatase and the regulation of estrogen biosynthesis – some new perspectives. Endocrinology **142**:4589-4594.

Streiff, R. R., Bender, J. F. (2001) Phase I study of N^1 -N^{11}- diethylnorspemine (DENSpm) administered TID for 6 days in patients with advanced malignancies. Invest. New Drugs **19**:29-39.

Takimoto, G. S., Graham, J. D., Jackson, T. A., Tung, L., Powell, R. L., Horwitz, L. D., Horwitz, K. B. (1999) Tamoxifen resistant breast cancer: coregulators determine the direction of transcription by antagonist-occupied steroid receptors. J. Steroid Biochem. Mo. Biol. **69**:45-50.

Tang, M.X., Szoka, F.C. (1997) The influence of polymer structure on the interactions of cationic polymers with DNA and morphology of the resultant complexes. Gene Ther. **4:** 823-832.

Thomas, T., Balabhadrapathruni, S., Gallo, M. A., Thomas, T. J. (2002) Development of polyamine analogs as cancer therapeutic agents. Oncol. Res.**13**:123-135.

Thomas, T., Thomas, T. J. (2003) Polyamine metabolism and cancer. J. Cell Mol. Med. **2**:113-126.

Thurlimann, B., Keshaviah, A., Coates, A. S., Mouridsen, H., Mauriac, L., Forbes, J. F., Paridaens, R., Catiglione-Gertsch, M., Gelber, R. D., Rabaglio, M., Smith, I., Wardly, A., Price, K. N., Godhirsch, A. (2005) BIG (Breast International Group), Group I-C: A comparison of letrozole and tamoxifen in postmenopausal women with early breast cancer. N. Engl. J. Med. **353**:2747-2757.

Tzukerman, M. T., Esty, A., Santiso-Mere, D., Danielian, P., Parker, M. G., Stein, R. B., Pike, J. W., McDonnell, D. P. (1994) Human estrogen receptor transactivational capacity is determined by both cellular and promoter context and mediated by two functionally distinct intramolecular regions. Mol. Endocrinol. **8**:21-30.

Van den Berg, H. W., Lynch, M., Martin, J., Nelson, J., Kickson, G. R., Crockard, A. D. (1989) Characterization of a tamoxifen-resistant variant of the ZR-75-1 human brast cancer cell line (ZR-75-8a1) and ability of the resistant phenotype. Br. J. Cancer **59**:522-526.

Varnado, B. L., Voci, C. J., Meyer, L. M., Coward, J. K. (2000) Circular dichroism and NMR studies of metabolically stable alpha-methylpolyamines: Spectral comparison with naturally occurring polyamines. Bioorg. Chem. **28**:395-408.

Vijayanathan, V., Thomas, T., Thomas, T.J. (2002) DNA nanoparticles and development of DNA delivery vehicles for gene therapy. Biochemistry **41:**4085-14094.

Vijayanathan, V., Venkiteswaran, S., Nair, S. K., Verma, A., Thomas, T. J., Zhu, B. T., Thomas, T. (2006) Physiologic levels of 2-methoxyestradiol interfere with nongenomic signaling of 17beta-estradiol in human breast cancer cells. Clin. Cancer Res. **12**:2038-48.

Vogel, V. G., Constantino, J. P., Wikerham, D. L., Cronin, W. M., Cecchini, R. S., Atkins, J. N., Bevers, T. B., Fehrenbacher, L., Pajon, E. R. Jr, Wade, J. L., Robidoux, A., Margolese, R. G., James, J., Lippman, S. M., Runowicz, C. D., Ganz, P. A., Reis, S. E., McCaskill-Stevens, W., Ford, L. G., Jordan, V. C., Wolmark, N.; National Surgical Adjuvant Breast and Bowel Project (NSABP). (2006) Effects of Tamoxifen vs Raloxifene on the risk of developing invasive breast cancer and other disease outcomes: The NSABP study of tamoxifen and raloxifene (STAR) P-2 Trial. JAMA **295**:2727-2741.

Wadhwa, M. S., Collard, W. T., Adami, R. C., McKenzie, D. L., Rice, K. G. (1997) Peptide-mediated gene delivery: influence of peptide structure on gene expression. Bioconjug. Chem., **8**, 81-88.

Wagner E. Polylysine-conjugate based DNA delivery, in Self-assembling complexes for Gene Delivery (Editors: Kabanov, A.V., Felgner, P.L., Seymour, L.W.) (1998) John Wiley & Sons 2nd Ed.:309-322.

Walter, P., Green, S., Green, G. Krust, A., Bornert, J., Jeltsch, J., Staub, A., Jensen, E., Scrace, G., Waterfield, M., Chambron, P. (1985) Cloning of the human estrogen receptor cDNA. Proc. Natl. Acad. Sci. USA **82**:7889-7893.

Wardley, A. M. (2002) Fulvestrant: a review of its development, preclinical and clinical data. Int. J. Clin. Pract. **56**:305-309.

Webb, P., Nguyen, P., Shinsako, J., Anderson, C., Feng, W., Nguyen, M. P., Chen, D., Huang, S. M., Subramanian, S., McKinerney, E., Katzenellenbogen, B. S., Stallcup, M. R., Kushner, P. J. (1998) Estrogen receptor activation function 1 works by binding p160 coactivator proteins. Mol. Endocrinol**. 11**:657-666.

Wijayratne, A. L., Nagel, S. C., Paige, L. A., Christensen, D. J., Norris, J. D., Fowlkes, D. M., McDonnell, D. P. (1999) Comparative analyses of mechanistic differences among antiestrogens. Endocrinology **140**:5828-5840.

Witorsch, R. J. (2002) Endocrine disruptors: can biological effects and environmental risks be predicted? Regul. Toxicol. Pharmacol. **36**:118-130.

Wolfert, M.A., Seymour, L.W. (1996) Atomic Force Microscopic Analysis of the Influence of the molecular weight of poly(L)lysine on the size of polyelectrolyte complexes formed with DNA. Gene Ther. **3:**269-273.

Wolff, A. C., Armstrong, D. K., Fetting, J. H., Carducci, M. K., Riley, C. D., Bender, J. F., Casero, R. A., Davidson, N. E. (2003) A Phase II study of the polyamine analog N^1,N^{11}-diethylnorspemine (DENSpm) daily for five days every 21 days in patients with previously treated metastatic breast cancer. Clin. Cancer Res. **9**:5922-5928.

Yager, J. D., Davidson, N. E. (2006) Estrogen Carcinogenesis in Breast Cancer. N. Engl. J. Med. **354**:270-282.

Yue, W., Santen, R. J., Wang, J. P., Li, Y., Verderame, M. F., Bocchinfuso, W. P., Korach, K. S., Devanesan, Pl, Todorovic, R., Rogan, E. G., Cavalieri, E. L. (2003) Genotoxic metabolites of estradiol in breast: potential mechanisms of estradiol induced carcinogenesis. J. Steroid Biochem. Mol. Biol. **86**:477-486.

Zhang, Q. X., Borg, A., Wolf, D. M., Oesterreich, S., Fuqua, S. A. (1997) An estrogen receptor mutant with strong hormone-independent activity from a metastatic breast cancer. Cancer Res. **57**:1244-1249.

Zhong, Y., Wang, Q. J., Li, X., Yan, Y., Backer, J. M., Chait, B. T., Heintz, N., Yue, Z. (2009) Distinct regulation of autophagic activity by Atg14L and Rubicon associated with Beclin 1-phoshatidylinositol 3-kinase complex. Nat. Cell Biol. Epub ahead of print.

Chapter 1

Regulation of Estrogenic Effects by Beclin 1 in Breast Cancer Cells

Shali John*, Irina Nayvelt*, Hui-Chen Hsu, PingAr Yang, Wensheng Liu,
Gokul Das, Thresia Thomas, and T. J. Thomas

*Joint First Authors
Cancer Research (2008), 68:7855-7863.

Abstract

Beclin 1 is an essential mediator of autophagy and a regulator of cell growth and cell death. We examined the effect of Beclin 1 overexpression on the action of estradiol (E_2) and 2 antiestrogens, raloxifene and 4-hydroxytamoxifen, in estrogen receptor α (ERα)-positive MCF-7 breast cancer cells. [^{3}H]-thymidine incorporation studies showed that Beclin 1 overexpressing cells (MCF-7.beclin) had a lower proliferative response to E_2 compared to cells transfected with vector control (MCF-7.control). There was only a 35% increase in [^{3}H]-thymidine incorporation, after 24 h of E_2 treatment of MCF-7.beclin cells compared to untreated cells, whereas this increase was 2-fold for MCF-7.control cells. E_2-induced changes in the expression of early-response genes were examined by real-time quantitative polymerase chain reaction (qPCR). There were significant differences in the pattern of expression of E_2-induced genes, c-myc, c-fos, Erg-1, and Nur77 between MCF-7.beclin and MCF-7.conrol cells, 2 h after treatment. While E_2-induced growth of MCF-7.control cells was completely inhibited by 500 nM raloxifene or 500 nM 4-hydroxytamoxifen, these concentrations of antiestrogens had no significant effect on the growth of MCF-7.beclin cells. Confocal microscopic and co-immunoprecipitation studies showed evidence for co-localization and association of Beclin 1 and ER$\tilde{\alpha}$ In addition, E_2 caused a decrease in Akt phosphorylation in MCF-7.beclin cells, compared to a 3-fold increase in MCF-7 cells, 5 min after treatment. These results indicate that Beclin 1 can down-regulate estrogenic signaling and growth response, and contribute to the development of antiestrogen resistance. This observation might be useful to define and overcome antiestrogen resistance of breast cancer.

Introduction

Beclin 1 is an essential gene in autophagy, a cell survival pathway that enables utilization of long-lived proteins as a source of amino acids under conditions of nutritional deprivation (1-4). In autophagy, Beclin 1 interacts with class III PI3 kinase (vps34) during autophagosomal membrane engulfing of damaged cytoplasmic organelles and long-lived proteins. Autophagy can

facilitate cell survival, delaying apoptotic death (5, 6). Alternatively, autophagy can facilitate a form of cell death referred to as autophagic or type II programmed cell death, characterized by autophagic vacuoles in the cytoplasm (7). Autophagy and Beclin 1 are important in the balance of breast cancer cell growth and death (8, 9). The function of Beclin 1 is, in part, defined by its interaction with the anti-apoptotic gene products, Bcl-2 and Bcl-xL (8, 9). Beclin 1 is also a tumor suppressor gene since one allele of Beclin 1 is lost in subsets of breast, prostate, and other tumors (10). Overexpression of Beclin 1 in MCF-7 breast cancer cells reduced tumorigenicity in nude mice (11). These results raise questions on molecular pathways by which Beclin 1 modifies estrogenic function in breast cancer.

Estrogens function through the receptors, ERα and ERβ, the ligand-activated transcription factors controlling the growth of ER-positive breast tumors and target tissues (12, 13). ERα mediates the proliferative stimulus of E_2 on ER-positive breast cancer cells, whereas ERα suppresses cell proliferation (14). Estrogenic ligands alter the conformation of ERs such that ERs recruit co-regulatory proteins to the promoter/enhancer sites of responsive genes to facilitate transcription (12, 13, 15). ER-recognition of estrogen response element and associated changes in chromatin stimulate a cell- and tissue-specific network of genes, enabling E_2 to exert multiple functions. In addition, estrogenic action includes nongenomic mechanism(s), involving membrane ERs and activation of kinase cascades in association with G protein coupled receptors or growth factor receptors (15-17).

Cell signaling through the ERα is pivotal to the regulation of breast cancer cell growth so that the ERα antagonist, tamoxifen, is the first targeted breast cancer therapeutic agent (18). 4-Hydroxytamoxifen is an active metabolite of tamoxifen, with higher affinity for ERα than tamoxifen (19). Although tamoxifen is initially effective against ERα positive tumors, resistance develops in most women (20). The agonistic activity of tamoxifen on uterine cells is also a cause for concern (21). Raloxifene is an antiestrogen with mixed agonist/antagonist activity, in a tissue specific manner (22, 23). Raloxifene is an agonist capable of enhancing bone density, whereas it is an antagonist on breast epithelial cells and the reproductive system. Understanding the basis of agonist activity of antiestrogens is an important aspect of overcoming antiestrogen resistance.

For a subset of ERα-positive tumors, cell growth is totally dependent on ERα (12, 13). Functions of ERα as a transcription factor and its ability to bind to accessory proteins and co-regulators are critical to the control of cancer cell growth (12, 13). Since Beclin 1 inhibited E_2-dependent MCF-7 tumor growth in immuno-deficient mice (10), an interaction between ERα signaling and Beclin 1 function appeared possible. We, therefore, examined the consequences of Beclin 1 overexpression on E_2-induced cell growth and cell signaling. We found that E_2-induced cell signaling and gene expression are modified by Beclin 1 and that an interaction of ERα and Beclin 1 might be involved in the inhibition of estrogenic cell signaling.

Materials and Methods

MCF-7 cell line was obtained from the American Type Culture Collection (Monasses, VA). We obtained MCF7.beclin cells expressing Beclin 1 from a tetracycline-repressible promoter (pTRE/flag-beclin 1) (11), and a control cell line containing empty vector (MCF7.control) from Dr. Beth Levine (University of Texas Southwestern Medical Center, Dallas, TX). Dulbecco's modified Eagles medium (DMEM), phenol red-free DMEM, fetal bovine serum (FBS), and anti-β-actin antibody were from Sigma Chemical Co. (St. Louis, MO). Antibiotics, trypsin, and other additives for cell culture medium were purchased from Invitrogen (Carlsbad, CA). Anti-Beclin 1, anti-phospho-Akt, anti-Akt, anti-pERK and anti-phospho-ERK antibodies were purchased from Cell Signaling Technology (Beverly, MA). Anti-ERα antibody was from Santa Cruz Biotechnology (Santa Cruz, CA). Secondary antibodies conjugated with Alexa Fluor 633 or Alexa Fluor 488 were from Invitrogen.

Cell Culture. MCF-7 cells were maintained in DMEM, supplemented with 100 units/ml penicillin, 100 µg/ml streptomycin, 40 µg/ml gentamycin, 2 µg/ml insulin, 0.5 mM sodium pyruvate, 50 mM nonessential amino acids, 2 mM L-glutamine, and 10% fetal bovine serum (FBS). MCF-7.control and MCF7.beclin 1 cells were maintained in DMEM supplemented with 10% FBS, 40 µg/ml gentamycin, 5 mg/ml G418, 2 µg/ml insulin, 200 µg/ml hygromycin and 2 µg/ml tetracycline. Prior to each experiment, cells were grown for 3 days in phenol red-free DMEM containing serum treated with dextran-coated charcoal (DCC) to remove serum-derived estrogenic compounds

(16). MCF-7.beclin cells were grown for 3 days in phenol red free DMEM without tetracycline, prior to plating under phenol red-free conditions.

[^{3}H]-Thymidine Incorporation. Cells (0.5 x 10^6) were seeded in 6-well culture plates in phenol red-free DMEM supplemented with DCC treated serum and additives. After 24 h of plating, cells were treated with 4nM E_2. DNA synthesis was measured by adding 4 μCi/ml of [^{3}H]-thymidine, 1 h prior to harvest (24). Cells were treated with 5% trichloroacetic acid followed by 1 N NaOH, and 1 N HCl. The radioactive thymidine in cellular DNA was quantified by liquid scintillation counting.

Cell Proliferation. MCF-7.beclin cells were seeded at a density of 5 x 10^4 cells/well in 24-well plates, in the presence of tetracycline in phenol red-free medium. A parallel study was set up with MCF-7.beclin cells without tetracycline. Cells were dosed 24 h after plating with 4 nM E_2, and re-dosed after 48 h. After appropriate treatment periods, live cells were counted using the trypan blue exclusion, using a hemocytometer.

CellTiter Glo assay. This assay measures cell viability by level of ATP content (25). Cells (5 x 10^3/well) were plated in 96-well plates. E_2/antiestrogens were added 24 h after plating. Cells were re-dosed with medium change at 48 h after the first dose. After 96 h, cells were treated with 0.1 ml of CellTiter Glo (Promega, Madison, WI) reagent, incubated for 5 min at 22 ^{o}C and luminescence recorded using a GloMax Luminometer (Promega).

qPCR. MCF-7.beclin-1 or MCF-7.control cells (1 x 10^6) were seeded in 60 mm culture dishes. After 24 h, cells were treated with E_2 (4 nM) for 0, 1 or 2 h. RNA was isolated using Trizol reagent (Invitrogen) and 2 μg RNA was reverse-transcribed using the first strand cDNA synthesis kit (Fermentas, Inc., Glen Burnie, MD) with random hexamers as primers. The expression of Tff1 (pS2), c- myc, c-fos, Erg-1, Nur77, and Gapdh genes was determined by real-time PCR using the SYBR Green PCR Master Mix (Bio-Rad) with the following primers: 5'-CAATGGCCACCATGGAGAAC-3' and 5'-AACGGTGTCGTCGAAACAGC-3' for Tff1 (188 bp); 5'-CTCCTCACAGCCCACTGGTC-3' and 5'-CTTGGCAGCAGGATAGTCCTTC-3' for c-Myc (101 bp); 5'-CGGGCTTCAACGCAGACTA-3' and 5'- GGTCCGTGCAGAAGTCCTG-3' for c-Fos (147 bp); 5'- ACCTGACCGCAGAGTCTTTTC-3' and 5'-GCCAGTATAGGTGATGGGGG-3' for Erg-1 (110 bp); 5'-CGCACAGTGCAGAAAAACG-3' and 5'- TGTCTGTTCGGACAACTTCCTT-3' for

Nur77 (145 bp) ; and 5'-CATGAGAAGTATGACAACAGCCT-3' and 5'-AGTCCTTCCACGATACCAAAGT -3' for Gapdh (113 bp). A final volume of 25 μl was used for qPCR in an IQ5^{TM} thermocycler (Bio-Rad). Amplification conditions were 95 °C for 3 min, followed by 40 cycles of 95 °C for 15 s and annealing for 30 s (57 °C for Tff1 and 55 °C for other genes). qPCR products were normalized relative to that of Gapdh to correct for differences in template input. Results are expressed as fold differences in expression of the indicated gene relative to that of Gapdh. Standard curves were generated for every target using six 4-fold serial dilutions.

Confocal Microscopy. Cells were plated in Labtek 6-well slide chamber and dosed after 24 h (16). Cells were fixed in 4% paraformaldehyde, blocked in normal goat serum (5%) in PBS, followed by incubation with anti-ERα antibody (mouse) and anti-Beclin 1 antibody (rabbit) in 2.5% goat serum in PBS. After washing, cells were incubated with appropriate secondary antibodies. Alexa Flour 633 conjugated anti-mouse IgG was used for ERα (deep red) and Alexa Fluor 488 conjugated anti-rabbit igG (green) was used for Beclin 1. Experiments were repeated using Alexa Fluor 488 conjugated anti-mouse IgG for detecting ERα (green) and Alexa Fluor 633 conjugated anti-rabbit IgG for detecting Beclin 1 (red). Nuclei were stained with DAPI (4'6'-diamidino-2-phenylindole, 1 nM). Images were recorded using a Zeiss 510 Laser scanning microscope with a 60X objective at identical intensity settings for all treatment groups. No fluorescence was detected when cells were treated with fluorescence labeled secondary antibody alone.

Immunoprecipitation. Cells (1.5 x 10^6/60 mm dish) were plated in dishes and allowed to attach for 24 h prior to treatments. After the specified treatments, cells were harvested and cell pellet lysed in buffer containing 50 mM Tris.HCl (pH 7.4), 150 mM NaCl, 1% Triton, 5 mM EDTA, 25 mM sodium fluoride, 25 mM sodium pyrophosphate, 2 mM sodium vanadate, 5% glycerol, 1 mM phenylmethylsulphonyl fluoride and 1 X protease inhibitor cocktail (Calbiochem, San Diego, CA) (26). Cell lysate (100 μg in 100 μl lysis buffer) was pre-cleared with Protein A/G agarose and incubated with 10 μl of anti-ERα (mouse monoclonal) antibody for 16 h at 4 °C. Reaction mixture was incubated with protein A/G-Sepharose for 1 h at 4 °C. Sepharose beads were washed 3

times with cold lysis buffer, extracted using Laemelli buffer and loaded on 12% SDS polyacrylamide gel for immunoblot analysis.

Western blot analysis. Cells (1.5 x 10^6/60 mm dish) were plated in dishes and allowed to attach for 24 h prior to treatments. After the specified treatments and time periods, cells were harvested and cell pellet was lysed in buffer (16). Proteins (25 µg) were separated on a 12% SDS-polyacrylamide gel, transferred to PVDF Polyscreen membrane and incubated with 1:200 to 1:1000 dilution of the primary antibody. Protein bands were visualized using horseradish peroxidase-conjugated secondary antibody (Santa Cruz Biotechnology, Santa Cruz, CA) and SuperSignal West Peco Chemiluminescent Substrate (Pierce, Woburn, MA). Membranes were stripped in stripping buffer (62.5 mM Tris.HCl, (pH 6.8), 2% SDS, 100 mM (fresh) β-mercaptoethanol) and washed 3 times in washing buffer (20 mM Tris.HCl (pH 7.6), 150 mM NaCl, and 0.05% Tween 20). A second primary antibody was then added and the membrane re-probed as needed. To verify equal protein loading, membranes were stripped and re-blotted with anti-β-actin antibody. Lightly exposed Kodak XAR Biomax films were scanned using an Epson B4 Scanner and band intensities quantified using the NIH Image J 1.34S program. Fold-changes in the intensity of the protein signals reported are the mean of the results from 3 experiments.

Chromatin immunoprecipitation assay (ChIP). ChIP assay was performed as described previously (27) with minor modifications. Cells ($8x10^6$) in 10 cm dishes were washed once with PBS and crosslinked with 1.5% formaldehyde at 37 °C for 10 minutes. After washing with PBS, cells were collected in 1.6 ml of lysis buffer (0.5% SDS, 5.6 mM EDTA, 33 mM Tris.HCl, pH8.1, 0.5% Triton X-100, 84 mM NaCl) and incubated on ice for 30 min. Cell lysate was sonicated using Sonicator 3000 (Misonix, NY). Samples were diluted 5-fold with dilution buffer (0.01% SDS, 1.2 mM EDTA, 16.7 mM Tris.HCl, pH 8.1, 1.1% Triton X-100, 167 mM NaCl) and then pre-cleared with salmon sperm DNA/Protein A agarose for 2 hours at 4 °C. anti-ERα antibody (5 µg) or rabbit IgG (Santa Cruz) was used to immunoprecipitation from 200 µg of protein. Immunoprecipitated DNA was amplified by PCR using AccuPrime TaqDNA polymerase and visualized with ethidium bromide staining. The following primers from pS2 promoter were used: 5'-

CTAGACGGAATGGGCTTC ATG-3' (forward) and 5'-TCCTCCAACCTG ACCTTAATCC-3' (reverse).

Statistical Analysis. All experiments were repeated at least three times. Statistical difference between control and treatment groups was determined by one-way ANOVA followed by Dunnet's post-test using SigmaStat statistical program. $P < 0.05$ was considered to be statistically significant.

Results

We tested the effect of E_2 on MCF-7.beclin cells that expressed Beclin 1 from a tetracycline-repressible promoter. MCF-7 cells transfected with control plasmid (MCF-7.control) were also treated with E_2 in the same manner. Cells were plated in 6-well plates and E_2 added 24 h later at 0.1 or 4 nM concentrations. At the time of dosing, 62 ± 3% of the cells were in the G1 phase, as determined by flow cytometry with propidium iodide staining. [^{3}H]-thymidine incorporation assay was conducted 24 and 48 h after E_2 treatment. Figure 2 (A & B) shows a comparison of E_2-induced DNA synthesis in MCF-7.beclin and MCF-7.control cells. MCF-7.control cells showed maximal DNA synthesis in the presence of 4 nM E_2 after 48 h of treatment. The level of DNA synthesis in E_2-treated cells was approximately 2.5-fold higher than that of untreated cells at the same time point. In contrast, Beclin 1 transfected cells showed only 75% increase in DNA synthesis at the 48 h time point in the presence of 4 nM E_2. At the 24 h time point, MCF-7.control cells showed a 2-fold increase in DNA synthesis due to E_2 treatment. However, only 35% increase in DNA synthesis was observed in MCF-7.beclin cells. To verify the level of Beclin 1 protein expression in MCF-7.beclin cells, Western immunoblots were conducted using Beclin 1 antibody. Our result (Figure 2C) showed that MCF-7.beclin cells had a 5-fold higher level of Beclin 1 compared to MCF-7.control cells, as expected from its over expression due to transfection.

We next examined E_2-induced changes in the expression of early response genes in MCF-7 control and MCF-7.beclin cells. As shown in Figure 1D, there were significant changes in the pattern of expression of E_2-induced genes between

MCF-7.beclin cells and MCF-7.conrol cells. As expected from the E_2 sensitivity of MCF-7.control cells, there was 2- to 3.5-fold higher levels of transcripts of Tff1, c-myc, c-fos, and Nur77 in these cells, after 2 h of E_2 treatment, compared to those of untreated cells. In contrast, only c-myc mRNA level showed a moderate increase at 2 h after E_2 treatment in MCF-7.beclin cells, while c-fos, Erg-1 and Nur77 mRNAs decreased, compared to those of untreated cells. All of the tested mRNAs showed lower levels in E_2-treated MCF-7.beclin cells, compared to E_2-treated MCF-7.control cells. These results indicate that the reduction of E_2-induced DNA synthesis in MCF-7.beclin cells is associated with altered expression of early-response genes.

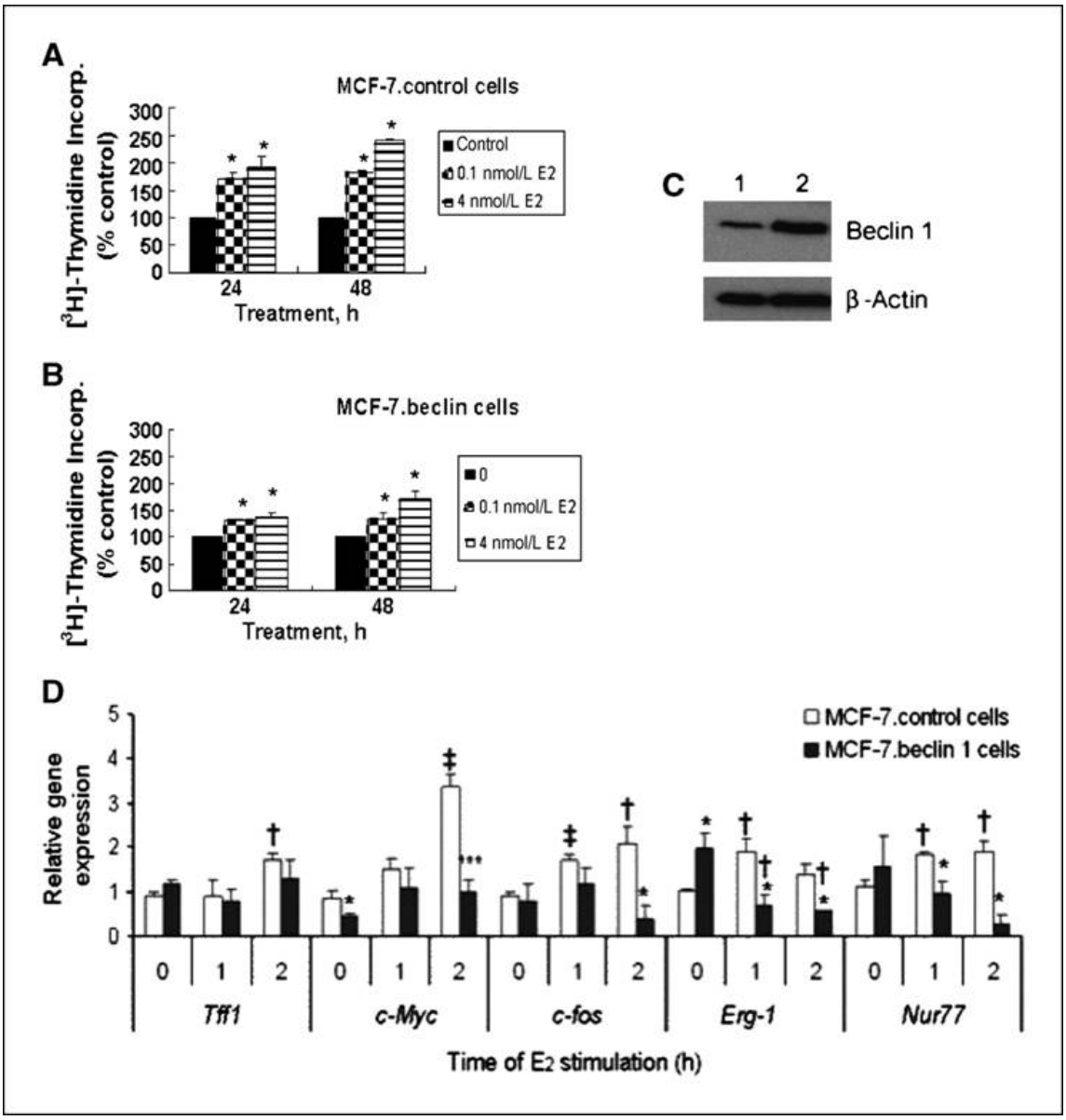

Figure 2. E_2-induced growth response of MCF-7.control and MCF-7.beclin cells. Cells growing in the absence of phenol red and tetracycline for 3 days were seeded in 6-well tissue culture plates at a density of 5 x10^5 cells/well with 3 ml medium. After 24 h, cells were treated with 0.1 or 4 nM E_2. [^{3}H]-thymidine was added 24 (A) or 48 h (B) after E_2-treatment, and cells harvested for scintillation counting 1 h after the addition of [^{3}H]-thymidine. Results are the mean ± SEM from 3 experiments. * Indicates statistical significance ($P < 0.05$), compared to the control. (C) Western blot analysis of Beclin 1 in MCF-7.control and MCF-7.beclin cells. Western immunoblots were conducted using anti-Beclin 1 antibody, followed by stripping and re-probing with anti-□-actin antibody. Results are representative of two different experiments. (D) qPCR analysis showing the effects of E_2 (4 nM) on the expression of the indicated gene in MCF7.control and MCF7.beclin cells at 0, 1, and 2 hr time points (n=3 per time point per group; *$p<0.05$, ***$p<0.005$ for the comparison of MCF-7.control vs MCF-7.beclin 1 cells at the same time point; $^{\dagger}p<0.05$, $^{\ddagger}p<0.005$ for the comparison of baseline versus E_2 stimulation in the same cell line, at the indicated time points.

E_2 is known to induce Akt phosphorylation as a part of non-genomic mechanism of action of ERα (16, 28, 29). We, therefore, examined whether E_2 response is modified in MCF-7.beclin cells. Cells were treated with 4 nM E_2 for 5, 10, 20, and 30 min. Cells were harvested and phospho-Akt levels determined by Western blots. We found a decrease in Akt phosphorylation in MCF-7.beclin cells treated with E_2, compared to untreated cells (Figure 3). In contrast, in MCF-7 cells, treatment with E_2 resulted in a 3-fold increase in Akt phosphorylation, 5 min after its addition (Figure 3). We also determined the levels of total Akt and phospho-ERK1/2 in MCF-7.beclin and control MCF-7 cells. While there was no change in the level of total Akt, p-ERK1/2 showed an increase, 10 min after E_2 treatment, in MCF-7.beclin and wild type cells. The level of β-actin was comparable in all lanes. These results indicate while E_2-induced Akt phosphorylation is down-regulated in the presence of Beclin 1 overexpression, increase in ERK1/2 phosphorylation remained intact.

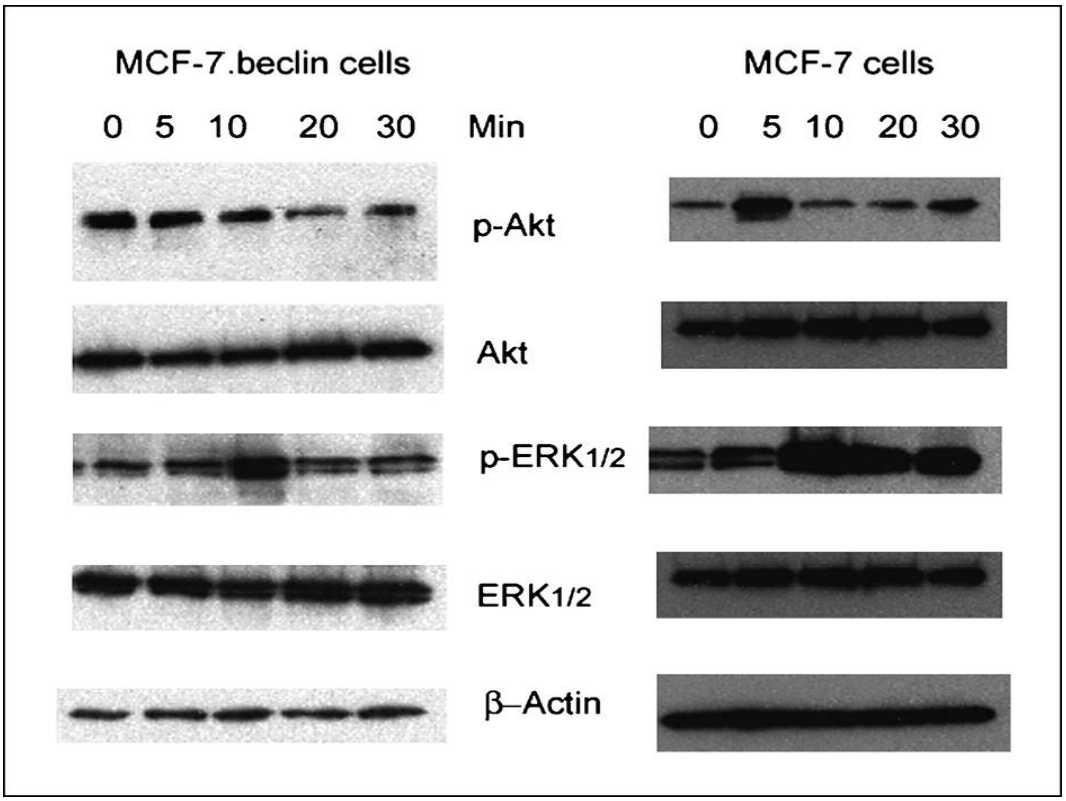

Figure 3. Effect of E_2 on Akt phosphorylation in MCF-7.beclin cells and MCF-7 cells. Cells (1.5 $x10^6$) were plated in 60 mm dishes and treated with 4 nM E_2. Cells were harvested after 5, 10, 20, and 30 min after E_2 treatment. Cellular extract was analyzed by Western blots using antibodies specific to phosphorylated (Ser-473) Akt, followed by sequential probing with antibodies specific to total Akt, phospho-ERK1/2, total ERK1/2, and β-actin. Similar results were obtained in 3 separate experiments.

We next examined the long-term effects of E_2, raloxifene and 4-hydroxytamoxifen, on MCF-7.beclin and MCF-7.control cells using CellTiterGlo assay. Cells were treated with E_2 or antiestrogens for 48 or 96 h. Assay at 96 h provided maximal responses to E_2 and antiestrogens. Our results (Figure 4) show that the presence of E_2 increased the luminescence of MCF-7.control cells by 2-fold, whereas there was only a 33% increase in luminescence in MCF-7.beclin cells. Raloxifene and 4-hydroxytamoxifen inhibited E_2 induced growth of MCF-7.control cells at 500 nM. In MCF-7.beclin cells, raloxifene had no significant effect even at 1000 nM. With 4-hydroxytamoxifen, E_2-induced proliferative response of MCF-7.beclin cells was not affected at 500 nM 4-hydroxytamoxifen, but it was inhibited at 1000 nM. However, the basal proliferation of

MCF-7.beclin cells or MCF-7.control cells in the absence of E_2 was not affected by these antiestrogens.

As an additional control for the effects of E_2 and antiestrogens in the absence of Beclin 1 overexpression, we studied MCF-7.beclin cells in the presence of tetracycline. E_2 response of cells containing tetracycline was similar to that of MCF-7 cells and antiestrogens suppressed the proliferative effect. However, when cells were treated with 4-hydroxytamoxifen and raloxifene in the absence of E_2, there was a 30 to 40% increase in proliferation, indicating that MCF-7.control and MCF-7.beclin cells containing tetracycline have some differences in antiestrogen responses.

We also examined E_2-induced response of MCF-7.beclin cells by trypan blue exclusion, using a hemocytometer (Figure 4B). Experiments were conducted in the presence and absence of tetracycline. After 48 h, E2 treatment induced only 20 to 30% increase in cell number, regardless of the presence of tetracycline. By 4 days, E_2 treatment of MCF-7.beclin cells showed a 2.5-fold increase in cell number in the presence of tetracycline. However, there was only about 50% increase in cell number in MCF-7.beclin cells in the absence of tetracycline. This result validates our findings on the influence of Beclin 1 on E_2 response, detected by CellTiter Glo assay.

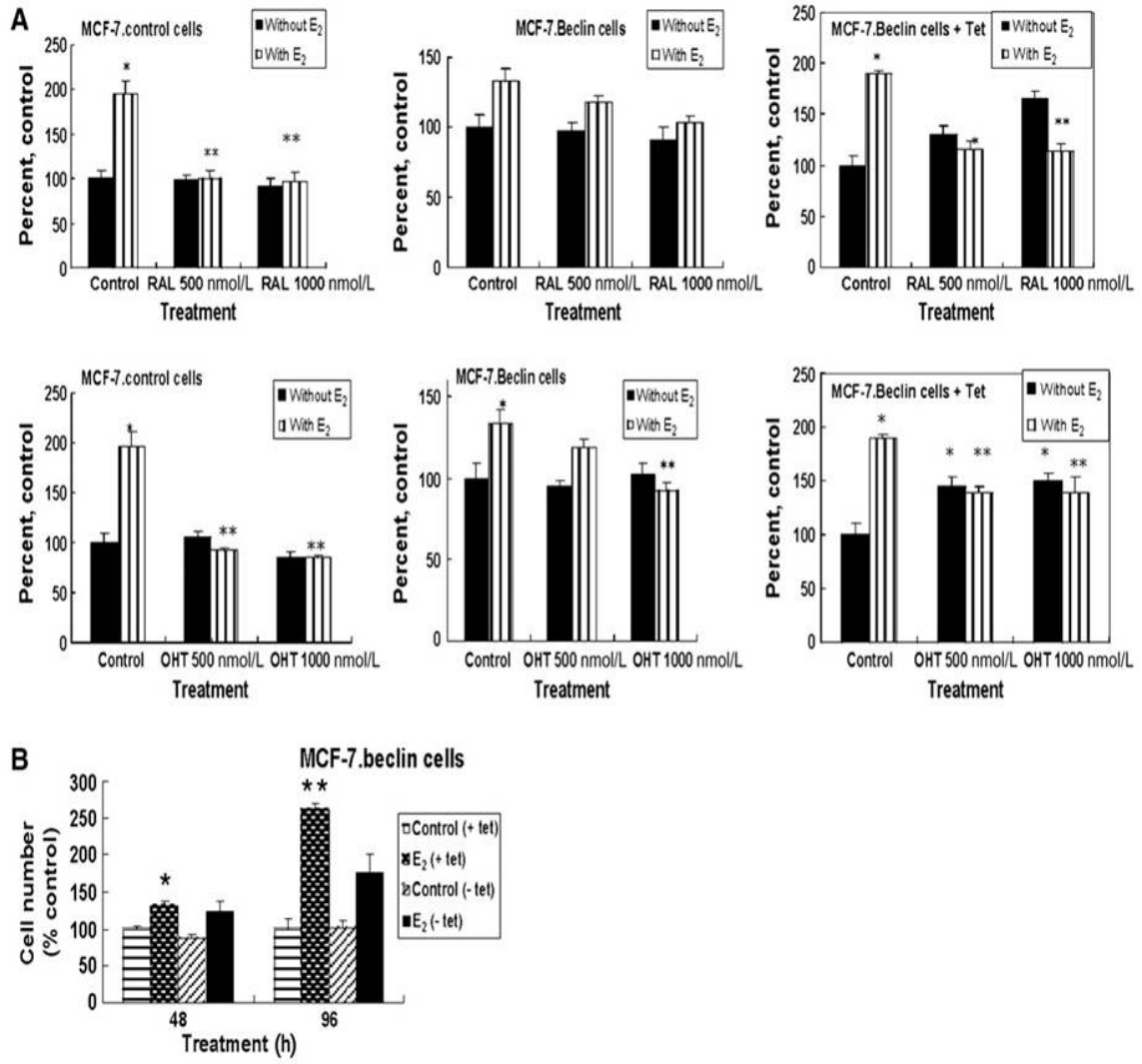

Figure 4. (A) Effects of E_2 and antiestrogens on the viability of MCF-7.control and MCF-7.beclin cells, and MCF-7.beclin cells containing tetracycline by CellTiter Glo assay. Cells were seeded in 96-well plates at a density of 5,000 cells/well in 0.1 ml medium. E_2, raloxifene (RAL), or 4-hydroxytamoxifen (OHT) were added 24 h after plating cells, at the indicated concentrations. Medium was withdrawn and cells were re-dosed 48 h after the first dose. After 96 h of treatment, cells were harvested by treatment with 0.1 ml of CellTiter Glo reagent. Luminescence was measured using Promega Glomax Lumniometer. Relative light units (RLU) were corrected for background, using readings of an equivalent amount of cell culture medium without cells. Values of RLU for control groups of MCF-7.beclin and MCF-7.control cells were in the range of 8 - 12 x 10^6 RLU. Results are the mean ± SEM from 3 experiments. RAL, raloxifene; OHT, 4-hydroxytamoxifen; *Statistical significance ($P < 0.05$) compared to the control; ** Statistical significance ($P < 0.05$) compared to E_2 treatment group. (B) Effect of E_2 on the growth of MCF-7.beclin cells in the presence and absence of tetracycline. Cells were allowed to grow in phenol red free medium for 3 days before plating in 24-well plates. Cell number was determined by trypan blue exclusion assay using a hemocytometer. Results are the mean and ± SEM from 3 experiments. *, **Indicates statistical significance compared to E_2 treatment group (* $P < 0.05$; ** $P < 0.001$).

ERα is known to re-distribute within the cell following the addition of E_2 (16, 30). Therefore, we examined whether ERα and Beclin 1 interact and re-distribute in the presence of E_2 by confocal microscopy (Figure 5). In untreated cells, Beclin 1 (green) was found distributed in both cytoplasm and occasionally in the nucleus. In contrast, ERα (red) was mainly found in the nucleus. Addition of E_2 caused a movement of Beclin 1 to the perinuclear area. Addition of E_2 caused a re-distribution of ERα throughout the cytoplasm and the nuclei in the case of mitotic cells (Figure 5A) and toward cytoplasm in the case of clusters of cells (Figure 5B). Addition of E_2 enhanced co-localization of ERα and Beclin 1, indicated by the yellow color in the merged photographs. Re-distribution of Beclin 1 and its accumulation in the perinuclear area was illustrated by the increased co-localization of Beclin 1 with Golgin-97 (Figure 5C) in E_2-treated cells. These results indicate that localization and function of Beclin 1 and ERα are being modified by E_2.

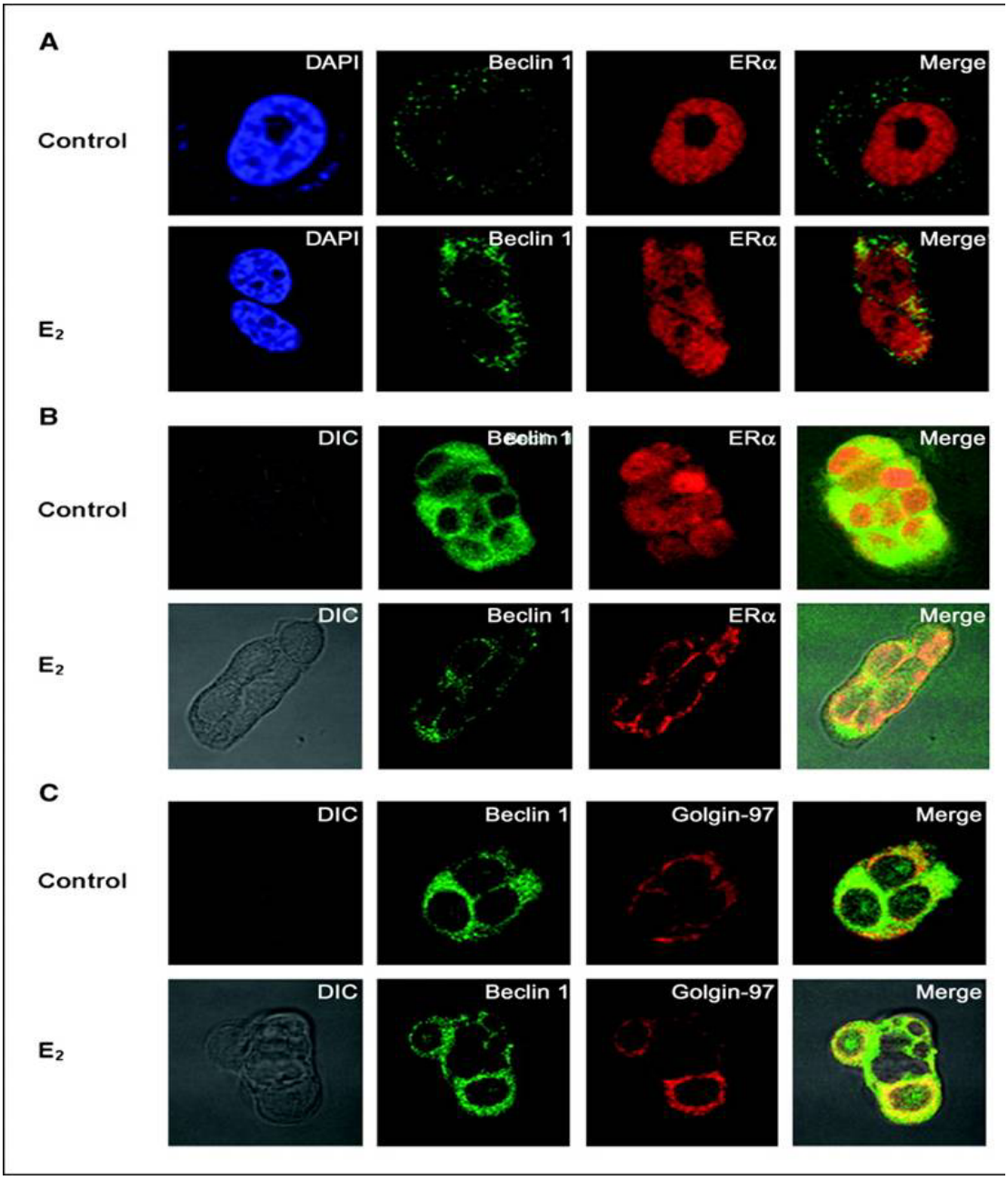

Figure 5. Effect of E_2 on the intracellular distribution of Beclin 1 and ERα. MCF-7.beclin cells (5 x 10^4) were seeded in Labtek 6-well chamber slides. Cells were dosed with E_2, 24 h after plating. Twenty-four hours after E_2 (4nM) treatment, cells were subjected to immunostaining procedure. Images were recorded using a Zeiss 510 Laser scanning microscope with a 60X objective at identical intensity settings for all treatment groups.
Nuclear staining was done using DAPI (4'6'-diamidino-2-phenylindole, 1 nM). ERα and Beclin 1 localization in the absence or the presence of E_2, observed in single or dividing cell (A) or in a group of cells (B). To confirm the perinuclear localization of Beclin 1 Golgin 97 localization was examined with Beclin 1 in the presence or absence of E_2 (C). Similar results were obtained in 3 separate experiments.

We next examined the effect of raloxifene and 4-hydroxytamoxifen on the localization of Beclin 1 and ERα in MCF-7.beclin cells. Figure 6 shows a representative confocal microscopic study of MCF7.beclin cells with and without raloxifene treatment. In these experiments green represents ERα and red Beclin 1. Although a different set of secondary antibodies were used, accumulation of ERα in the nucleus and distribution of Beclin 1 throughout the cell remained similar to previous studies (11, 16). However, the intensity Beclin 1 signal was much stronger for Alexa Fluor 633 conjugated (red) antibody (Figure 6), compared to Alexa Fluor 488 conjugated (green) antibody (Figure 5). Addition of raloxifene caused a re-organization of ERα or Beclin 1 so that these proteins were found throughout cytoplasm and nucleus, including membrane projections (Figure 6). Merge pictures showed association of ERα and Beclin 1 with a strong yellow color, indicating co-localization of ERα and Beclin 1 (Figure 6) in the presence of raloxifene. Co-localization of Beclin 1 and ERα was also observed in the presence of 4-hydroxytamoxifen (results not shown).

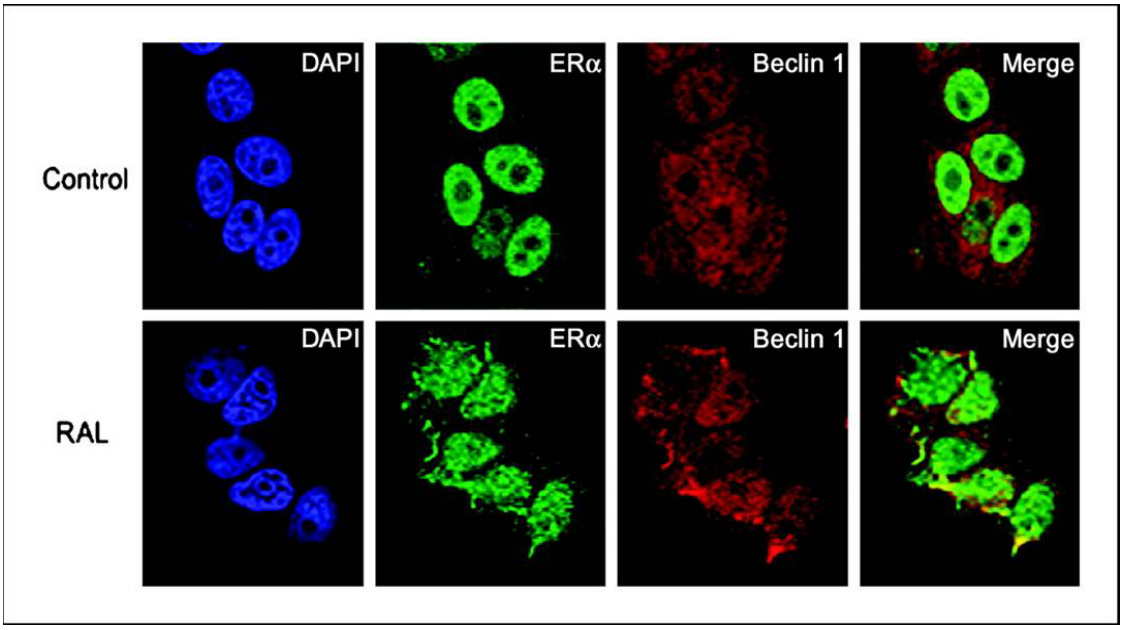

Figure 6. Effect of raloxifene on the co-localization of Beclin 1 and ERα in MCF-7.beclin cells. Cells (5 x 10^4) were plated in Labtek 6-well chamber slides, treated with 1 μM raloxifene (RAL) for 24 h and subjected to immunofluorescent staining. Images were recorded using a Zeiss 510 Laser scanning microscope. Nuclear staining with DAPI (4'6'-diamidino-2-phenylindole, 1 nM); ERα staining green; Beclin 1 staining red, and merge pictures are given. Similar results were obtained in 3 separate experiments.

Subsequently, we examined the interaction of ERα and Beclin 1 by co-immunoprecipitation. Our results (Figure 7A) showed that Beclin 1 was immunoprecipitated in association with ERα. Interestingly, addition of E_2 caused a 1.5- to 2-fold increase in the level of Beclin 1 associated with ERα, whereas the presence of raloxifene caused a 6-fold increase. The presence of 4-hydroxytamoxifen increased the level of Beclin 1 associated with ERα by 2.5-fold. Taken together, results of immunoprecipitation and subsequent immunoblotting confirmed the association of Beclin 1 with ERα, as observed in confocal microscopic studies. Although co-immunoprecipitation of ERα and Beclin 1 was found in untreated cells as well as in E_2- and raloxifene-treated cells, maximal level of co-immunoprecipitated proteins were found in raloxifene-treated cells.

To examine whether band intensities in the immunoprecipiation study has contributions from changes in the level of ERα and Beclin 1, we conducted direct Western blot analysis. Representative blots from 24 h treatment are shown in Figure 7B. Beclin 1 level did not undergo any major change due to treatment with E_2 or antiestrogens. ERα level decreased (10 to 25%) in the presence of E_2 and slightly increased in the presence of antiestrogens (1.5 to 2-fold) after normalizing to β-actin level. These changes in ERα are consistent with reports on the effects of E_2 and antiestrogens on ERα stability (16, 28).

We next conducted ChIP assay to elucidate the mechanistic differences in the action of E_2 and antiestrogens in MCF-7 and MCF-7.beclin cells. A comparison of the effects of E_2, 4-hydroxytamoxifen and raloxifene on MCF-7 cells and MCF-7.beclin cells is presented in Figure 7C. ChIP assay showed comparable E_2 responses on ERα occupation of pS2 promoter in both MCF-7 and MCF-7.beclin cells. Thus, the partial inhibition of the growth of MCF-7.becln cells is not associated with ERα binding to pS2 promoter. In the presence of 4-hydroxytamoxifen and raloxifene, ERα occupation on pS2 promoter was lower in MCF-7.beclin cells than that in MCF-7 cells. This result argues against a role for Beclin 1 as a repressor that binds to both ER□ and DNA. Thus, the lack of antiestrogen response in the presence of Beclin 1 might involve the interaction between ERα and Beclin 1, physically sequestering ERα away from promoter sites.

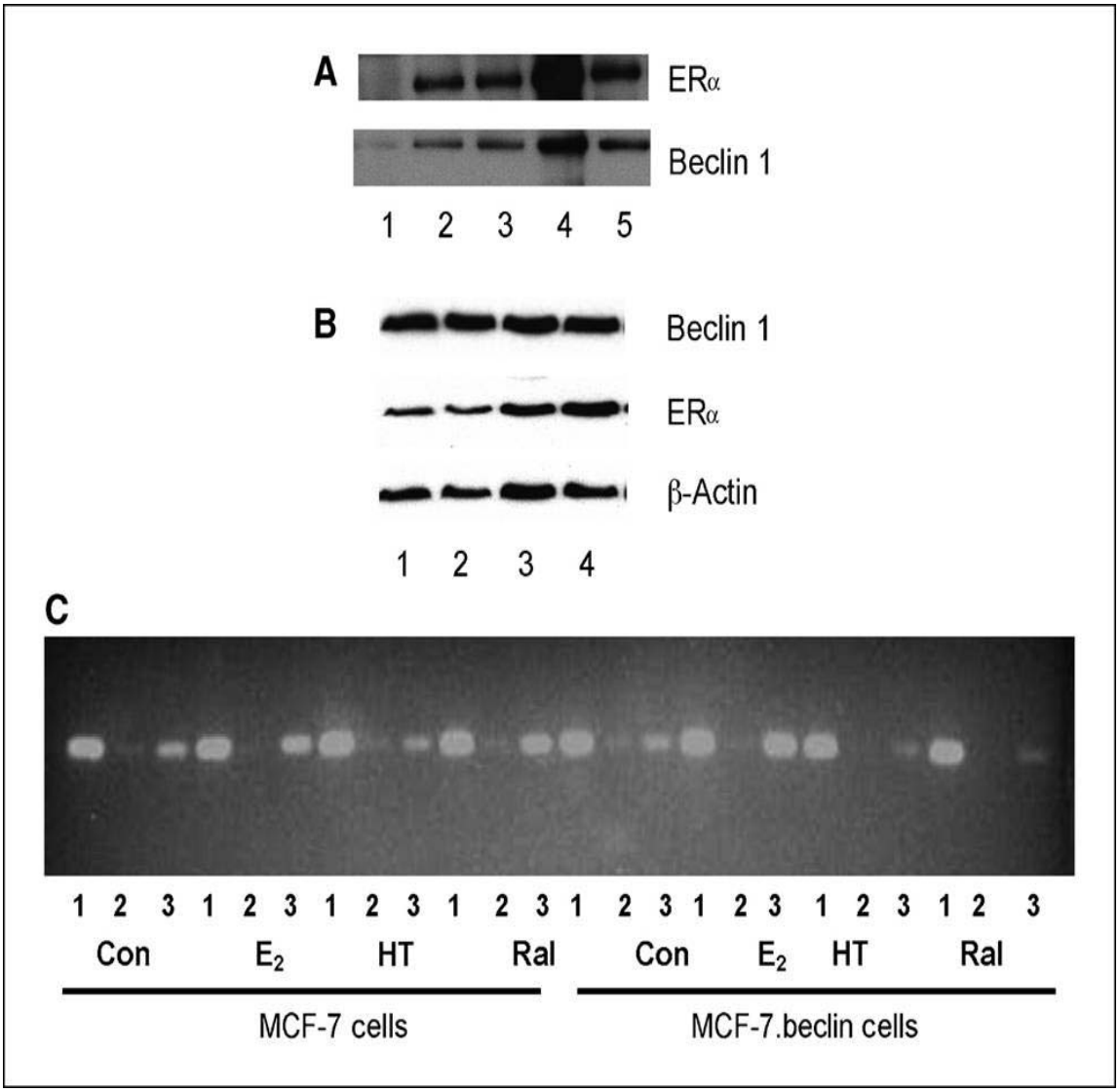

Figure 7. (A) Co-immunoprecipitation of ERα and Beclin 1 by anti-ERα antibody. MCF-7.beclin cells were plated in 60 mm culture plate and treated for 24 h with 4 nM E_2, 1 μM raloxifene, or 1 μM 4-hydroxytamoxifen. Cellular proteins were immunoprecipitated using anti-ERα (mouse IgG) anitobody. Immunoprecipitate was collected and subjected to Western blots, using a rabbit antibody specific to Beclin 1. The membrane was stripped and re-probed using anti-ERα (rabbit) antibody. Lane 1, an equivalent amount of protein, precipitated by normal (control) IgG; lane 2, immunoprecipitate (using ERα from untreated cells; lane 3, from E_2-treated cells; lane 4, from raloxifene-treated cells; and lane 5, from 4-hydroxytamoxifen-treated cells. (B) Direct Western blot of cells treated with E_2, raloxifene and 4-hydroxytamoxifen. Treatments represent lane 1, control; lane 2, E_2; lane 3, raloxifene; and lane 4, 4-hydroxytamoxifen. Blots were sequentially probed using anti-Beclin 1, anti-ERα, and anti-β-actin antibodies. Similar results were obtained in 3 separate experiments. (C) Results of ChIP assay showing ERα occupancy on pS2 (Tff1) promoter, 2 h after E_2 treatment. MCF7 cells and MCF-7.beclin cells were treated with vehicle (con), E_2, HT (4-hydroxytamoxifen) or Ral (raloxifene) and then harvested and subjected to ChIP assay. Sample shown are: input DNA (1), and immunoprecipitation with rabbit IgG (2) or ERα antibody (3) for each treatment group. Input lane represents DNA from 1% of material used for immunoprecipitation.

Discussion

In this study, we examined the effect of Beclin 1 on E_2 function and found that Beclin 1 overexpressing cells had reduced proliferative response to E_2. qPCR analysis of gene expression showed that several E_2-responsive genes were down-regulated in cells expressing Beclin 1. E_2 caused a decrease in Akt phosphorylation in Beclin 1 transfected cells. Growth inhibitory responses of antiestrogens, raloxifene and 4-hydroxytamoxifen were also limited by Beclin 1 transfection. In contrast, E_2-induced growth of MCF-7.control cells was totally inhibited by antiestrogens. The presence of E_2 caused a re-organization and accumulation of Beclin 1 in the perinucelar areas of cells. Importantly, we found a co-localization of ERα and Beclin 1 by confocal microscopy in MCF-7.beclin cells. An interaction between Beclin 1 and ERα was also evident from the results of co-immunoprecipitation, followed by Western immunoblotting. ChIP assay results suggest that interaction of ERα and Beclin 1 in the presence of antiestrogens leads to decreased promoter occupancy. Our results show that Beclin 1 can down-regulate estrogen-induced signaling events and cell growth in ERα-positive breast cancer cells. Our results further suggest that Beclin 1 may alter sensitivity of antiestrogens to breast cancer cells.

There have been extensive efforts to understand tamoxifen resistance in breast cancer cells (31). While a primary mechanism of estrogen insensitivity involves the loss of ERα, tamoxifen resistance often occurs in the presence of ERα. Since ERα has a down-regulatory effect on many estrogenic responses, it is the growth-stimulatory responses of ERα that are generally targeted by tamoxifen (20, 32). A basic mechanism for acquired tamoxifen resistance is that ERα becomes insensitive, as the essential growth regulatory circuits are taken over by growth factor receptors, including members of the HER-2 family of receptors, or G-protein coupled receptors (20, 33). Our results show that overexpression of Beclin 1 provides a context under which ERα does not transmit cell signaling responses such as Akt phosphorylation. Down-regulation of E_2-responsive genes, such as c-fos, Erg-1 and Nur77, is indicative of an altered molecular environment for estrogenic function. ChIP assay results showed decreased receptor occupancy of pS2 promoter due to increased Beclin 1 expression, especially in the presence antiestrogens.

Both tamoxifen and raloxifene are selective estrogen receptor modulators (SERMs), dependent on the presence of coactivator/co-repressor proteins (34). Interaction of ligands with ERα and ERβ induces subtle conformational changes which amplified by the binding of tissue specific proteins (35, 36). Raloxifene was first approved for the prevention of osteoporosis because it enhanced bone density (37, 38). Following a large comparative study of tamoxifen and raloxifene (STAR trial), raloxifene was found to decrease the incidence of breast cancer and was less prone to induce endometrial cancer, compared to tamoxifen (39). Cell culture studies have demonstrated raloxifene resistance (40). The observation that both 4-hydroxytamoxifen and raloxifene showed a lack of sensitivity in MCF-7.beclin cells, indicates that a common factor in antiestrogen resistance might be the functional availability of ERα, when the receptor is complexed with proteins such as Beclin 1. Such an interaction might allow sequestering of Beclin 1, until conditions of nutritional deprivation or stress arise.

Beclin 1 overexpressig cells were first investigated by Liang et al (11). Although these cells had decreased clonogenicity and showed a different morphology from that of wild type MCF-7 cells, nutritional deprivation was necessary to produce a large number of autophagosomes (11). While Beclin 1 was localized in the endoplasmic reticulum, mitochondria, perinuclear membrane as well as the nucleus, Beclin 1 mutants deficient in nuclear export, were unable to facilitate autophagy (8). Interestingly, ERα also shuttles between nucleus, cytoplasm and peripheral membrane and interacts with multiple proteins in these locations in regulating E_2-induced expression of hundreds of proteins (29). Thus the interaction of ERα and Beclin 1 may affect the function of both Beclin 1 and ERα.

Our results on DNA synthesis and CellTiter Glo assays showed that MCF-7.beclin cells had a reduced growth response in the presence of E_2, compared to vector control cells. However, E_2-response was still present, yielding 30 to 75% increase in DNA synthesis at 24 and 48 h, respectively. Phospho-Akt levels in MCF-7.beclin cells showed a decrease after treatment with E_2. Since E_2-induced phosphorylation of Akt is dependent on active ERα (15), the association of ERα and Beclin 1 may be involved in decreased Akt phosphorylation. In contrast, ERK1/2 was activated by E_2 in Beclin 1 overexpressing cells. ER-

dependent non-genomic functions are dependent on many co-regulators, including modulator of nongenomic actions of receptor (MNAR) (41) and growth factor receptors (42, 43). E_2 facilitates an interaction between ERα and epidermal growth factor receptor member, ERBB4 (43). Cross-talk also exists between ERα and ERBB2 (HER-2) signaling and insulin-like growth factor pathways, contributing to tamoxifen resistance (42, 44). Different G-protein coupled receptors and G proteins, (such as Gαi and Gβγ) may be also involved in E_2 responses (45).

Recent studies suggest that Bcl-2 binding domain of Beclin 1 serves as a point of cross-talk between autophagic and apoptotic pathways (46). Bcl-2 down-regulation by an antisense oligonucleotide provoked autophagic cell death in HL-60 cells (47). Interestingly, crystallographic studies identified Beclin 1 as a Bcl-2 homology domain 3-only (BH3-only) protein (9, 48). This observation would classify Beclin 1 along with other pro-apoptotic BH3-only proteins, such as Bim, Bid, and Bok, suggesting a pro-apoptotic function that might be activated under unique tissue/cellular context (49). Whether the interaction of ERα with Beclin 1 modulates pro-apoptotic function by sequestering essential growth stimulatory proteins needs to be investigated.

In summary, our results reveal an interaction between ERα and Beclin 1 in breast cancer cells. This interaction may modulate the function of ERα and Beclin 1. In the context of ERα function, we found that Beclin 1 transfected cells were less sensitive to E_2-induced growth stimulation and to the growth inhibitory effects of antiestrogens. Thus, a novel function for Beclin 1 might involve down-regulation of the action of ERα, contributing to resistance of breast cancer cells to antiestrogens.

Acknowledgments

Grant support: National Cancer Institute grants CA80163 (T.J & T. T.) and CA42439 (T. T. & T. J).

We gratefully acknowledge the receipt of MCF-7.Beclin and MCF-7.control cells from Dr. Beth Levine (University of Texas Southwestern Medical Center, Dallas, TX).

References

1. Rubinsztein DC, Gestwicki JE, Murphy LO, Klionsky DJ. Potential therapeutic applications of autophagy. Nat Rev Drug Discov 2007;6:304-12.

2. Takeshige K, Baba M, Tsuboi S, Noda T, Ohsumi Y. Autophagy in yeast demonstrated with proteinase-deficient mutants and conditions for its induction. J Cell Biol 1992;119:301-11.

3. Aita VM, Liang XH., Murty VV, et al. Cloning and genomic organization of beclin 1, a candidate tumor suppressor gene on chromosome 17q21. Genomics 1999;59:59-65.

4. Kametaka S, Okano T, Ohsumi M, Ohsumi Y. Apg14p and Apg6/Vps30p form a protein complex essential for autophagy in the yeast, Saccharomyces cerevisiae. J Biol Chem 1998;273:22284-91.

5. Abedin MJ, Wang D, McDonnell MA, Lehmann U, Kelekar A. Autophagy delays apoptotic death in breast cancer cells following DNA damage. Cell Death Differ 2007;14:500-10.

6. Karantza-Wadsworth V, Patel S, Kravchuk O, et al. Autophagy mitigates metabolic stress and genome damage in mammary tumorigenesis. Genes Dev 2007;21:1621-35.

7. Gewirtz D. Autophagy as a mechanism of radiation senstization in breast cancer cells. Autophagy 2007;3:540-548.

8. Pattingre S, Tassa A, Qu X, et al. Bcl-2 antiapoptotic proteins inhibit Beclin 1-dependent autophagy. Cell 2005;122:927-39.

9. Feng W, Huang S, Wu H, Zhang M. Molecular basis of Bcl-xL's target recognition versatality revealed by the structure of Bcl-xL in complex with BH3 domain of Beclin-1. J.Mol. Biol. 2007;372:223-35.

10. Liang XH, Jackson S, Seaman M, et al. Induction of autophagy and inhibition of tumorigenesis by beclin 1. Nature 1999;402:672-76.

11. Liang XH, Yu J, Brown K, Levine B. Beclin 1 contains a leucine-rich nuclear export signal that is required for its autophagy and tumor suppressor function. Cancer Res 2001;61:3443-49.

12. Thomas T, Gallo MA, Thomas TJ. Estrogen receptors as targets for drug development for breast cancer, osteoporosis and cardiovascular diseases. Curr Cancer Drug Targets 2004;4:483-99.

13. Cordera F, Jordan VC. Steroid receptors and their role in the biology and control of breast cancer growth. Semin Oncol 2006;33:631-41.

14. Williams C, Edvardsson K, Lewandowski S, Strom A, Gustafsson JA. genomewide study of the repressive effects of estrogen receptor beta on estrogen receptor alpha signaling in breast cancer cells. Oncogene 2008;27:1019-32.

15. Pedram A, Razandi M, Levin ER. Nature of functional estrogen receptors at the plasma membrane. Mol Endocrinol 2006;20:1996-2009.

16. Vijayanathan V, Venkiteswaran S, Nair SK, et al. Physiologic levels of 2-methoxyestradiol interfere with nongenomic signaling of 17beta-estradiol in human breast cancer cells. Clin Cancer Res 2006;12:2038-48.

17. Gururaj AE, Rayala SK, Vadlamudi RK, Kumar R. Novel mechanisms of resistance to endocrine therapy: genomic and nongenomic considerations. Clin Cancer Res 2006;12:1001s-7s.

18. Jensen EV, Jordan VC. The estrogen receptor: a model for molecular medicine. Clin Cancer Res 2003;9:1980-9.

19. Vijayanathan V, Thomas TJ, Nair S K, Shirahata A, Gallo MA, Thomas T. Bending of the estrogen response element by polyamines and estrogen receptors alpha and beta: a fluorescence resonance energy transfer study. Int J Biochem Cell Biol 2006;38:1191-206.

20. Massarweh S, Schiff R. Unraveling the mechanisms of endocrine resistance in breast cancer: new therapeutic opportunities. Clin Cancer Res 2007;13:1950-4.

21. Labrie F. Drug insight: breast cancer prevention and tissue-targeted hormone replacement therapy. Nat Clin Pract Endocrinol Metab 2007;3:584-93.

22. Jordan VC. Beyond raloxifene for the prevention of osteoporosis and breast cancer. Br J Pharmacol 2007;150:3-4.

23. Jordan VC, Brodie AM. Development and evolution of therapies targeted to the estrogen receptor for the treatment and prevention of breast cancer. Steroids 2007;72:7-25.

24. Lewis JS, Thomas TJ, Klinge CM, Gallo MA, Thomas T. Regulation of cell cycle and cyclins by 16alpha-hydroxyestrone in MCF-7 breast cancer cells. J Mol Endocrinol 2001;27:293-307.

25. Wesierska-Gadek J, Gueorguieva M, Rasmussen C, Zerza-Schnitzhofer. A new multiplex assay allowing simultaneous detection of the inhibition of cell proliferation and induction of cell death. J. Cell Biochem 2006;96:1-7.

26. Shah N, Thomas TJ, Lewis JS, et al. Regulation of estrogenic and nuclear factor kappa B functions by polyamines and their role in polyamine analog-induced apoptosis of breast cancer cells. Oncogene 2001;20:1715-29.

27. Liu W, Kounduri, SD, Bansal S, et al. Estrogen receptor-alpha binds p53 tumor suppressor protein directly and represses its function. J Biol Chem 2006;281:9837-40.

28. Kiang DT, Kollander RE, Thomas T, Kennedy BJ. Up-regulation of estrogen receptors by nonsteroidal antiestrogens in human breast cancer. Cancer Res 1989;49:5312-6.

29. Levin ER, Pietras RJ. Estrogen receptors outside the nucleus in breast cancer. Breast Cancer Res Treat 2008;108:351-61.

30. Song RX, Barnes CJ, Zhang Z, Bao Y, Kumar R, Santen RJ. The role of Shc and insulin-like growth factor 1 receptor in mediating the translocation of estrogen receptor alpha to the plasma membrane. Proc Natl Acad Sci U S A 2004;101:2076-81.

31. Frasor J, Chang EC, Komm B, et al. Gene expression preferentially regulated by tamoxifen in breast cancer cells and correlations with clinical outcome. Cancer Res 2006;66:7334-40.

32. Chang EC, Frasor J, Komm B, Katzenellenbogen BS. Impact of estrogen receptor beta on gene networks regulated by estrogen receptor alpha in breast cancer cells. Endocrinology 2006;147:4831-42.

33. Milano A, Dal Lago L, Sotiriou C, Piccart M, Cardoso F. What clinicians need to know about antioestrogen resistance in breast cancer therapy. Eur J Cancer 2006;42:2692-705.

34. Lonard D, O'Malley B. Nuclear receptor co-regulators: judges, juries, and executioners of cellular regulation. Mo Cell 2007;27:691-700.

35. McDonnell D P, Clemm DL, Hermann T, Goldman ME, Pike JW. Analysis of estrogen receptor function in vitro reveals three distinct classes of antiestrogens. Mol Endocrinol 1995;9:659-69.

36. Lupien M, Jeyakumar M, Hebert E, et al. Raloxifene and ICI182,780 increase estrogen receptor-alpha association with a nuclear compartment via overlapping sets of hydrophobic amino acids in activation function 2 helix 12. Mol Endocrinol 2007;21:797-816.

37. Cauley JA, Norton L, Lippman ME, et al. Continued breast cancer risk reduction in postmenopausal women treated with raloxifene: 4-year results from the MORE trial. Multiple outcomes of raloxifene evaluation. Breast Cancer Res Treat 2001;65:125-34.

38. Black LJ, Sato M, Rowley ER, et al. Raloxifene (LY139481 HCl) prevents bone loss and reduces serum cholesterol without causing uterine hypertrophy in ovariectomized rats. J Clin Invest 1994;93:63-9.

39. Vogel VG, Costantino JP, Wickerham DL, et al. Effects of tamoxifen vs raloxifene on the risk of developing invasive breast cancer and other disease outcomes: the NSABP Study of Tamoxifen and Raloxifene (STAR) P-2 trial. JAMA 2006;295:2727-41.

40. O'Regan RM, Osipo C, Ariazi E, et al. Development and therapeutic options for the treatment of raloxifene-stimulated breast cancer in athymic mice. Clin Cancer Res 2006;12:2255-63.

41. Vadlamudi RK, Kumar R. Functional and biological properties of the nuclear receptor coregulator PELP1/MNAR. Nucl Recept Signal 2007;5:e004.

42. Xia W, Bacus S, Hegde P, et al. LA model of acquired autoresistance to a potent ErbB2 tyrosine kinase inhibitor and a therapeutic strategy to prevent its onset in breast cancer. Proc Natl Acad Sci U S A 2006;103:7795-800.

43. Zhu Y, Sullivan LL, Nair SS, et al. Coregulation of Estrogen Receptor by ERBB4/HER4 Establishes a Growth-Promoting Autocrine Signal in Breast Tumor Cells. Cancer Res 2006;66:7991-8.

44. Song RX, Zhang Z, Chen Y, Bao Y, Santen RJ. Estrogen signaling via a linear pathway involving insulin-like growth factor I receptor, matrix metalloproteinases, and epidermal growth factor receptor to activate mitogen-activated protein kinase

in MCF-7 breast cancer cells. Endocrinology 2007;148:4091-101.
45. Kumar P, Wu Q, Chambliss KL, et al. Direct Interactions with G alpha i and G beta gamma mediate nongenomic signaling by estrogen receptor alpha. Mol Endocrinol 2007;21:1370-80.

46. Maiuri MC, Zalckvar E, Kimchi A, Kroemer G. Self-eating and self-killing: crosstalk between autophagy and apoptosis. Nat Rev Mol Cell Biol 2007;8:741-52.

47. Kim R, Emi M, Matsuura K, Tanabe K. Antisense and nonantisense effects of antisense Bcl-2 on multiple roles of Bcl-2 as a chemosensitizer in cancer therapy. Cancer Gene Ther 2007;14:1-11.

48. Oberstein A, Jeffrey PD, Shi Y. Crystal structure of the Bcl-XL-Beclin 1 peptide complex: Beclin 1 is a novel BH3-only protein. J Biol Chem 2007;282:13123-32.

49. Erlich S, Mizrachy L, Segev O, et al. Differential Interactions between Beclin 1 and Bcl-2 family members. Autophagy 2007;3:561-8.

Chapter 2

A Bis(ethyl) Polyamine Analogue, 1,15-bis(ethylamino)4,8,12-triazapentadecane (BE-3-3-3-3), Mimics Estradiol and Induces Autophagy in Breast Cancer Cells

Irina Nayvelt, Shali John, Hui-Chen Hsu, PingAr Yang, Akira Shirahata, Rajesh Patel, Thresia Thomas and T. J. Thomas

ABSTRACT

Polyamines are ubiquitous cellular cations with multiple functions in cell proliferation and cell death. Bis(ethyl) polyamine analogues have been synthesized and tested as chemotherapeutic agents for different subsets of cancer. 1,15-bis(ethylamino)4,8,12-triazapentadecane (BE-3-3-3-3) is a polyamine analogue with therapeutic potential for breast cancer. We examined the effect of BE-3-3-3-3 on MCF-7 cells in the presence and absence of E_2. In the presence of E_2, there was a concentration-dependent decrease of cell growth, as measured by [^{3}H]-thymidine incorporation. In the absence of E_2, low concentrations (1.25 to 10 μM) of BE-3-3-3-3 increased [^{3}H]-thymidine incorporation at 24 and 48 h of treatment. However, growth inhibition was observed by 96 h of treatment. BE-3-3-3-3-induced changes in the expression of E_2-responsive genes as determined by real-time quantitiative polymerase chain reaction (qPCR). Significant changes in the transcript levels were observed for the following genes: c-myc, c-fos, c-jun, c-myb, Cyclin B1, and PTEN. Akt phosphorylation was increased in the presence of BE-3-3-3-3. Delayed growth inhibition in the absence of E_2 was associated with the induction of autophagy, as evidenced by elevated levels of autophagy-related proteins, Beclin 1 and MAP LC3 II. Electron microscopic studies confirm the induction of autophagy in the presence of BE-3-3-3-3. Confocal microscopy also demonstrated higher levels of Beclin 1 in BE-3-3-3-3-treated cells, and showed Beclin 1 accumulation around the nucleus. These results provide evidence for the ability of BE-3-3-3-3 to modulate gene expression and proliferation of breast cancer cells. In addition, our results indicate a novel pathway for the action of bis(ethyl) polyamine analogues in the balance of cell growth and autophagy.

Introduction

Putrescine ($H_2N(CH_2)_4NH_2$), spermidine ($H_2N(CH_2)_3NH(CH_2)_4NH_2$), and spermine ($H_2N(CH_2)_3NH(CH_2)_4NH(CH_2)_3NH_2$) are ubiquitous cellular cations involved in cell growth and differentiation (Casero et al. 2007, Gerner et al. 2004). These polyamines are delicately regulated in the cell by biosynthetic enzymes, catabolic enzymes, and by uptake/efflux pathways (Casero et al. 2007, Thomas et al. 2003). Transfection of ODC gene in NIH 3T3 cells transformed them to a

malignant phenotype (Moshier et al., 1993). Alterations in polyamine levels and metabolism are causatory factors of carcinogenesis in animal models and humans (Gerner et al., 2004). Breast cancer tissues were found to have increased levels of polyamines compared to adjacent normal tissues (Canizares et al. 1999, Leveque et al. 2000). Our research (Shah et al. 2001, Thomas and Thomas 1994) and other reports (Manni et al. 1992, Leveque et al. 2000) show an essential role of polyamines in estrogenic pathway of breast cancer cell growth.

Estrogenic action in target cells is mediated through the estrogen receptors, ERα and ERβ. In the genomic mode of ER action, estradiol (E_2) binding to the nuclear receptor induces a conformational change, leading to co-activator recruitment and the stimulation of transcription from either the promoter/enhancer site of E_2-responsive genes, or through protein-protein interactions with other transcription factors such as the activating protein 1 (AP-1) and the stimulating protein 1 (SP-1). E_2 can also elicit a fast, non-genomic response through cellular membrane-associated ERs. These receptors may interact with G-proteins or other cell membrane growth receptors (EGFR, IGF, etc.), and stimulate events such as calcium flux, phospholipase C activation, production of cAMP and inositol triphosphate (IP_3) (Levin et al., 2001). The aforementioned second messengers stimulate kinase cascades, which can lead to the modulation of multiple genes involved in cell growth and proliferation (Levin et al. 2001, Yager et al. 2006). Polyamines play a key role in E_2-mediated cell growth, which involves the regulation of ER–ERE and transcription factor binding, as well as of the cell cycle progression (Thomas and Thomas, 2001).

Previous studies on polyamine analogues in our laboratory (Faaland et al. 2000, Shah et al. 2001) and others (Casero et al., 2007) often used ER-positive breast cancer cells growing in the presence E_2, as these cells represented a major class of ER-positive human breast cancer. In MCF-7 cells, 1,15-bis(ethylamino)-4,8,12-triazapentadecane (BE-3-3-3-3) inhibited cell proliferation, induced apoptosis, and increased SSAT activity (Faaland et al., 2000). BE-3-3-3-3 was more effective than the commonly used analogue, bis(ethyl) norspermine (BE-3-3-3), in inhibiting tumor growth in a transgenic mouse model of breast cancer (Shah et al., 1999).

BE-3-3-3 inhibited cancer cell growth in vitro (Shappell et al., 1992), and tumor growth in animal models (Bernacki et al. 1992, Porter et al. 1993), but failed to produce an objective therapeutic effect in patients during phase I and II clinical trials (Creaven et al. 1997, Streiff et al. 2001, Wolff et al. 2003). A possible explanation for BE-3-3-3's ineffectiveness as a therapeutic agent derives from a study by Minchin et al. (2006), which showed that BE-3-3-3 stimulated cell proliferation of melanoma cells at low concentrations (up to 10 μM).

In several studies, polyamine analogues (i.e. BE-3-3-3) induced the formation of large lysosomal vacuoles, and led us to suspect the involvement of autophagy in the action of these compounds (Dai et al. 1999, Porter et al. 1990, Kramer et al. 1998). Autophagy is a pathway for the recycling of long-lived cytoplasmic proteins and organelles, in which these cellular components are enclosed into double-membrane vesicles, termed autophagic vacuoles or autophagosomes, and delivered to the lysosome for degradation (Klionsky, 2000). Basal levels of autophagy are essential for proper cellular maintenance and tissue remodeling. However, autophagy is upregulated in conditions of stress, such as nutrient or growth factor deprivation, or oxidative stress, and promotes cell survival by providing energy from the recycling of non-essential cellular components (Levine et al., 2005). On the other hand, prolonged activation of autophagy can result in Type II Programmed Cell Death, which is different from apoptosis. Studies have demonstrated that autophagy can delay apoptotic cell death, and that an inhibition of autophagy can sensitize cells to apoptosis-inducing drugs, such as doxorubicin (Daniel et al. 2006, Abedin et al. 2007).

Beclin 1 is a homologue of yeast Atg6/Vps30p gene, and is essential for autophagy in mammals (Liang et al., 1999). It forms a complex with phosphotidyl inositol kinase III (PI3K) and p150 protein kinase, and plays a key role in autophagosome formation (Yang et al., 2005). Another autophagy-related protein is microtubule-associated protein 1 light chain 3 (LC3), the mammalian orthologue of Atg8 (Yang et al., 2005). A modified form of this protein, LC3-II, is firmly attached to membranes of preautophagosomes and autophagosomes, and serves as an excellent marker of the induction and inhibition of autophagy in mammalian cells (Klionsky et al., 2008).

Our purpose in this study was to identify conditions and subsets of breast cancer cells responding to BE-3-3-3-3, and to define the role of autophagy in the action of this polyamine

analogue. We found that BE-3-3-3-3 induced cell proliferation and stimulated Akt phoshorylation in the absence of E_2. BE-3-3-3-3 also increased the expression of autophagy-related proteins, Beclin 1 and MAP LC II, and caused autophagosome formation and Beclin 1 accumulation around the nucleus. These findings indicate that BE-3-3-3-3 has an estrogen-mimetic effect on breast cancer cell growth at low concentrations (up to 10 μM), which may become important during optimization of therapeutic treatment.

Materials and Methods

Materials. MCF-7, T-47D, and MDA-MB-231 cell lines were obtained from the American Type Culture Collection (Monasses, VA). Dulbecco's modified Eagles medium (DMEM), phenol red-free DMEM, RPMI-1640, phenol red-free RPMI-1640, Minimal Essential medium (MEM), fetal bovine serum (FBS), and anti-β-actin antibody were obtained from Sigma Chemical Co. (St. Louis, MO). Antibiotics, trypsin, and other additives for cell culture medium were purchased from Invitrogen (Carlsbad, CA). Anti-phospho-Akt, anti-Akt antibodies, and anti-Beclin 1 antibodies were purchased from Cell Signaling Technology (Beverly, MA). Anti-MAP LC3 antibody was purchased from Santa Cruz Biotechnology (Santa Cruz, CA). Secondary antibody conjugated with Alexa Fluor 488 was obtained from Invitrogen. 1,15-bis(ethylamino)4,8,12-triazapentadecane (BE-3-3-3-3) was synthesized as described earlier (Musso et al.,1997).

Cell Culture. MCF-7 cells were maintained in DMEM, supplemented with 100 units/ml penicillin, 100μg/ml streptomycin, 40 μg/ml gentamicin, 2 μg/ml insulin, 0.5 mM sodium pyruvate, 50 mM nonessential amino acids, 2 mM L-glutamine, and 10% fetal bovine serum. T-47D cells were maintained in RPMI-1640 medium, supplemented with 100 units/ml penicillin, 100μg/ml streptomycin, 40 μg/ml gentamicin, 2 μg/ml insulin, 0.5 mM sodium pyruvate, 2 mM L-glutamine, and 10% fetal bovine serum. MDA-MB-231 cells were maintained in MEM, supplemented with 100 units/ml penicillin, 100μg/ml streptomycin, 40 μg/ml gentamicin, 0.5 mM sodium pyruvate, 2 mM L-glutamine, and 10% fetal bovine serum. MCF-7 and T-47D cells were grown for 3-4 days in phenol red-free DMEM or phenol-red free RPMI-1640, respectively, containing serum treated

with dextran-coated charcoal (DCC) to remove serum-derived estrogenic compounds, prior to each experiment (Vijayanathan). DCC suspension contained 0.05% dextran, 0.5% charcoal and 25 mM sucrose. Serum was subjected to three 10 min cycles of DCC treatment, centrifugation, and passed through a 0.2 μm membrane filter.

[^{3}H]-Thymidine Incorporation. Cells (0.5 x 10^6) were seeded in 6-well culture plates in phenol red-free DMEM supplemented with DCC treated serum and additives. After 24 h of plating, cells were treated with estradiol and/or polyamine analogues as indicated in the text and Figure Legends. Control cells received ethanol vehicle, which was maintained at less than 0.1%. DNA synthesis was measured by adding 4 μCi/ml of [^{3}H]-thymidine to cells 1 h prior to harvest. Cells were washed twice with ice-cold PBS and treated with ice-cold 5% trichloroacetic acid. The cell layer was then solubilized in 1 N NaOH and neutralized with 1 N HCl. The radioactive thymidine incorporated in cellular DNA was quantified by liquid scintillation counting.

qPCR. MCF-7 cells (1 x 10^6) were seeded in 60 mm culture dishes. After 24 h, cells were treated with 0, 5, and 10 μM BE-3-3-3-3 for 0, 2, 4, and 8 h. RNA was isolated using Trizol reagent (Invitrogen) and 2 μg RNA was reverse-transcribed using the first strand cDNA synthesis kit (Fermentas, Inc., Glen Burnie, MD) with random hexamers as primers. The expression of c- myc, c-fos, c-jun, cyclin B1, c-myb, PTEN, and Gapdh genes was determined by real-time PCR using the SYBR Green PCR Master Mix (Bio-Rad) with the following primers: 5'-CTCCTCACAGCCCACTGGTC-3' and 5'-CTTGGCAGCAGGATAGTCCTTC-3' for c-Myc (101 bp); 5'-CGGGCTTCAACGCAGACTA-3' and 5'- GGTCCGTGCAGAAGTCCTG-3' for c-Fos (147 bp); 5'-TGCCTCCAAGTGCCGAAAAA-3' and 5'-TGACTTTCTGTTTAAGCTGTGCC-3' for c-jun (143 bp); 5'-ATTGCCAATTATCTCCCGAATCG-3' and 5'-CCAATTCTCCCCTTTAAGTGCT-3' for c-myb (185 bp); 5'-TGGTTGATACTGCCTCTCC-3' and 5'-GACTGCTTGCTCTTCCTC-3' for cyclin B1 (200 bp); 5'-GGACGAACTGGTGTAATG-3' and 5'-GTGCCACTGGTCTATAATC-3' for PTEN (193 bp); and 5'-CATGAGAAGTATGACAACAGCCT-3' and 5'-AGTCCTTCCACGATACCAAAGT -3' for Gapdh (113 bp). A final volume of 25 □l was used for qPCR in an IQ5^{TM} thermocycler (Bio-Rad). Amplification conditions were 95 °C for 3 min,

followed by 40 cycles of 95 °C for 15 s and annealing for 30 s at 55 °C. qPCR products were normalized relative to that of Gapdh to correct for differences in template input. Results are expressed as fold differences in expression of the indicated gene relative to that of Gapdh. Standard curves were generated for every target using six 4-fold serial dilutions.

Western blot analysis. Cells (1.5 x 10^6/60 mm dish) were plated in dishes and allowed to attach for 24 h prior to treatments. After the specificed treatments and time periods, medium was removed and cells were scraped off the plates using a disposable Cell Lifter (Fisher Scientific) in ice-cold phosphate buffered saline (PBS). Cells were centrifuged, and the pellet was stored at -80°C. Cell pellet was lysed by the addition of ice-cold lysis buffer (50 mM Tris.HCl (pH 7.4), 150 mM NaCl, 1% Triton, 5 mM EDTA, 25 mM sodium fluoride, 25 mM sodium pyrophosphate, 2 mM sodium vanadate, 5% glycerol and 1X concentration of a protease inhibitor cocktail (Calbiochem, San Diego, CA). Twenty micrograms of protein (determined by the Bradford protein assay) was diluted in 2X SDS-PAGE Laemmli buffer (150 mM Tris.HCl, pH 6.8, 30% glycerol, 4% SDS, 7.5 mM dithiothreitol, 0.01% bromophenol blue) and separated on a 12% SDS-polyacrylamide gel. Proteins were transferred to PVDF Polyscreen membrane. After blocking with 5% nonfat milk, membrane was immunoblotted with a 1:200 to 1:1000 dilution of the primary antibody. Protein bands were visualized using horseradish peroxidase-conjugated secondary antibody (Santa Cruz Biotechnology, Santa Cruz, CA) and SuperSignal West Peco Chemiluminescent Substrate (Pierce, Woburn, MA).

Membranes were stripped in stripping buffer (62.5 mM Tris.HCl, (pH 6.8), 2% SDS, 100 mM, beta-mercaptoethanol) and washed 3 times in washing buffer (20 mM Tris. HCl (pH 7.6),150 mM NaCl, and 0.05% Tween 20). Another primary antibody was then added and the membrane re-probed as needed. To verify equal protein loading, membranes were stripped and re-blotted with anti-β-actin monoclonal antibody. The blots were developed using Kodak XAR Biomax film. Exposed films were scanned using an Epson B4 Scanner and band intensities quantified using the NIH Image J 1.34S program.

Confocal Microscopy. Cells were plated in Labtek 6-well slide chamber and dosed

after 24 h (ref.). Cells were fixed in 4% paraformaldehyde, blocked in normal goat serum (5%) in PBS, followed by incubation with an anti-Beclin 1 antibody (rabbit) in 2.5% goat serum in PBS. After washing, cells were incubated with appropriate secondary antibodies. Alexa Fluor 488 conjugated anti-rabbit IgG (green) was used for Beclin 1. Nuclei were stained with DAPI (4'6'-diamidino-2-phenylindole, 1nM). Images were recorded using a Zeiss 510 Laser scanning microscope with a 60X objective at identical intensity settings for all treatment groups. No fluorescence was detected when cells were treated with fluorescence labeled secondary antibody alone.

Electron Microscopy. Cells were treated with 4 nM E_2 and 10 μM BE-3-3-3-3 and harvested at 24 h. Cells were trypsinized, centrifuged, and fixed in a solution containing 2.5 % glutaraldehyde, 4% paraformaldehyde, 0.1 M sodium cacodylate (pH 7.4) and 8 mM $CaCl_2$. Cells were post-fixed with 1% osmium tetroxide, dehydrated in graded alcohols, embedded in Epon 812, sectioned with ultra microtome, stained with uranyl acetate and lead citrate. Cells were visualized using the JEOL 1200EX electron microscope at 3000 X.

Results

BE-3-3-3-3 stimulates cell growth in the absence of E_2. We first examined the effect of BE-3-3-3-3 on cell growth in estrogen receptor (ER)-positive (MCF-7 and T-47D) and ER-negative (MDA-MB-231) breast cancer cells. Cells were treated with 0, 1.25, 2.5, 5, and 10 μM BE-3-3-3-3 alone, or in combination with E_2, and [^{3}H]-thymidine incorporation was determined 24, 48, and 96 h after dosing. At 24 and 48 hours of treatment, BE-3-3-3-3 treatment in the absence of E_2 produced a 3- to 5-fold increase in DNA synthesis in MCF-7 cells (Figure 8A). A similar increase was detected in T-47D cells (Figure 8C). Inhibition of DNA synthesis was observed at 96 h in MCF-7 cells, at 10 μM BE-3-3-3-3 (Figure 8A), and also in T-47D cells (data not shown). In the presence of E_2, BE-3-3-3-3 inhibited DNA synthesis in MCF-7 cells, starting at 48 h at 10 μM BE-3-3-3-3 (Figure 8B), and also in T-47D cells, at 1.25 μM BE-3-3-3-3 after 24 h of treatment (Figure 8D). Effects of BE-3-3-3-3 on ER-negative, MDA-MB-231 cells are represented in Figure 8E. A modest increase in DNA synthesis, 1.3 to 1.5 fold, was observed at 48 h, at 1.25 and 2.5

μM μM BE-3-3-3-3, respectively. Growth inhibition also occurred at this time point (48 h), at higher concentrations of BE-3-3-3-3, 5 and 10 μM. Our results show that at low concentrations BE-3-3-3-3 has, at first, an estrogenic, growth-stimulatory effect on ER-positive breast cancer cells, which converts into a growth inhibitory effect by 96 h.

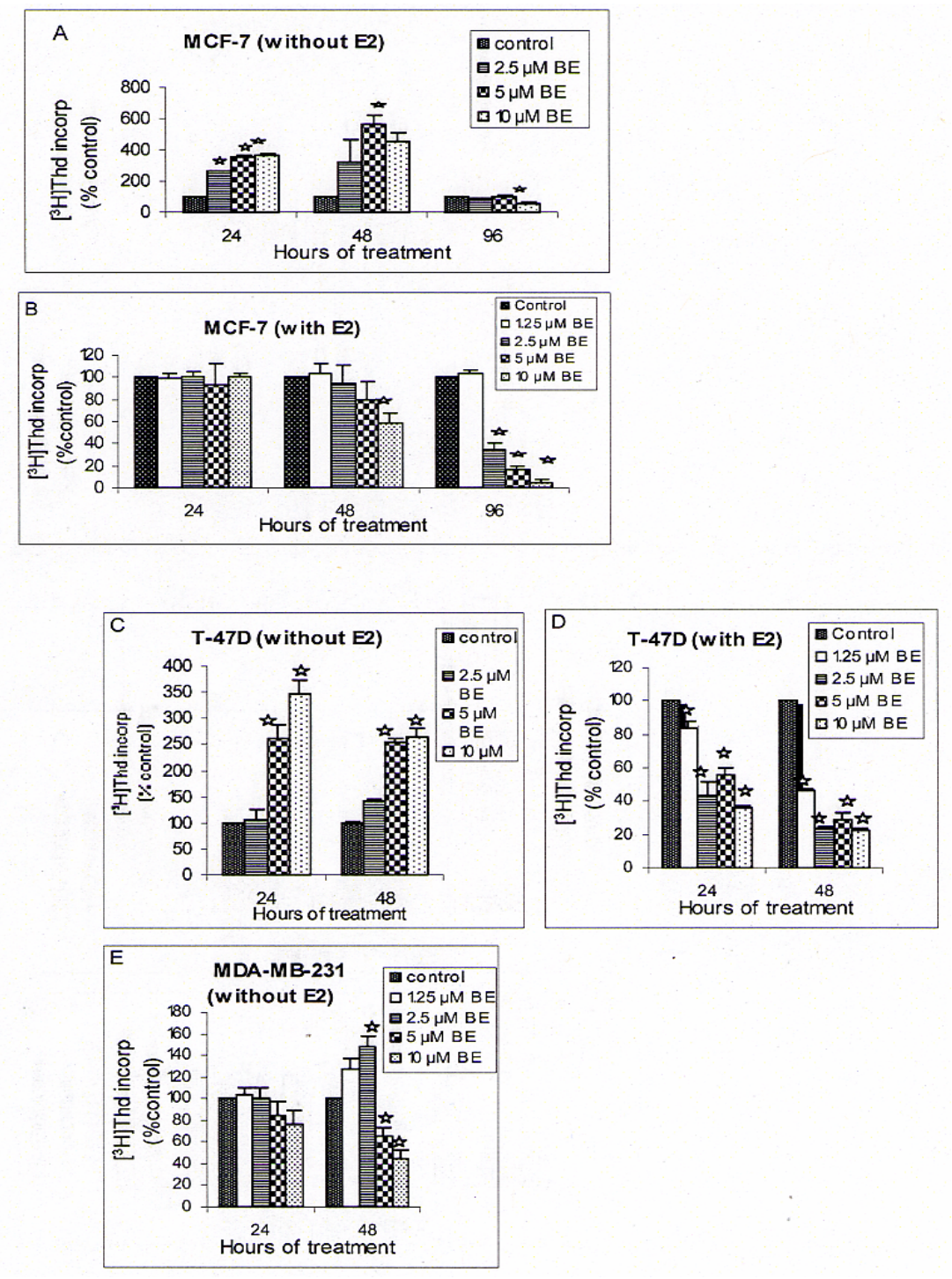

Figure 8. Effect of BE-3-3-3-3 on cell growth of ER-positive and ER-negative breast cancer cells in the presence and absence of E_2. Cells growing in the absence of phenol red (except for MDA-MB-231) for 3 days were seeded in 6-well tissue culture plates at a density of 5 $x10^5$ cells/well with 2 ml medium. After 24 h, cells were treated with BE-3-3-3-3 alone, or in combination with 4 nM E_2. [^{3}H]-thymidine was added 24, 48, or 96 h after treatment, and cells harvested for scintillation counting 1 h after the addition of [^{3}H]-thymidine. (A) MCF-7 cells treated with BE-3-3-3-3 alone. (B) MCF-7 cells treated with BE-3-3-3-3 and/or 4 nM E_2. (C) T-47D cells treated with BE-3-3-3-3 alone. (D) T-47D cells treated with BE-3-3-3-3 and/or 4 nM E_2. (E) MDA-MB-231 cells treated with BE-3-3-3-3. Results are the mean ± SEM from 3 experiments. Star indicates statistical significance ($P < 0.05$), compared to the control.

BE-3-3-3-3 stimulates Akt signaling. Akt serine/threonine kinase is a key mediator of cell survival, resistance to apoptosis and sensitivity to chemotherapeutic agents. Since E_2-stimulated cell signaling involves the phosphorylation of Akt by ERα, we investigated whether the estrogen-mimetic, cell-proliferative effect of BE-3-3-3-3 was also associated with increased Akt phosphorylation. Accordingly, we determined the effect of BE-3-3-3-3 on Akt phosphorylation in the presence and absence of E_2, in MCF-7 cells. Cells were dosed with 0, 1.25, 2.5, 5, and 10 μM BE-3-3-3-3 alone or together with 4 nM E_2, and collected after 48 hours of treatment. Protein levels were determined by Western blotting. BE-3-3-3-3 caused a 2.5- to 3-fold increase in phospho-Akt (p-Akt) levels compared to control in the presence and absence of E_2 (Figure 9). In the absence of E_2, increased Akt phosphorylation was observed starting at 2.5 μM, while in the presence of E_2, the increase was observed at 1.25 μM, suggesting a permissive/synergistic effect of E_2 on BE-3-3-3-3-stimulated cell signaling. Interestingly, Akt phosphorylation level at 48h of treatment was similar in the control and the E_2–treated cells. This may indicate that the bifuscation of growth stimulatory and inhibitory pathways is not represented by Akt phoshorylation. Total Akt levels were unchanged, except for the group containing 10 μM BE-3-3-3-3 and E_2, demonstrating that increased Akt phosphorylation was not the result of altered Akt protein levels.

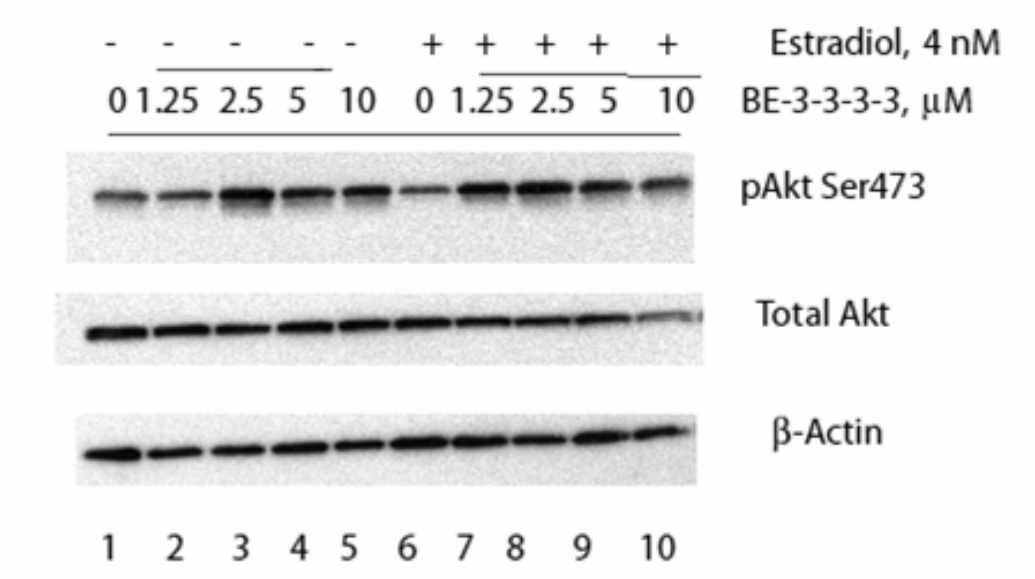

Figure 9. Effect of BE-3-3-3-3 on Akt phosphorylation in the presence and absence of E_2 in MCF-7 cells. Cells (1.5×10^6) were plated in 60 mm dishes, and treated with 0, 1.25, 2.5, 5, and 10 μM BE-3-3-3-3 alone (lanes 1-5, respectively), or in the presence of 4 nm E_2 (lanes 6-10, respectively). Cells were harvested at 48 h, and analyzed by Western blots using antibodies specific to phosphorylated (Ser-473) Akt, followed by sequential probing with antibodies specific to total Akt, and β-actin. Similar results were obtained in 3 separate experiments.

Effect of BE-3-3-3-3 on E_2-regulated genes. Since previous experiments demonstrated that BE-3-3-3-3 has an estrogen-like, growth-promoting effect on MCF-7 cells within 48 h, we examined whether this effect was also associated with regulation of E_2-responsive genes by this polyamine analogue. Cells were treated with 0, 5, and 10 μM BE-3-3-3-3 in the absence of E_2, and the RNA was harvested at 0, 2, 4, and 8 h. Significant increase in transcript levels compared to control was observed in the early response genes c-jun, 3-fold at 2 and 4 h, and c-myc, 2.5-fold at 2h (Figure 10). However, c-myc was later inhibited by 10 μM BE-3-3-3-3 at 8 h. c-Fos, another early response gene, showed a non-significant induction at 2 and 4 h at 5 μM BE-3-3-3-3, but was inhibited by 10 μM BE-3-3-3-3 at 4 h. Cyclin B1 gene expression was significantly reduced (~ 35%) by BE-3-3-3-3 at 4 h. Transcript levels of the c-myb proto-oncogene showed a 4-fold decrease in the presence of BE-3-3-3-3 at all hours of treatment. RNA levels of the tumor suppressor gene, PTEN, showed a 1.5-2-fold decrease at 4h, in the presence of 5 μM BE-3-3-3-3.

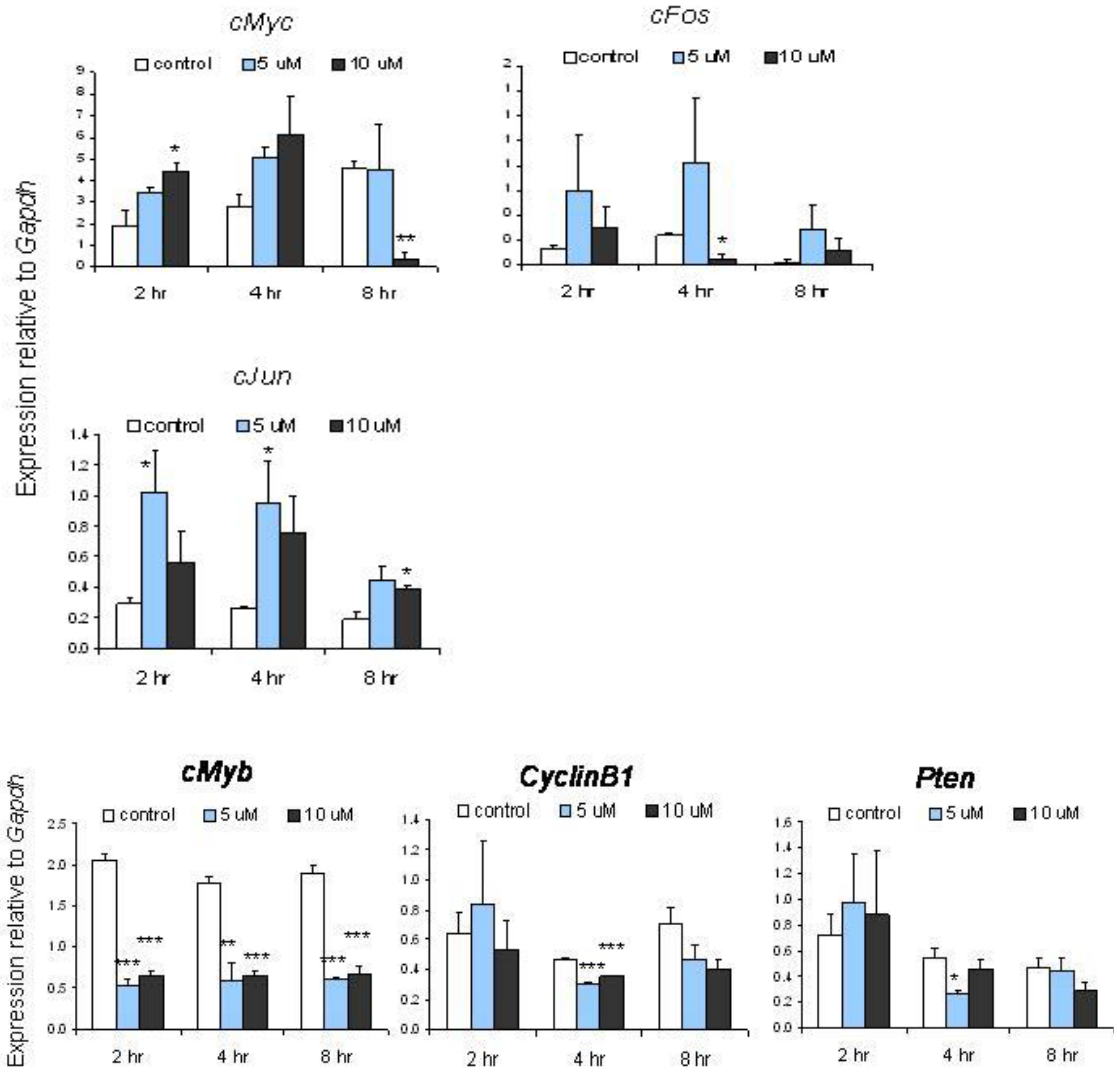

Figure 10. qPCR analysis showing the effects of treatment with 5 and 10 μM BE-3-3-3-3 on the expression of E_2-modulated genes in MCF-7 cells at 2, 4 and 8 hr time points (n= 4 per time point per group; *p<0.05 vs. control, **p<0.01 vs. control, ***p<0.001 vs. control). Y-axis units in all graphs indicate gene expression relative to Gapdh.

Induction of Beclin 1 and microtubule-associated protein 1 light chain 3 II (MAP LC3 II) expression during the action of BE-3-3-3-3. In the next set of experiments we examined whether the delayed growth inhibition of BE-3-3-3-3 is related to the induction of autophagy in MCF-7 cells. Therefore, we examined the effect of this polyamine analogue on the expression

of Beclin 1and MAP LC3-II proteins, which serve as markers of autophagy, a known mechanism of cell survival in response to nutritional starvation and stress. MCF-7 cells were treated with 1.25, 2.5, 5, and 10 μM BE-3-3-3-3 and harvested at 48 h after dosing. Western blot analysis was conducted using the anti-beclin antibody. Figure 11A shows the effect of BE-3-3-3-3 on Beclin 1 levels at 48 h. There was a dose-dependent increase in the level of Beclin 1 in cells treated with BE-3-3-3-3. The observation of Beclin 1 in untreated (control) MCF-7 cells is consistent with recent reports (Scarlatti et al. 2008, Abedin et al. 2007), although some early work indicated otherwise (Liang et al., 1999). In similar experiments, we examined the induction of MAP LC 3-II in BE-3-3-3-3 treated cells (Figure 11B). Western blots using anti-MAP LC3 antibody showed a dose-dependent increase in the production of 16 kD modified form of LC3 II (lower band in B, LC3 blot), with a maximum induction observed at 5 μM. The induction of Beclin 1 and MAP LC3-II indicate that the growth-stimulatory, pro-survival action of BE-3-3-3-3 involves the autophagy pathway.

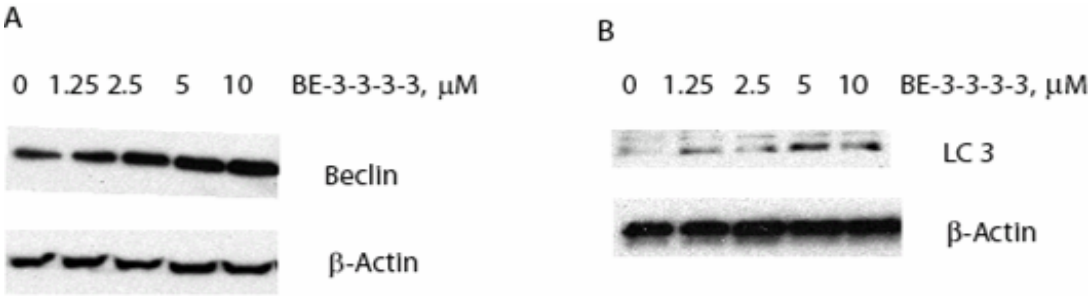

Figure 11. Effect of BE-3-3-3-3 on the levels of Beclin 1 (A) and MAP LC3 (B) in MCF-7 cells. Cells (1.5×10^6) were plated in 60 mm dishes, and treated with 0, 1.25, 2.5, 5, and 10 μM BE-3-3-3-3. After 48 h, cells were harvested and analyzed by Western blots using anti-beclin (A) and anti-MAP LC3 (B) antibodies. The blots were stripped and then re-probed with a β-actin antibody. Results are representative of 3 different experiments.

Electron microscopy (EM) of MCF-7 cells treated with BE-3-3-3-3. Our previous experiments demonstrated that treatment with BE-3-3-3-3 elevated the expression levels of MAP LC3-II, which are indicative of increased autophagosome formation. In order to visualize the ultra-structural changes in cells treated with BE-3-3-3-3, we conducted electron microscopy studies. Figure 12a shows untreated (control) MCF-7 cells, and denotes the absence of autophagy-related cellular

alterations. Figure 12b depicts typical autophagosomes produced in Beclin 1-overexpressing MCF-7 cells during nutritional starvation maintained for 4h. Treatment with 10 μM BE-3-3-3-3 induced autophagy in MCF-7 cells after 24h, demonstrated by the presence of autophagosomes in the cytoplasm (Figure 12c, further expanded in 12d). These results indicate that autophagy plays a role in the estrogen-like growth stimulatory effect of BE-3-3-3-3, delaying the growth inhibitory action of this polyamine analog.

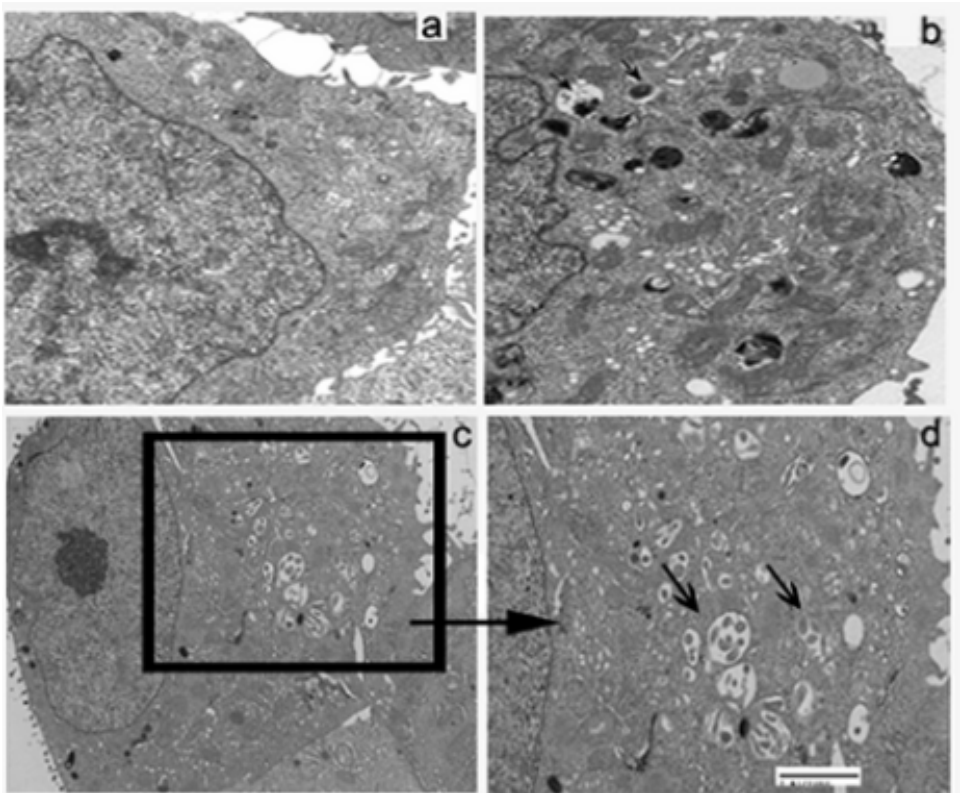

Figure 12. Ultrastuctural changes in MCF-7 cells treated with BE-3-3-3-3 for 24 h. (a) Untreated MCF-7 cells (negative control). (b) Beclin-transfected cells after nutritional starvation for 4h (positive control). Arrows indicate autophagosomes. (c) MCF-7 cells treated with 10 μM BE-3-3-3-3. (d) Expanded region of panel c, showing autophagic vacuoles (arrows). Bar represents 2 μm.

Beclin 1 localization in the presence of BE-3-3-3-3. Next, we determined the effect of BE-3-3-3-3 on the cellular localization of Beclin 1 in MCF-7 cells, 24 h after treatment (Figure 13). In the absence of the polyamine analogue, Beclin 1 fluorescence signal was weak, indicating low protein levels, and Beclin 1 was widely distributed around the nucleus (Fig. 13A). E_2 treatment (alone) increased the strength of Beclin 1 signal, which corresponded to increased protein levels,

and stimulated the accumulation of Beclin 1 around the nucleus (Fig. 13B). BE-3-3-3-3-treatment (in the absence of E_2) produced a noticeable increase in the fluorescence intensity and levels of Beclin 1 protein compared to control (Fig. 13C). Beclin 1 was localized around the nucleus, in a fashion similar to that observed in the E_2-treated cells.

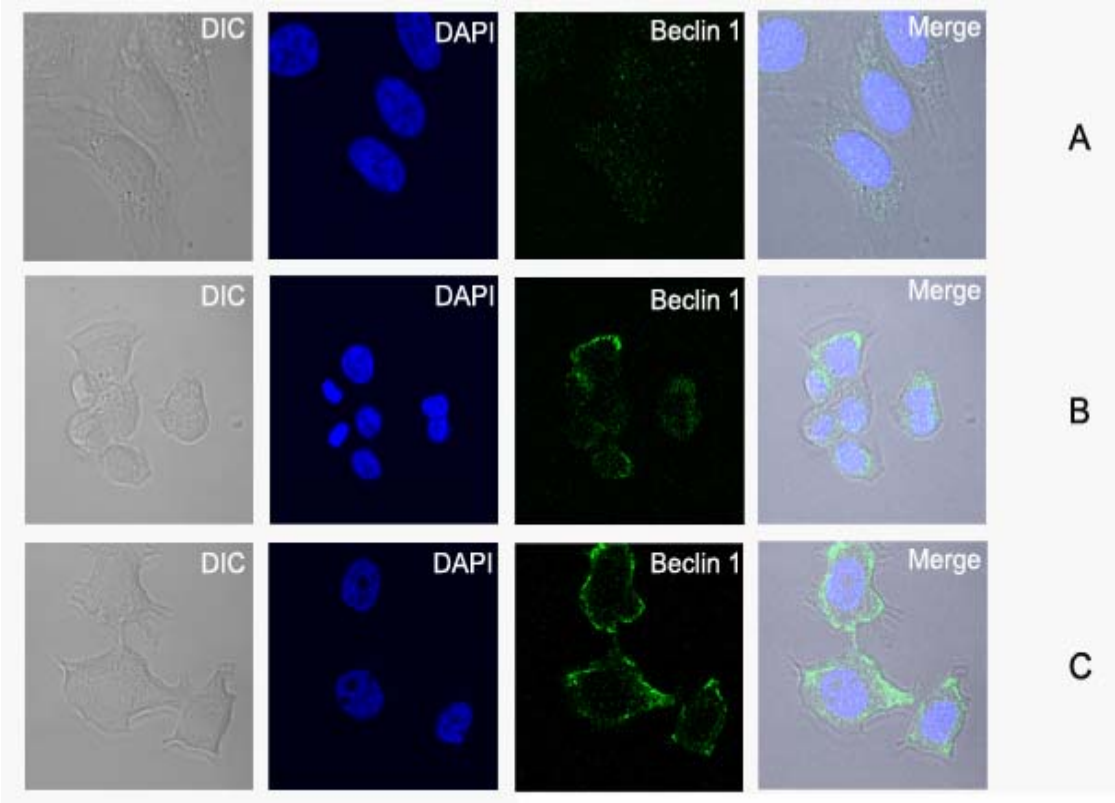

Figure 13. Effect of BE-3-3-3-3 treatment on Beclin 1 distribution in MCF-7 cells. Cells (5×10^4) were seeded in Labtek 6-well chamber slides, and either left untreated (panel A, control) or dosed after 24 h with E_2 (panel B), or 5 μM BE-3-3-3-3 (panel C). Twenty-four hours after treatment, cells were subjected to immunostaining procedure. Images were recorded using a Zeiss 510 Laser scanning microscope with a 60X objective at identical intensity settings for all treatment groups. Nuclear staining was done using DAPI (4'6'-diamidino-2-phenylindole, 1 nM). Similar results were obtained in 3 separate experiments.

Discussion

In this study, we examined the effect BE-3-3-3-3 on ERα-positive breast cancer cell growth, and found that while it was growth-inhibitory in the presence of E_2, it stimulated DNA synthesis in the absence of E_2 up to 48 h after treatment. In MCF-7 cells, this estrogen-mimetic growth

stimulation was accompanied by the modulation of several E_2–regulated genes. Delayed growth inhibition of MCF-7 cells was associated with elevated levels of autophagy-related proteins, Beclin 1 and MAP LC3-II, and autophagosome formation in the presence of BE-3-3-3-3. Confocal microscopic studies also showed increased Beclin 1 levels in BE-3-3-3-3- treated cells, as well as an accumulation of this protein around the nucleus.

Previous studies with polyamine analogues in ER-positive breast cancer cells have been conducted in the presence of E_2. Under these conditions, BE-3-3-3-3 inhibited cell growth and induced apoptosis (Faaland et al., 2000). In addition, BE-3-3-3-3 was a more potent inhibitor of tumor growth in vivo than BE-3-3-3 (Shah et al., 1999). BE-3-3-3 was recently tested in Phase I and II clinical trials. However, it produced neurotoxic side effects, and lacked a therapeutic effect in treated patients (Creaven et al., 1997, Wolff et al. 2003). A reason for BE-3-3-3's failure in vivo might involve the growth stimulatory effect of this polyamine analogue at low concentrations. These concentrations generally correspond to plasma concentration of the polyamine analog after intravenous administration.

Minchin et al. (2006) observed a growth-stimulatory effect of low concentration of BE-3-3-3 (up to 10 μM) on melanoma cells. Our [^{3}H]-incorporation experiments also showed that BE-3-3-3-3's growth-promoting effect occurred within 48 of treatment. In contrast with our data, the increased proliferation of melanoma cells was observed 4 days after treatment, and may depend on the experimental cell type. BE-3-3-3-3's growth-stimulatory effect was similar to E_2-stimulated DNA synthesis induction observed in our laboratory. The estrogenic growth properties of BE-3-3-3-3 may become important in the selection of treatment for postmenopausal women, who have very low endogenous levels of E_2. In this population, BE-3-3-3-3 might actually stimulate cancer growth instead of promoting regression.

Estrogen-mimetic behavior of BE-3-3-3-3 is further evidenced by its stimulatory effect on the expression of E_2–regulated early response genes, c-myc, c-jun, and c-fos. Transcriptional activation by the polyamine analogue probably does not result from direct DNA binding, and may involve interactions with some of the same transcription factors and co-activators (i. e. p160, p300/ CBP) used by E_2 (Karmakar et al. 2009, Sasaki et al. 2008, Cheng et al. 2006).

Alternatively, BE-3-3-3-3 may modulate gene expression through non-genomic mechanisms, such as activation of the G-protein-coupled receptor homologue GPR30 (Maggiolini et al., 2004). Downregulation of Cyclin B1 gene expression by the polyamine analogue is consistent with a previously reported degradative/downregulatory effect of E_2 on cyclin B1 mRNA during G1 phase (Thomas and Thomas, 1994). Approximately 62% of the MCF-7 cells in our study were in G1 phase, as determined by flow cytometry (unpublished data). The inhibition of c-myb expression by BE-3-3-3-3, however, contradicted the stimulatory effect of E_2, which increased c-myb mRNA levels 20-fold in ER-positive breast cancer cells (Gudas et al., 1995). Transcript levels of the tumor-suppressor gene, PTEN, were downregulated by BE-3-3-3-3. In contrast, E_2 transiently increased PTEN protein expression in human endometrial stromal cells (Guzeloglu-Kayisli et al., 2003). PTEN has also been reported to have a stimulatory effect on autophagy by relieving the autophagy-inhibiting effect of PI3K/PKB (Wurmser et al., 2002). Decreased PTEN expression in our study was observed at an early time point (4 h), whereas autophagy induction was demonstrated after 24 h. Further investigation is needed to assess the role of PTEN in the induction and progression of autophagy in MCF-7 cells.

Another estrogenic action of BE-3-3-3-3 was increased Akt phosphorylation. The proliferative effect of E_2 include the stimulation of Akt phosphorylation as part of non-genomic cell signaling of ERα (Levin et al., 2008). Akt serine/threonine kinase is a key mediator of cell survival, resistance to apoptosis and sensitivity to chemotherapeutic agents (Cicenas, 2008). Thus, BE-3-3-3-3-induced cell growth during the 48 h after treatment may involve mechanisms similar to those involved in E_2–stimulated cell growth.

Previous studies have reported that certain polyamine analogues induced the formation of large lysosomal vacuoles in treated cells (Dai et al. 1999, Porter et al. 1990, Kramer et al. 1998). Porter et al. detected vacuole formation and growth in L1210 leukemia cells after a few hours of treatment with 2.5-diamino-3-hexyne (Porter et al., 1990). This vacuolation could be completely resolved by the removal of the polyamine analogue for 12 h. Large cytoplasmic vacuoles were also observed by Kramer et al. after 24 h of treatment with BE-3-3-3 (DENSPM) in S-Adenosylmethionine Decarboxylase (AdoMetDC) overexpressing CHO/100 cells (Kramer et al.,

1998). As in the previous study, vacuolar growth could be reversed by the removal of the drug. Vacuole formation in these cells was associated with only a modest growth inhibition by BE-3-3-3, even at high intracellular polyamine analogue concentration. The explanation offered by the author(s) suggested that vacuolar sequestration of BE-3-3-3 limited its growth-inhibitory effects. We now speculate that the presence of these vacuoles indicated the activation of autophagy in response to treatment with BE-3-3-3, which promoted cell survival and delayed growth inhibition by recycling the intracellular components within the observed vacuoles. Dai et al. also observed vacuole formation after 4 h of treatment with a polyamine oxidase inhibitor MDL-72,527, in hematopoietic cells (Dai et al., 1999). In these cells, vacuoles grew in size over time, eventually engulfing key cytoplasmic organelles such as mitochondria. Vacuolar growth could, once again, be reversed with the removal of the drug. The characteristic morphology and their reversible growth and appearance of these vacuoles led us to hypothesize the involvement of autophagy in the action of these polyamine analogues.

Based on these findings, we decided to investigate whether autophagy plays a role in the delayed MCF-7 cell growth inhibition by BE-3-3-3-3 in the absence of E_2. Our EM analysis demonstrated the presence of autophagosomes, indicators of autophagy, after treatment with 10 μM BE-3-3-3-3. Additional evidence for the stimulation of autophagy comes from the polyamine analogue-mediated increase in the expression of autophagy-related proteins, Beclin 1 and MAP LC3 II.

Atg6/Beclin 1 was initially identified as a protein mediating autophagy in yeast and subsequently in mammalian cells (Liang et al., 1999). In autophagy, Beclin 1 interacts with class III PI3 kinase (vps34) in the nucleation step of the autophagosomal membrane that engulfs damaged cytoplasmic organelles and long-lived proteins targeted for lysosomal degradation (Zhong et al., 2009). Recent studies show that autophagy delayed apoptotic death of breast cancer cell death following DNA damage (Abedin et al., 2007). In another case, silencing Beclin 1, and thereby autophagy, enhanced doxorubicin-induced apoptosis (Daniel et al., 2006). These results raised the possibility that autophagy works against the apoptosis-inducing chemotherapeutic agents. In a previous study, we found that Beclin 1 modulated estrogenic

signaling by interacting with ERα in Beclin 1-overexpressing breast cancer cells. This interaction promoted antiestrogen resistance, as evidenced by decreased growth inhibition of breast cancer cells in response to treatment with tamoxifen and raloxifene. Therefore, we hypothesize that elevated expression of Beclin 1 in response to BE-3-3-3-3-treatment indicates that autophagy activation resulted in the resistance to growth-inhibitory action of this analogue, and promoted cell survival during 48 h after treatment.

MAP LC3 is a mammalian homologue of yeast Atg8, and is essential for autophagosome formation (Noda et al. 2008, Tanida et al. 2004). It is synthesized as pro-LC3, and proteolytically processed and modified during autophagy to produce MAP LC3-II (Kabeya et al., 2000). MAP LC3-II is found on the pre-autophagic membranes and autophagosomes, and is a widely accepted marker of the detection of autophagy (Kadowaki et al. 2009, Klionsky et al. 2008). Thus, an increase in the levels of this protein in response to BE-3-3-3-3 treatment indicates the induction of autophagosome formation, which is supported by our EM data.

Confocal microscopic investigation showed higher levels of Beclin 1 in the presence of BE-3-3-3-3, supporting our data on Beclin 1 protein expression. In addition, BE-3-3-3-3 caused the accumulation of the protein around the nucleus. Similar results were observed in E_2-treated cells, indicating that BE-3-3-3-3 behaves in an estrogen-mimetic manner. In a previous study, we demonstrated E_2–stimulated Beclin 1 re-localization to the perinuclear area in Beclin 1-overexpressing, MCF-7 cells (John et al., 2008). Confocal microscopy analysis of Beclin 1 distrubution in Beclin 1-overexpressing MCF-7 cells by Liang et al. (2001) showed that the protein was localized in the endoplasmic reticulum, mitochondria, perinuclear membrane as well as the nucleus. In addition, nuclear export of Beclin 1 was essential to the induction of autophagy in these cells (Liang et al., 2001).

Taken together, these results demonstrate the differential behavior of BE-3-3-3-3 in the presence and absence of E_2. It stimulated cell growth in the absence of E_2, an effect that was abolished by 96 h after treatment. In contrast, it inhibited cell growth in the presence of E_2. Early response genes in the E_2–induced growth regulatory pathways were influenced by BE-3-3-3-3. We also showed the involvement of autophagy in the 48 h growth-stimulatory phase BE-3-3-3-3,

which promoted cell survival and delayed growth inhibition in response to this polyamine analogue. Based on our findings, we propose that therapeutic agents specifically targeted for modulating autophagy might be useful in combination with polyamine analogues in controlling breast cancer cell growth in the absence of E_2.

References

Abedin, M. J., Wang, D., McDonnell, M. A., Lehmann, U., Kelekar, A. (2007) Autophagy delays apoptotic death in breast cancer cells following DNA damage. Cell Death Differ. **14**:500-10.

Anderson, E., Clarke, R. B. (2004) Steroid receptors and cell cycle in normal mammary epithelium. J. Mammary Gland Biol. Neoplasia **9**:3-13.

Bernacki, R. J., Bergeron, R. J., Porter, C. W. (1992) Antitumor activity of N^1,$N^{'}$-bis-(ethyl)spermine homologues against human MALME-3 melanoma xenografts. Cancer Res. **52**:2424-2430.

Canizares, F., Salinas, J., De Las Heras, M., Diaz, J., Tovar, I., Martinez, P., Penafiel, R. (1999) Prognostic valued of ornithine decarboxylase and polyamines in human breast cancer: Correlation with clinicopathologic parameters. Clin. Cancer Res. **5**:2035-41.

Casero, R. A., Marton, L. J. (2007) Targeting polyamine metabolism and function in cancer and other hyperproliferative diseases. Nat. Rev. Drug Discov. **6**:373-390.

Cicenas, J. (2008) The potential role of Akt phosphorylation in human cancers. Int. J. Biol. Markers. **23**:1-9.

Cheng, A. S., Jin, V. X., Fan, M., Smith, L. T., Liyanarachchi, S., Yan, P. S., Leu, Y., Chan, M. W., Plass, C., Nephew, K. P., Davuluri, R. V., Huang, T. H. (2006) Combinatorial analysis of transcription factor partners reveals recruitment of c-myc to estrogen receptor-α responsive promoters. Mol. Cell **21**:393-404.

Creaven, P. J., Perez, R., Pendyala, L., Meropol, N. J., Loewen, G., Levine, E., Berghorn, E., Raghavan, D. (1997) Unusual central nervous system toxicity in a Phase I study of N^1N^{11} diethylnorspemine in patients with advanced malignancy. Invest. New Drugs **15**:227-234.

Dai, H., Kramer, D. L., Yang, C., Murti, G., Porter, C. W., Cleveland, J. L. (1999) The polyamine oxidase inhibitor MDL-72,527 selectively induces apoptosis of transformed hematopoietic cells through lysosomotropic effects. Cancer Res. **59**:4944-4954.

Daniel, F., Legrand, A., Pessayre, D., Vadrot, N., Descatoire, V., Bernauau, D. (2006) Partial Beclin 1 silencing aggravates doxorubicin- and Fas-induced apoptosis in HepG2 cells. World J. Gastroenterol. **12**:2895-2900.

Faaland, C. A., Thomas, T. J., Balabhadrapathruni, S., Langer, T., Mian, S., Shirahata, A., Gallo, M. A., Thomas, T. (2000) Molecular correlates of the action of bis(ethyl)polyamines in breast cancer cell growth inhibition and apoptosis. Biochem. Cell Biol. **78**:415-426.

Gerner, E. W., Meyskens, F. L. (2004) Polyamines and cancer: old molecules, new understanding. Nat. Rev. Cancer **4**:781-792.

Gudas, J. M., Klein, R. C., Oka, M., Cowan, K. H. (1995) Posttrascriptional regulation of the c-myb proto-oncogene in estrogen receptor-positive breast cancer cells. Clin. Cancer Res. **1**:235-243.

Guzeloglu-Kayisli, O., Kayisli, U. A., Al-Rejjal, R., Zheng, W., Luleci, G., Arici, A. (2003) Regulation of PTEN (Phosphatase and tensin Homolog deleted on chromosome 10) expression by estradiol and progesterone in human endometrium. J. Clin. Endocrinol. Metab. **88**:5017-5026.

John, S., Nayvelt, I., Hsu, H. C., Yang, P., Liu, W., Das, G. M., Thomas, T., Thomas, T. J. (2008) Regulation of estrogenic effects by beclin 1 in breast cancer cells. Cancer Res. **68**:7855-7863.

Kabeya, Y., Mizushima, N., Ueno, T., Yamamoto, A., Kirisako, T., Noda, T., Kominami, E., Ohsumi, Y., Yoshimori, T. (2000) LC3, a mammalian homologue of yeast Apg8p, is localized in autophagosome membranes after processing. EMBO J. **19**:5720-5728.

Kadowaki, M., Karim, R. (2009) Cytosolic LC3 ratio as a quantitiative index of macroautophagy. Methods Enzymol. **452**: 199-213.

Karmakar, S., foster, E. A., Smith, C. L. (2009) Unique roles of p160 coactivators for regulation of breast cancer cell proliferation and estrogen receptor-(transcriptional activity. Endocrinology **150**:1588-1596.

Klionsky, D. J., Abeliovich, H., Agostinis, P., Agrawal, D. K., Aliev, G. et al. (2008) Guidelines for the use and interpretation of assays for monitoring autophagy in higher eukaryotes. Autophagy **4**:151-175.

Kramer, D. L., Black, J. D., Mett, H., Bergeron, R. J., Porter, C. W. (1998) Lysosomal sequestration of polyamine analogues in Chinese hamster ovary cells resistant to the s-adenosylmethionine decarboxylase inhibitor, CGP-48664. Cancer Res. **58**:3883-3890.

Leveque J., Foucher, F., Bansard, J. Y., Havouis, R., Grall, J. Y., Moulinoux, J. P. (2000) Polyamine profiles in tumor, normal tissue of the homologous breast, blood, and urine of breast cancer sufferers. Breast Cancer Res.Treat. **60**:99-105.

Leveque, J., Foucher, F., Havouis, R, Desury, D., Grall, J. Y., Moulinoux, J. P. (2000) Benefits of complete polyamine deprivation in hormone responsive and hormone resistant MCF-7 human breast adenocarcinoma in vivo. Anticancer Res. **20**:97-101.

Levin, E. R., Pietras, R. J. (2008) Estrogen receptors outside the nucleus in breast cancer. Breast Cancer Res. Treat.**108**:351-361.
Levine, B., Yuan, J. (2005) Autophagy in cell death: an innocent convict? J. Clin. Invest. **115**:2679-2688.

Liang, X. H., Jackson S, Seaman M, Brown, K., Kempkes, B., Hibshoosh, H., Levine, B. (1999) Induction of autophagy and inhibition of tumorigenesis by beclin 1. Nature **402**:672-76.

Liang, X. H., Yu, J., Brown, K., Levine, B. (2001) Beclin 1 contains a leucine-rich nuclear export signal that is required for its autophagy and tumor suppressor function. Cancer Res. **61**:3443-49.

Maggiolini, M., Vivacqua, A., Fasanella, G., Recchia, A. G., Sisci, D., Pezzi, v., Montanaro, D., Musti, A. M., Picard, D., Ando S. (2004) The G protein-coupled receptor GPR30 mediates c-fos up-regulation by 17β-estradiol and phytoestrogens in breast cancer cells. J. Biol. Chem. **279**:27008-27016.

Manni, A., Badger, B., Martel, J., Demers, L. (1992) Role of polyamines in the growth of hormone-responsive and -resistant human breast cancer cells in nude mice. Cancer Lett. **66:**1-9.

Minchin, R. F., Knight, S., Arulpragasam, A., Fogel-Petrovic, M. (2006) Concentration-dependent effects of N^1, N^{11}-diethylnorspermine on melanoma cell proliferation. Int. J. Cancer **118**:509-512.

Moshier, J. A., Dosescu, J., Skunca, M., Luk, G. D. (1993) Transformation of NIH/3T3 cells by ornithine decarboxylase overexpression. Cancer Res. **53**:2618-2622.

Musso, M., Thomas, T., Shirahata, A., Sigal, L. H., Van Dyke, M. W., Thomas, T. J. (1997) Effects of chain length modification and bis(ethyl) substitution of spermine analogs on purine-purine-pyrimidine triplex DNA stabilization, aggregation, and conformational transitions. Biochemistry **36**:1441-1449.

Noda, N. N., Kumeta, H., Nakatogawa, H., Satoo, K., Adachi, W., Ishii, J., Fujioka, Y., Ohsumi, Y., Inagaki, F. (2008) Structural basis of target recognition by Atg8/LC3 during selective autophagy. Genes Cells **13**:1211-1218.

Porter, C. W., Bernacki, R. J., Miller, J., Bergeron, R. J. (1993) Antitumor activity of N^1,N^{11}-bis-(ethyl)spermine against human melanoma xenografts and possible biochemical correlates of drug action. Cancer Res. **53**:581-586.

Porter, C. W., McManis, J., Casero, R. A., Bergeron, R. J. (1987) Relative abilities of bis(ethyl) derivatives of putrescine, spermidine, and spermine to regulate polyamine biosynthesis and inhibit L1210 leukemia cell growth. Cancer Res. **47**:2821-2825.

Porter, C. W., Stanek, J., Black, J., Vaughan, M., Ganis, B., Pleshkewych, A. (1990) Morphological evidence for an apparent lysosomotropic activity by unsaturated putrescine analogues. Cancer Res. **50**:1929-1935.
Sasaki, H., Hayakawa, J., Terai, Y., Kanemura, M., Tanabe-Kimura, A., Kamegai, H., Seino-Noda, H., Ezoe, S., Kanakura, Y., Sakata, M., Tasaka, K., Ohmichi, M. (2008) Oncogene **27**:2737-2745.

Scarlatti, F., Maffei, R., Beau, I., Codogno, P., Ghidoni, R. (2008) Role of non-canonical Beclin 1-independent autophagy in cell death induced by resveratrol in human breast cancer cells. Cell Death Differ. **15**:1318-1329.

Shah, N., Antony, T., Haddad, S., Amenta, P., Shirahata, A.,Thomas, T. J., Thomas, T. (1999) Antitumor effects of bis(ethyl)polyamine analogs on mammary tumor development in FVB/NTgN (MMTVneu) transgenic mice. Cancer Lett. **146**: 15-23.

Shah, N., Thomas, T. J., Lewis, J. S., Klinge, C. M., Gelinas, C., Thomas, T. (2001) Regulation of estrogenic and nuclear factor κB function by polyamines and their role in polyamine analog-induced apoptosis of breast cancer cells. Oncogene **20**:1715-1729.

Shappell, N. W., Miller, J. T., Bergeron, R. J., Porter, C. W. (1992) Differential effects of the spermine analog, N^1,N^{12}-bis-(ethyl)spermine, on polyamine metabolism and cell growth in human melanoma cell lines and melanocytes. Anticancer Res. **12**:1083-1090.

Streiff, R. R., Bender, J. F. (2001) Phase 1 study of N^1N^{11} diethylnorspemine (DENSPM) administered TID for 6 days in patients with advanced malignancies. Invest. New Drugs **19**:29-39.

Tanida, I., Ueno, T., Kominami, E. (2004) LC3 confugation system in mammalian autophagy. Int. J. Biochem. Cell Biol. **36**:2503-2518.

Thomas, T., Balabhadrapathruni, S., Gallo, M. A., Thomas, T. J. (2002) Development of polyamine analogs as cancer therapeutic agents. Oncol. Res.**13**:123-135.

Thomas, T., Thomas, T. J. (1994) Estradiol control of ornithine decarboxylase mRNA, enzyme activity, and polyamine levels in MCF-7 breast cancer cells: therapeutic implications. Breast Cancer Res. Treat. **29**:189-201.

Thomas, T., Thomas, T. J. (2003) Polyamine metabolism and cancer. J. Cell Mol. Med. **2**:113-126.

Thomas, T., Thomas, T. J. (2001) Polyamines in cell growth and cell death: molecular mechanisms and therapeutic applications. Cell Mol. Life Sci. **58**:244-258.

Thomas, T., Thomas, T. J. (1994) Regulation of cyclin B1 by estradiol and polyamines in MCF-7 breast cancer cells. Cancer Res. **54**:1077-1084.

Vijayanathan, V., Venkiteswaran, S., Nair, S. K., Verma, A., Thomas, T. J., Zhu, B. T., Thomas, T. (2006) Physiologic levels of 2-methoxyestradiol interfere with nongenomic signaling of 17beta-estradiol in human breast cancer cells. Clin. Cancer Res. **12**:2038-48.

Watanabe, J., Kamata, Y., Seo, N., Okayasu, I., Kuramoto, H. (2007) Stimulatory effect of estrogen on the growth of endometrial cancer cells is regulated by cell-cycle regulators. J. Steroid Biochem. Mol. Biol. **107**:163-171.

Wolff, A. C., Armstrong, D. K., Fetting, J. H., Carducci, M. K., Riley, C. D., Bender, J. F., Casero, R. A., Davidson, N. E. (2003) A Phase II study of the polyamine analog N^1,N^{11}-diethylnorspemine (DENSpm) daily for five days every 21 days in patients with previously treated metastatic breast cancer. Clin. Cancer Res. **9**:5922-5928.

Yager, J. D., Davidson, N. E. (2006) Estrogen Carcinogenesis in Breast Cancer. N. Engl. J. Med. **354**:270-282.

Yang, Y., Liang, Z., Gu, Z., Qin, Z. (2005) Molecular mechanism and regulation of autophagy. Acta Pharmacol. Sin. **26**:1421-1434.

Zhong, Y., Wang, Q. J., Li, X., Yan, Y., Backer, J. M., Chait, B. T., Heintz, N., Yue, Z. (2009) Distinct regulation of autophagic activity by Atg14L and Rubicon associated with Beclin 1-phoshatidylinositol 3-kinase complex. Nat. Cell Biol. Epub ahead of print.

Chapter 3

Specificity of α-methylated polyamine stereosisomers on polyamine-DNA interactions

Irina Nayvelt, Ipsit Pandya, Alex R. Khomutov, Rajesh Patel, and T.J. Thomas

Abstract

We compared the abilities of spermine and its α,α'-dimethylated stereoisomers (Me_2Spm), R,R-Me_2Spm, S,S-Me_2Spm, R,S-Me_2Spm, and racemic (R,R; R,S; S,S)- Me_2Spm, to provoke calf thymus (CT) DNA condensation. Condensation efficiency was determined by measurement of EC_{50} (polyamine concentrations at which 50% of the DNA is in compacted form). RR-, RS-, and Rac-Me_2Spm's were more efficient condensing agents than spermine, with significantly lower EC_{50} values ($p \leq 0.01$ RR and RS, $p \leq 0.05$ Rac). On the other hand, SS-Me_2Spm's condensing ability was comparable to that of spermine. Hydrodynamic radii (R_h) of nanoparticles ranged between 39.6 – 48.4 nm. Only R,R- and S,S-Me_2Spm isomers demonstrated significantly larger condensates than spermine ($p \leq 0.01$). Electron microscopic investigation showed the presence of toroids and spheroids in DNA condensates. Melting temperature investigation did not show any significant difference in the ability of different analogues to stabilize duplex DNA. Our findings indicate that Me_2Spm isomers are efficient DNA packaging agents, and may be considered as possible gene delivery vehicles. Our study also reveals hidden stereospecificity of these isomers in DNA interaction and condensation.

Introduction

The natural polyamines, putrescine, spermidine and spermine, are ubiquitous intracellular components whose presence is necessary for cell growth and proliferation.[1] Although several studies have shown that polyamines are involved in a variety of cellular processes, including DNA packaging, replication, transcription and translation, their exact role in cell proliferation has not been elucidated.[2-4] Under physiological conditions, positively charged polyamines interact electrostatically with negatively charged DNA, and induce DNA compaction when 89-90% of the charges have been neutralized.[5,6] We recently found that the attractive component of the free energy is always 2.3 ± 0.2 times larger than the repulsive component of the free energy at force-balance equilibrium.[7] DNA condensation by multivalent ions is believed to occur when the ions have at least three positive charges, and ions with higher valence are able to promote DNA compaction at lower concentrations. Polyamines facilitate the coil-globule transition by lowering the free energy threshold, and DNA in the globule remains in the B-form.[8]

Under conditions of low salt and low DNA concentration, intramolecular condensation is believed to be favored, whereas high salt conditions lead to intermolecular condensation and aggregation.[9.10] Polyamine-mediated DNA condensation has been shown to produce tightly compacted structures such as toroids, rods, and spheroids.[11-13] Toroids are believed to contain B-form DNA, and have a columnar hexagonal liquid crystalline order of packaging.[14] Dynamic light scattering and electron microscopic studies conducted with spermine found that the size of nanoparticles is in the range of 50-130 nm.[6,13] Several studies have demonstrated that in addition to non-specific electrostatic interactions, polyamine structure plays a large role in its DNA binding and compaction.[7,15] Experiments performed with polyamine analogues with various structural modifications found corresponding changes in DNA binding affinity, condensing ability, and DNA arrangement of the condensed products.[6,16]

Strict control of polyamine levels within cells is necessary for normal cell proliferation, and failure to maintain polyamine homeostasis leads to metabolic disorders.[1,17] High levels of polyamines are found in cancer cells, and they promote increased cell proliferation.[18,19] Low levels of cellular polyamines can also have deleterious effects, leading to growth inhibition and

apoptosis. Compounds that affect polyamine homeostasis have been studied in an effort to discover cures for conditions that involve disorders of polyamine metabolism.[20,21] Several studies have demonstrated that polyamine analogues can downregulate polyamine synthesis and cellular uptake, and/or activate catabolism. However, while terminal amino group-alkylated polyamine analogues are able to downregulate polyamine levels in the cell, they are unable to perform the needed cellular functions of polyamines.[22,23]

A new type of polyamine analogues, in which methyl group(s) are attached to backbone carbon atom have shown several promising characteristics.[24,25] They are actively transported into cells and can substitute for the function of natural polyamine counterparts in maintaining cell growth. The methyl group addition interferes with acetylation by SSAT and prevents degradation of these compounds. A recent study demonstrated that administration of 1-methylspermidine was able to prevent severe pancreatitis caused by pancreatic polyamine depletion, indicating that this analogue was successfully internalized by pancreatic cells and was resistant to degradation.[26]

To examine the impact of polyamine structure on DNA condensation, we compared the ability of spermine (Spm) and several α,α'-dimethylated spermine (α,α'-Me_2Spm) stereoisomers to condense and stabilize CT DNA. We found some significant differences in the DNA condensing abilities of these compounds, indicating that polyamine geometry plays a part in DNA condensation.

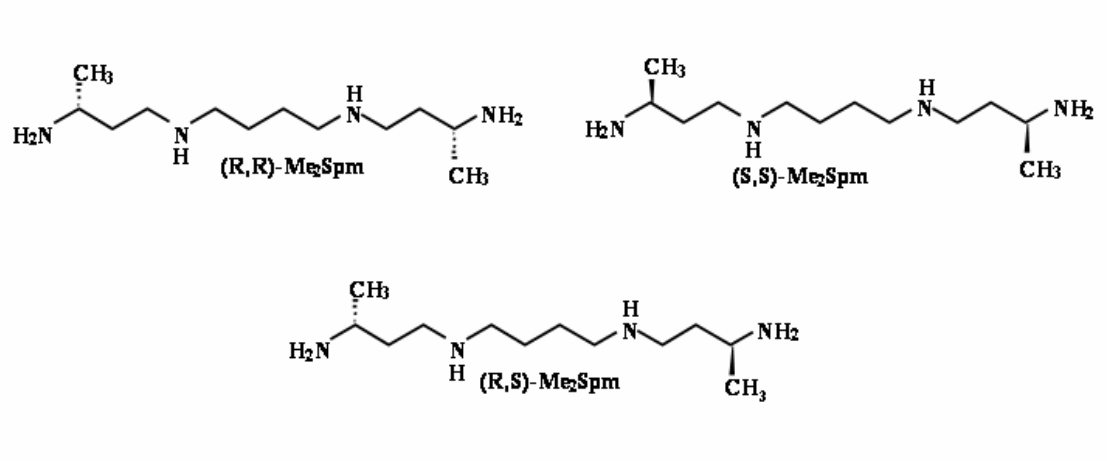

Figure 14. Chemical structure of spermine stereoisomers used in this study.

MATERIALS AND METHODS

DNA. Calf Thymus (CT) DNA was purchased from Worthington Biochemical Corporation (Lakewood, NJ), and was used for all experiments. It was dissolved in 1 mM Na cacodylate buffer (1 mM Na cacodylate, 0.5 mM EDTA, pH 7.4), and dialyzed against the same buffer for 3 hours. The average molecular weight of the DNA, determined by multiangle laser light scattering and Zimm plot, was 6 x 10^6. DNA solution's absorbance ratio (A_{260}/A_{280}) was measured at 1.9, indicating that the DNA was free from protein contamination.

Reagents. Spermine.4HCl was purchased from Sigma Chemical Co. (St. Louis, MO). α,α'-Dimethylated spermine (Me_2Spm) isomers were tetra hydrochloride salts, and were synthesized and characterized by one of us (ARK). Stereoisomer structures are represented in Figure 14.

Total Intensity Light Scattering. Static light scattering experiments were performed using a Fluoromax-2 spectrofluorometer (Jobin Yvon-Spex Instruments S. A., Inc., Edison, NJ).[7,15] The excitation and emission monochromators were both set to a wavelength of 305 nm with 5 nm band pass. The scattered light intensity was collected at a 90° angle with respect to the incident beam. Small quantities of spermine and/or isomers were added to the CT DNA/buffer solution (0.5 μg/ml DNA) in 2 ml borosilicate glass tubes to achieve the desired concentration of the condensing agent. The solutions were vortexed gently for 5s and allowed to equilibrate for 30

minutes at room temperature. They were then centrifuged in a Beckman GS 6KR centrifuge for 10 minutes at 500 x g to avoid light scattering from aggregated particles. Centrifugation at 500 x g did not induce phase separation or a reduction in DNA concentration in solution. Therefore, the light scattering measurements are representative of the DNA concentrations used.

Dynamic Laser Light Scattering. Dynamic light scattering experiments were performed using DynaPro model MSX equipment (Protein Solutions, Inc., Charlottesville, VA).[7,15] Spermine and/or isomer solutions were added to DNA solutions (0.5 μg/ml) to achieve the desired condensing agent concentrations. The samples were mixed and allowed to attain equilibrium for 30 minutes at 22 °C. Samples were centrifuged for 10 minutes at 500 x g and 4 °C to remove aggregate particles. Hydrodynamic radii were measured by transferring 45 μl of sample solution to a standard quartz cuvette, and the scattered light was detected at a 90° angle to the incident beam. All measurements were performed in the same cuvette to avoid variations introduced by minor differences between cuvettes. The cuvette was washed with double distilled water and vacuum-dried before each measurement.

A laser beam from a 2W laser (800 nm wavelength) was passed through a quartz cell holding the sample, and the scattered light was detected at a 90° angle with respect to the incident beam. The scattered light was analyzed with an autocorrelator in order to generate the first-order autocorrelation function. The following equation describes the autocorrelation function, $g^{(l)}(\tau)$, for monodisperse particles that are much smaller than the incident beam:

$$g^{(l)}(\tau)=\exp[-Dq^2(\tau)]$$

In this equation, τ is the decay time, q (= $4\pi n/[\lambda_o \sin(\theta/2)]$) is the scattering vector which is a function of the incident beam wavelength λ_o, the scattering angle θ, the refractive index of the solvent n, and the diffusion coefficient D. The hydrodynamic radius (R_h) is calculated from the diffusion coefficient using the Stokes-Einstein equation:

$$R_h = kT/6\pi\eta D,$$

where T is the absolute temperature, η is solvent viscosity, and k is the Boltzmann constant. Data were analyzed by a Dynamics Version 6 software package obtained from Protein Solutions, Inc.

Electron Microscopy. Structural morphology of condensates was analyzed using a JEOL 1200EX electron microscope. Samples were prepared by adding appropriate amounts of spermine/isomer solutions to CT DNA/buffer solutions (0.5 μg/ml) or (2.5 μg/ml). The solutions were vortexed lightly and allowed to equilibrate for 30 minutes. Formvar-coated copper grids were glow discharged for 60 seconds. Samples were placed on the grids for 30 minutes, and excess solution was blotted using a filter paper. The grids were stained with either 1% uranyl acetate or 1% phosphotungstenic acid solution (pH ~ 7.0) for a minute and allowed to air dry.

Melting Temperature (T_m) Measurements. T_m experiments were performed using a Beckman DU640 spectrophotometer. T_m cell block contained six cells, one of which was filled with buffer (used as a blank). Other cells were filled with DNA solution alone or with an appropriate concentration of spermine/isomer reagent. Melting temperature was obtained by increasing the temperature of the sample at a rate of 0.5 °C/min, within a range of 50-95 °C, and monitoring the absorbance (A) every 30 seconds. T_m values were taken as the temperature at which half of the complex was dissociated. Computer-generated first derivative of the melting curve, dA/dT (where A is absorbance and T is temperature) was also used for determining T_m. T_m measurements obtained by both methods did not deviate by more than 1 °C.

RESULTS

Total Intensity Light Scattering. In this set of experiments, we studied the DNA condensing abilities of spermine and α,α'-dimethylated spermine (Me_2Spm) stereoisomers, R,R-Me_2Spm, S,S-Me_2Spm, R,S-Me_2Spm, and Rac-Me_2Spm (33.3% R,R; 33.3% S,S; 33.3% R,S). In Figure 15, total intensity of scattered light is graphed against concentration of each spermine compound. At a critical concentration of the condensing reagent, we observed a sharp rise in scattered light intensity. At higher concentrations, the scattered light intensity reached a plateau, which

corresponded to complete condensation of CT DNA at this concentration range. We compared DNA condensing ability of each compound by calculating their EC_{50} values (Table 3), which correspond to spermine/isomer concentrations at which half of the DNA was in the compacted form. The condensing efficiency of spermine and its isomers appeared as follows: RR-Me_2Spm>RS-Me_2Spm>Rac-Me_2Spm>SS-Me_2Spm>Spm. RR-, RS-, and Rac- Me_2Spm's EC_{50} values were significantly different from spermine ($p \leq 0.01$ RR and RS, $p \leq 0.05$ Rac).

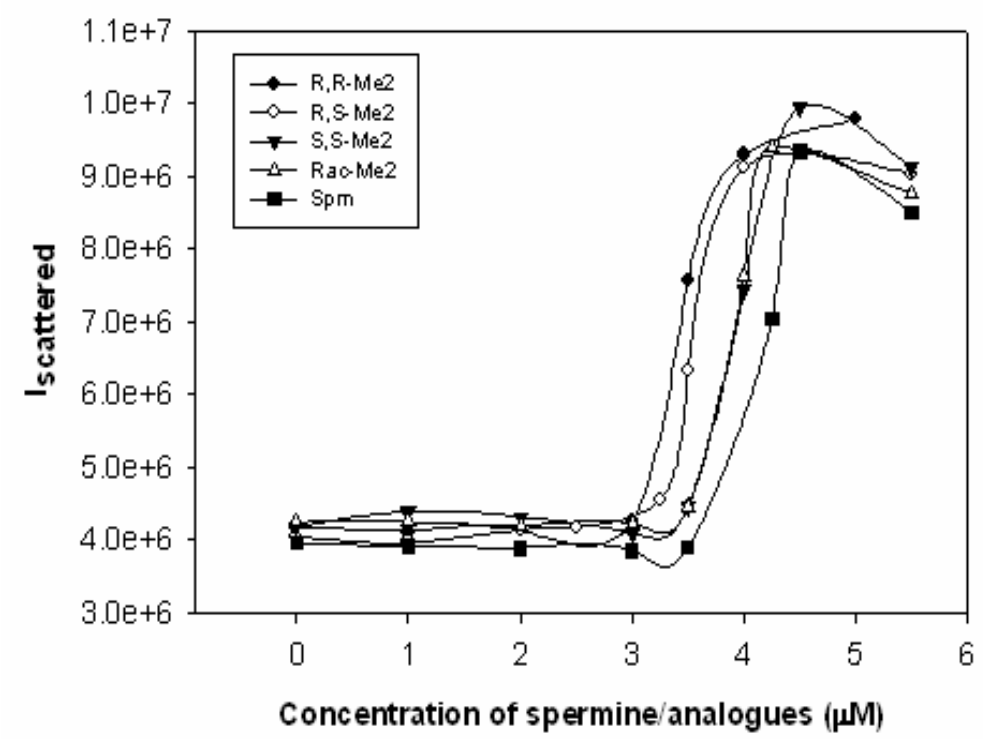

Figure 15. Typical plots of relative intensity of scattered light at 90° against concentrations of spermine and Me_2Spm analogues. The CT DNA solution had a concentration of 0.5 μg/ml. The experiment was performed in 1 mM Na cacodylate buffer (pH 7.4), and repeated at least 3 times.

Table 3. EC_{50} values of spermine and its Me_2Spm stereoisomers.

	EC_{50}, μM*
	Mean ± SD
Spm	4.17 ± 0.06 [4,5,7]
SS	3.97 ± 0.12 [4,5]
RR	3.4 ± 0.1 [2,3,6]
RS	3.55 ± 0.06 [2,3,6]
Rac	3.94 ± 0.12 [1,4,5]

*Measurements were made in 1 mM Na cacodylate buffer (pH 7.4), with CT DNA concentration of 0.5 μg/ml. ± indicates SD from at least 4 separate experiments. Standard deviations in EC_{50} values were less than 5%. [1] $p \leq 0.05$ vs spermine; [2] $p \leq 0.01$ vs. spermine; [3] $p \leq 0.01$ SS; [4] $p \leq 0.01$ RR; [5] $p \leq 0.01$ RS; [6] $p \leq 0.01$ Rac; [7] ≤ 0.05 Rac.

Hydrodynamic Radius Measurement of Condensates. In the next series of experiments, we determined the sizes of nanoparticles produced during CT DNA condensation by spermine and its isomers in the presence of 1 mM Na cacodylate buffer, pH 7.4. Spermine/isomer concentrations found in the plateau regions of static light scattering curves were used in these experiments, indicating that the DNA was in the fully condensed form. Hydrodynamic radii (R_h) of the condensates ranged from 39.6±1.1 nm (RS- Me_2Spm) to 48.4±1.2 nm (SS-Me_2Spm), and did not follow the same pattern as the EC_{50} values (Table 4). Particle sizes increased in the following order: RS- Me_2Spm < Spm < Rac-Me_2Spm < RR- Me_2Spm < SS-Me_2Spm (Table 4). R_h values of nanoparticles prepared from the SS- and RR-Me_2Spm differed significantly from those produced by spermine ($p \leq 0.01$).

Table 4. Hydrodynamic radii (R_h) of condensates formed in the presence of spermine and Me_2Spm stereoisomers.

Hydrodynamic Radii (nm)	
	Mean ± SD
Spm	40.4 ± 1.0 [3,5]
SS	48.4 ± 1.2 [1,6,8,10]
RR	45.1 ± 2.5 [2,4,7]
RS	39.6 ± 1.1 [3,5,11]
Rac	42.6 ± 2.4 [3,9]

Measurements were made in 1 mM Na cacodylate buffer (pH 7.4). ± indicates SD from 4-6 separate experiments. Standard deviations in R_h values were less than 5%. [1] indicates $p \leq 0.01$ vs spermine; [2] $p \leq 0.001$ vs. spermine; [3] $p \leq 0.01$ vs. SS, [4] $p \leq 0.05$ vs. SS; [5] $p \leq 0.001$ vs RR; [6] $p \leq 0.05$ vs. RR; [7] $p \leq 0.001$ vs. RS; [8] $p \leq 0.01$ vs. RS; [9] $p \leq 0.05$ vs. RS; [10] $p \leq 0.01$ vs. Rac; [11] $p \leq 0.05$ vs. Rac.

Electron Microscopy (EM). In this series of experiments we analyzed the shapes and sizes of nanoparticles produced in the course of CT DNA condensation by spermine and Me_2Spm analogues in 1mM Na cacodylate buffer, pH 7.4. Representative electron micrographs of condensate structures are shown in Figure 16. In the absence of condensing agents, DNA remained in an aggregated, uncoiled state (Panels A). Upon the addition of polyamines, spheroids and toroids were formed (Panel B-F). While spermine and other isomers generally produced round-shaped structures, SS-Me_2Spm also formed spindle-shaped particles (Panels C, b-c). Particle size varied, but was similar, overall, to our dynamic light scattering measurements. It should be noted that the larger structures shown in Figure 16 do not represent the majority of nanoparticle population, but were selected due to better negative staining.

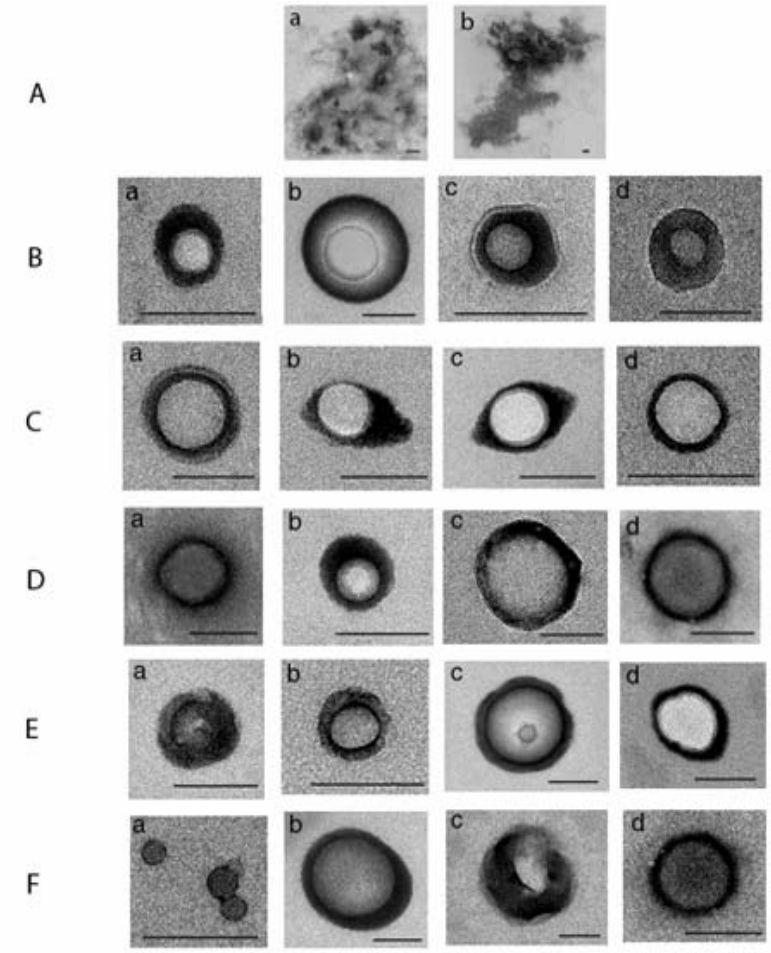

Figure 16. Representative electron micrographs of CT DNA alone (Panel A), and CT DNA condensed in the presence of spermine (Panel B), SS-Me_2Spm (Panel C), RR-Me_2Spm (Panel D), RS-Me_2Spm (Panel E), and Rac-Me_2Spm (Panel F). Scale bar is 100 nm.

T_m determination of spermine/isomers-DNA complexes. We compared DNA stabilizing property of spermine and Me_2Spm isomers by comparing the T_m values obtained for each compound. T_m data was obtained by monitoring the UV absorbance of CT DNA at 260 nm as the temperature varied from 50 to 95 °C. At a critical temperature, a sharp rise in UV absorbance is observed in the melting profile of each compound, which corresponds to DNA strand separation/melting. Figure 17 shows representative absorbance-temperature profiles of CT DNA in the presence of increasing concentration of Rac-Me_2Spm. Each compound induced DNA stabilization in a concentration-dependent manner, as evidenced by the increasing T_m readings

(65 – 90 °C), as the spermine/analogue concentrations varied from 0-100 μM (Figure 18 and Table 5). However, the most efficient DNA condensing agents did not provide the greatest degree of duplex stabilization. In fact, spermine demonstrated the greatest DNA stabilizing ability, as evidenced by its T_m values at concentrations of 10-100 μM. These results indicate that DNA condensation and stabilization may occur through divergent mechanisms.

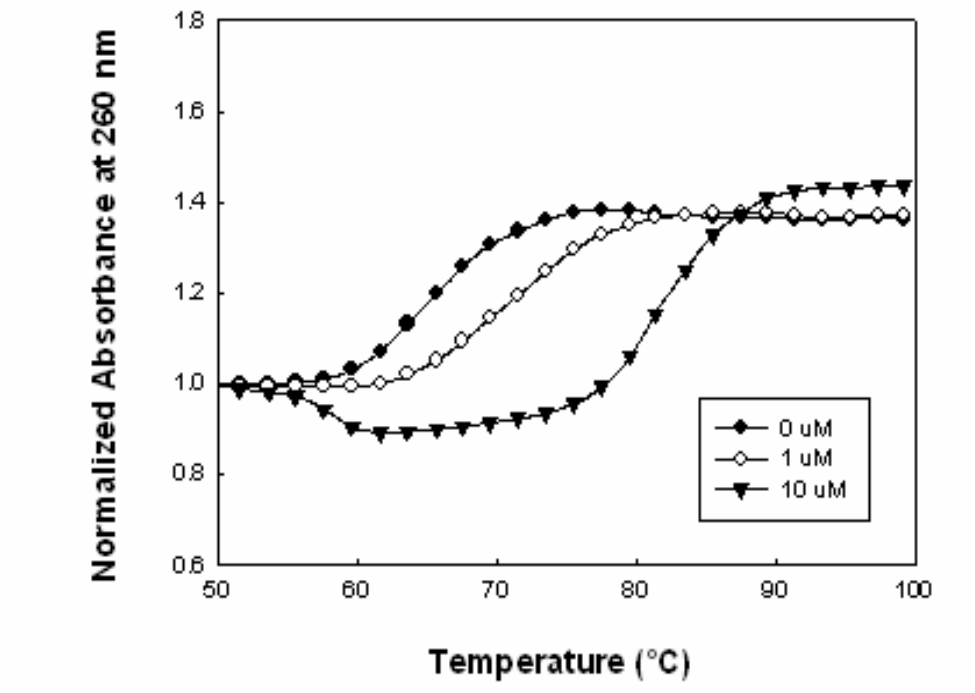

Figure 17. Representative melting profiles of CT DNA in the presence of Rac-Me_2Spm. The Tm measurements were conducted with a DNA concentration of 6.25 μg/ml, in 1 mM Na cacodylate buffer (pH 7.4). Heating rate was 0.5 °C/minute.

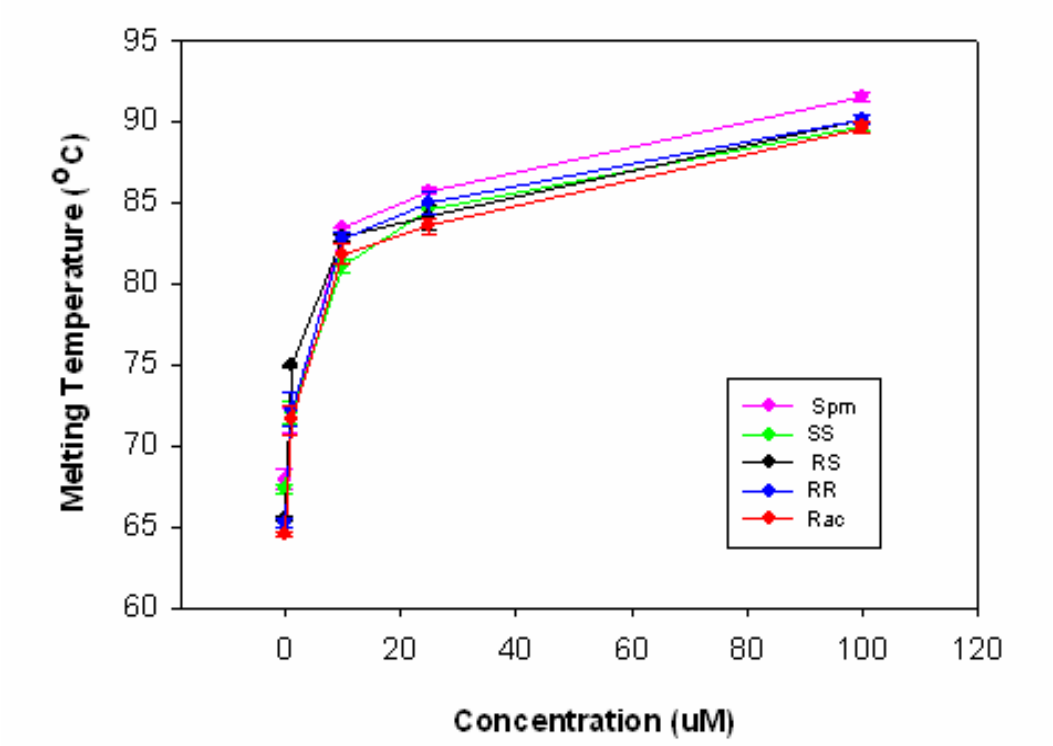

Figure 18. Effect of increasing spermine and Me_2Spm analogue concentrations on the DNA melting temperature. Experiments were performed with 6.25 μg/ml of CT DNA, and 1 mM Na cacodylate buffer. Error bars indicate standard deviation from at least 3 experiments, and in many cases are small enough to be contained within the symbol.

Table 5. Effects of spermine and Me_2Spm analogues on the melting T_m (°C) of DNA.

Conc. (μM)	Spermine Mean ± SD	SS-Me_2Spm Mean ± SD	RS-Me_2Spm Mean ± SD	RR-Me_2Spm Mean ± SD	Rac-Me_2Spm Mean ± SD
0	66.1 ± 1.4	66.1 ± 1.4	66.1 ± 1.4	66.1 ± 1.4	66.1 ± 1.4
1	71.6 ± 0.8 [i]	72 ± 0.7	74.9 ± 0.1 [b,l]	72.3 ± 1.1	71.6 ± 0.9 [i]
10	83.5 ± 0.1 [d,l]	81.1 ± 0.4 [a,g,i]	82.8 ± 0.21 [e]	82.8 ± 0.4 [e]	81.8 ± 0.7 [b]
25	85.7 ± 0.2 [f,j,l]	84.6 ± 0.6 [c]	84.1 ± 0.72 [c]	85 ± 0.7 [m]	83.5 ± 0.5 [b,h]
100	91.5 ± 0.3 [d,g,i,k]	89.7 ± 0.3 [a]	90.1 ± 0.3 [b]	90.1 ± 0.3 [b]	89.6 ± 0.3 [a]

T_m measurements were performed in at least 3 separate experiments, with 6.25 μg/ml of CT DNA in 1 mM Na cacodylate buffer. The SD in T_m measurements was ≤ 1 °C.
[a] p≤0.001 vs. spermine; [b] p≤0.01 vs. spermine; [c] p≤0.05 vs. spermine; [d] p≤0.001 vs. SS; [e] p≤0.01 vs. SS; [f] p≤0.05 vs. SS; [g] p≤0.01 vs. RR; [h] p≤0.05 vs. RR; [i] p≤0.01 vs. RS; [j] p≤0.05 vs. RS; [k] p≤0.001 vs. Rac; [l] p≤0.01 vs. Rac; [m] p≤0.05 vs. Rac.

Discussion

Our results indicate that in addition to positive charge, spatial arrangement of multivalent ions like spermine and its α,α'-methylated stereoisomers could influence DNA compaction efficiency and the sizes of resultant nanoparticles. We found that R,R-, R,S- and Rac- Me_2Spm isomers are more efficient DNA condensing agents than spermine, as evidenced by their significantly lower EC_{50} values ($p \leq 0.1$, $p \leq 0.1$, and $p \leq 0.5$, respectively). Hydrodynamic radii ranged from 39.6 ± 1.1 to 48.4 ± 1.2 nm, and only S,S- and R,R- Me_2Spm produced significantly larger condensates than spermine ($p \leq 0.1$). Melting temperature studies demonstrated that Spm conferred the greatest duplex stability at concentrations .

Most studies on polyamine analogues focused on alkylated derivatives, in which the N groups undergo modification.[27-29] Alkylated analogues were shown to be cytotoxic against tumor cell lines, and efforts have been directed toward improving their cytotoxicity while reducing their negative side effects.[30-32] On the other hand, the α,α'-dimethyl modification leaves the primary amino groups intact and does not affect the charge distribution of a polyamine moiety.[33] Me_2Spm was shown to be metabolically stable, resisting acetylation by SSAT and subsequent degradation by oxidazes. During in vivo studies, prior administration of methylated spermine and spermidine analogues was able to prevent the development of pancreatitis in transgenic mice, leading to the conclusion that methylspermine analogues have the ability to substitute for the metabolic function of natural polyamines.[19] The physico-chemical properties of methylspermine analogues have not been extensively investigated to date. Therefore, we examined DNA condensing abilities and particle properties of Me_2Spm isomers.

Evidence from tissue culture and other studies suggests that stereoisomer structure has an impact on its biological activity.[34,35] Vijayanathan et al. found that structural characteristics of spermine homologues, such as the number of methylene spacings between the secondary amine groups, play an important role in their DNA condensing abilities and the sizes of resultant nanoparticles.[7] Valasinas et al. found that a cis-decamine isomer was less efficient at inducing DNA aggregation and less cytotoxic than other decamines.[36] This finding was attributed to its less stretched conformation, and resulting differences in binding to DNA. The study of salicyl diamines

of different conformations by Gao et al. showed that the R,R stereoisomer was the most effective cytotoxic agent in MCF-7 cells.[37] The isomer also had the greatest effect on cyclin D1 mRNA expression, downregulating it to 40% of control, compared to other isomers that were able to lower mRNA expression only to 68-71% of control. In a study of putrescine analogues, Higashi et al. found that distance between amino groups and spatial orientation influenced analogues' ability to stimulate antizyme synthesis by inducing frame shifting.[38]

Sizes of nanoparticles produced in this study generally correspond to sizes of polyamine-DNA condensates previously reported in literature. Particle size measurements can be influenced by many factors, including the size of the DNA undergoing condensation, starting reactant concentrations, ionic conditions, mixing protocol, as well as the method of measurement. In a previous study, Thomas and Bloomfield observed T4 DNA-spermidine condensates with hydrodynamic radii of 48-49 nm.[39] Using both dynamic light scattering (DLS) and atomic force microscopy (AFM), Vijayanathan et al. reported particle formation between PGL-3 plasmid (> 5 kb in size) and polyamines/polyamine analogues with radii of 51-96 nm.[12] Sizes of nanoparticles decreased with increasing positive charge of the compacting agent. A DLS study with λ-phage DNA (size: ~ 48.5 kb, MW: 31.5×10^6 Da), produced nanoparticles of similar size, 41 nm, to those observed in our study conducted with shorter DNA. The size of λ-DNA condensates depended on their structural specificity, increasing with the length of the methylene spacer between the secondary amino groups.

Our melting temperature investigation demonstrates that spermine and its stereoisomers stabilize CT-DNA in a concentration-dependent manner. These findings are in agreement with other melting studies by Thomas and Bloomfield[40] and Saminathan et al.[41] The lack of correlation between DNA-condensing and duplex-stabilizing abilities of various isomers in our study may be attributed to the fact that DNA condensation and stabilization occur through different mechanisms. This hypothesis is supported by Terui et al., who found that although longer polyamines stabilized DNA more effectively than shorter counterparts, the mechanism of stabilization was similar and independent of polyamine chemical structure.[42]

Studies with protamines and polyamines demonstrate their preferential binding in the minor groove of DNA.[43] We hypothesize that differences in spatial arrangement of methylated stereoisomers can influence their steric interactions with DNA, thereby affecting condensing abilities and particle size.

In summary, our study demonstrates that in addition to ion valence, spatial arrangement of spermine stereoisomers plays an important role in their DNA condensation efficiency. Nanoparticle sizes were also dependent on structural conformation of the condensing agents. These finding may help in the configuration of efficient gene delivery vehicles.

Acknowledgment.

National Institutes of Health (CA080163 to T.J.T. and T.T.).

References

(1) Thomas, T.; Thomas, T. J. Polyamines in cell growth and cell death: molecular mechanisms and therapeutic applications.Cell. Mol. Life Sci. **2001**, 58, 244-258.

(2) Gerner, E. W.; Meyskens, F. L., Jr. Polyamines and cancer: old molecules, new understanding. Nat. Rev. Cancer **2004,** 4, 781-792.

(3) Casero, R. A., Jr.; Marton, L. J. Targeting polyamine metabolism and function in cancer and other hyperproliferative diseases. Nat. Rev. Drug Discov. **2007,** 6, 373-390.

(4) Wilson, R. W.; Bloomfield, V. A. Counterion-induced condensation of deoxyribonucleic acid. A light-scattering study. Biochemistry **1979,** 18, 2192-2196.

(5) Thomas, T. J.; Bloomfield, V. A. Quasielastic laser light scattering and electron microscopy studies of the conformational transitions and condensation of poly(dA-dT).poly(dA-dT). Biopolymers **1985**, 24, 2185-2194.

(6) Vijayanathan, V.; Thomas, T.; Thomas, T. J. DNA nanoparticles and development of DNA delivery vehicles for gene therapy. Biochemistry **2002,** 41, 14085-14094.

(7) Todd, B. A.; Parsegian, V. A.; Shirahata, A.; Thomas, T. J.; Rau, D. C. Attractive forces between cation condensed DNA double helices. Biophys. J. **2008,** 94, 4775-4782.

(8) Baigi, D.; Yoshikawa, K. Dielectric control of counterion-induced single-chain folding transition of DNA. Biophysical J. **2005,** 88, 3486-3493.

(9) Pelta, J.; Livolant, F.; Sikorav, J. L. DNA aggregation induced by polyamines and cobalthexamine. J. Biol. Chem. **1996,** 271, 5656-5662.

(10) Saminathan, M.; Antony, T.; Shirahata, A.; Sigal, L. H.; Thomas, T.; Thomas, T. J. Ionic and structural specificity effects of natural and synthetic polyamines on the aggregation and resolubilization of single-, double-, and triple-stranded DNA. Biochemistry **1999,** 38, 3821-3830.

(11) Arscott, P. G.; Li, A. Z.; Bloomfield, V. A. Condensation of DNA by trivalent cations. 1. Effects of DNA length and topology on the size and shape of condensed particles. Biopolymers **1990,** 30, 619-630.

(12) Vijayanathan, V.; Thomas, T.; Antony, T.; Shirahata, A.; Thomas, T. J. Formation of DNA nanoparticles in the presence of novel polyamine analogues: a laser light scattering and atomic force microscopic study. Nucleic Acids Res. **2004,** 32, 127-1234.

(13) Sarkar, T.; Vitoc, I.; Mukerji, I.; Hud, N. V. Bacterial protein HU dictates the morphology of DNA condensates produced by crowding agents and polyamines. Nucleic Acids Res. **2007,** 35, 951-961.

(14) Saminathan, M.; Thomas, T.; Shirahata, A.; Pillai, C. K. S.; Thomas, T. J. Polyamine structural effects on the induction and stabilization of liquid crystalline DNA: potential applications to DNA packaging, gene therapy and polyamine therapeutics. Nucleic Acids Res. **2002,** 30, 3722-3731.

(15) Vijayanathan, V.; Thomas, T.; Shirahata, A.; Thomas, T. J. DNA condensation by polyamines: a laser light scattering study of structural effects. Biochemistry **2001**, 40, 13644-13651.

(16) N'soukpoé-Kossi, C. N.; Ouameur, A. A.; Thomas, T.; Shirahata,; A, Thomas, T. J.; Tajmir-Riahi, H. A. DNA interaction with antitumor polyamine analogues: a comparison with biogenic polyamines. Biomacromolecules **2008,** 9, 2712-2718.

(17) García-Faroldi, G.; Sánchez-Jiménez, F.; Fajardo, I. The polyamine and histamine metabolic interplay in cancer and chronic inflammation. Curr. Opin. Clin. Nutr. Metab. Care **2009,** 12, 59-65.

(18) Thomas, T.; Thomas, T. J. Polyamine metabolism and cancer. J. Cell. Mol. Med. 2003, 7, 113-126.

(19) Abe, K.; Saito, T.; Kitamura, S.; Konaka ,R. Elevated spermidine level in pleural fluid of patients with lung cancer. Clin. Chim. Acta. **1990**, 188, 183-184.

(20) Moinard, C.; Cynober, L.; de Bandt, J. P. Polyamines: metabolism and implications in human diseases. Clin. Nutr. **2005,** 24, 184-197.

(21) Linsalata, M.; Russo, F. Nutritional factors and polyamine metabolism in colorectal cancer. Nutrition **2008,** 24, 382-389.

(22) Seiler, N. Thirty years of polyamine-related approaches to cancer therapy. Retrospect and prospect. Part 2. Structural analogues and derivatives. Curr. Drug Targets **2003,** 4, 565-585.

(23) Thomas, T. Balabhadrapathruni, S. Gallo, M. A.; Thomas, T. J. Development of polyamine analogs as Cancer Therapeutic Agents. Oncol. Res. **2002,** 13, 123-135.

(24) Faaland, C. A.; Thomas, T. J.; Balabhadrapathruni, S.; Langer, T.; Mian, S.; Shirahata, A.; Gallo, M. A.; Thomas, T. Molecular correlates of the action of bis(ethyl)polyamines in breast cancer cell growth inhibition and apoptosis. Biochem. Cell Biol. **2000,** 78, 415-426.

(25) Keinanen, T. A.; Jarvinen, A.; Uimari, A.; Vepsalainen, J.; Khomutov, A. R.; Grigorenko, N. A.; Hyvonen, M. T.; Cerrada-Gimenez, M.; Alhonen, L.; Janne, J. α-Methylated polyamines as potential drugs and experimental tools in eEnzymology. Mini Rev. Med. Chem. **2007**, 7, 813-820.

(26) Jarvinen, A.; Cerrada-Gimenez, M; Grigorenko, N. A.; Khomutov, A. R.; Vepsalainen, J.; Sinervirta, R. M.; Keinanen, T. A.; Alhonen, L I..; Janne, J. α-Methyl polyamines: efficient synthesis and tolerance studies in vivo and in vitro. first evidence for dormant stereospecificity of polyamine oxidase. J. Med. Chem. **2006**, 49, 399-406.

(27) Rasanen, T. L.; Alhonen, L.; Sinervirta, R.; Keinanen, T.; Herzig, K.H.; Suppola, S.; Khomutov, A.R.; Vepsalainen, J.; Janne J. A polyamine analogue prevents acute pancreatitis and restores early liver regeneration in transgenic rats with activated polyamine catabolism. J. Biol. Chem. **2002**, 277, 39867.

(28) Jin, H. T.; Lämsä, T.; Hyvönen, M. T.; Sand, J.; Räty, S.; Grigorenko, N.; Khomutov, A. R.; Herzig, K. H.; Alhonen, L.; Nordback, I. A polyamine analog bismethylspermine ameliorates severe pancreatitis induced by intraductal infusion of taurodeoxycholate. Surgery **2008,** 144, 49-56.

(29) Vijayanathan, V.; Lyall, J.; Thomas, T.; Shirahata, A.; Thomas, T. J. Ionic, structural, and temperature effects on DNA nanoparticles formed by natural and synthetic polyamines Biomacromolecules **2005,** 6, 1097-1103.

(30) Nayvelt, I.; Thomas, T.; Thomas, T. J. Mechanistic differences in DNA nanoparticle formation in the presence of oligolysines and poly-L-lysine. Biomacromolecules **2007,** 8, 477-484.

(31) Thomas, T. J.; Bloomfield, V. A. Ionic and structural effects on the thermal helix-coil transition of DNA complexed with natural and synthetic polyamines. Biopolymers **1984**, 23, 1295-1306.

(32) Venkiteswaran, S.; Vijayanathan, V.; Shirahata, A.; Thomas, T.; Thomas, T. J. Antisense recognition of the HER-2 mRNA: effects of phosphorothioate substitution and polyamines on DNA.RNA, RNA.RNA, and DNA.DNA duplex stability. Biochemistry **2005**, 44, 303-312.

(33) Hyvönen, M. T.; Herzig, K. H.; Sinervirta, R.; Albrecht, E.; Nordback, I.; Sand, J.; Keinänen, T. A.; Vepsäläinen, J.; Grigorenko; N.; Khomutov, A. R.; Krüger; B.; Jänne, J.; Alhonen, L. Activated polyamine catabolism in acute pancreatitis: alpha-methylated polyamine analogues prevent trypsinogen activation and pancreatitis-associated mortality. Am. J. Pathol. **2006,** 168, 115-122.

(34) Hyvönen, M. T.; Howard, M.T., Anderson, C.B., Grigorenko; N.; Khomutov, A. R.; Vepsäläinen, J.; Alhonen, L; Janne, J.; Kienanen, T. Divergent Regulation of the key enzymes of polyamine metabolism by chiral α-methylated polyamine analogues. Manuscript submitted.

(35) Hyvönen, M. T.; Sinervirta, R.; Kienanen, T.; Fashe, T.; Grigorenko; N.; Khomutov, A. R.; Vepsäläinen, J.; Alhonen, L. Acute pancreatitis induced by activated polyamine catabolism is associated with coagulopathy: Effects of α-methylated polyamine analogues on homeostatis. Manuscript submitted.

(36) Valasinas, A.; Sarkar, A.; Reddy, V. K.; Marton, L. J.; Basu, H. S.; Frydman, B. "Conformationally Restricted Analogues of ^{1}N,^{14}N-Bisethylhomospermine (BE-4-4-4): Synthesis and Growth Inhibitory Effects on Human Prostate Cancer Cells" J. Med. Chem. **2001**, 44, 390-403.

(37) Gao, J.; Liu, Y.; Zhou, Y.; Zingaro, R. A. "Chiral Salicyl Diamines: Potent Anticancer Molecules" ChemMedChem **2007**, 2, 1723.

(38) Higashi, K.; Yoshida, K.; Nishimura, K.; Momiyama, E.; Kashiwagi, K.; Matsufuji, S.; Shirahata, A.; Igarashi, K. "Structural and Functional Relationship among Diamines in Terms of Inhibition of Cell Growth" J. Biochem. **2004**, 136, 533.

(39) Thomas, T.J.; Bloomfield, V.A. Collapse of DNA caused by trivalent cations: pH and ionic specificity effects. Biopolymers **1983**, 22, 1097-1106.

(40) Thomas, T.J.; Bloomfield, V.A. Ionic and structural effects on the thermal helix-coil transition of DNA complexed with natural and synthetic polyamines. Biopolymers **1984**, 23, 1295-1306.

(41) Saminathan, M.; Antony, T.; Shirahata, A,; Sigal, L.H.; Thomas, T.; Thomas, T.J. Ionic and structural specificity effects of natural and synthetic polyamines on the aggregation and resolubilization of single-, double-, and triple-stranded DNA. Biochemistry **1999**, 38, 3821-3830.

(42) Terui, Y.; Ohnuma, M.; Hiraga, K.; Kawashima, E.; Oshima, T. Stabilization.of nucleic acids by unusual polyamines produced by an extreme thermophile, Thermus thermophilus. Biochem. J. **2005**, 388, 427-33.

(43) Schmid, N.; Behr, J.P. Location of spermine and other polyamines on DNA as revealed by photoaffinity cleavage with polyaminobenzenediazonium salts. Biochemistry **1991**, 30, 4357-4361.

Chapter 4

Mechanistic Differences in DNA Nanoparticle Formation in the Presence of Oligolysines and Poly-L-lysine

Irina Nayvelt, Thresia Thomas, and T. J. Thomas

Biomacromolecules (2007), 8:477-484

ABSTRACT

We studied the effectiveness of trilysine (Lys_3)-, tetralysine (Lys_4)-, pentalysine (Lys_5)**-,** and poly-L-lysine (PLL) (MW: 50,000) on λ-DNA nanoparticle formation, and characterized the size, shape and stability of nanoparticles. Light scattering experiments showed EC_{50} (lysine concentration at 50% DNA compaction) values of ~0.0036, 2, and 20 μmoles/liter, respectively, for PLL, Lys_5, and Lys_4 at 10 mM [Na^+]. Plots of log[EC_{50}] versus log[Na^+] showed positive slopes of 1.09 and 1.7, respectively, for Lys_4 and Lys_5 and a negative slope of -0.1 for PLL. Hydrodynamic radii of oligolysine-condensed particles increased (48-173 nm) with increasing [Na^+], whereas no significant change occurred to nanoparticles formed with PLL. There was an increase in the size of nanoparticles formed with Lys_5 at >40 °C, whereas no such change occurred with PLL. DNA melting temperature increased with oligolysine concentration. These results indicate distinct differences in the mechanism(s) by which oligolysines and PLL provoke DNA condensation to nanoparticles.

INTRODUCTION

DNA condensation to nanoparticles has been extensively studied to understand the energetic forces involved in the control of DNA compaction in viral capsids and in chromosomes, and to develop novel gene delivery vehicles.[1] Natural and synthetic polyamines, basic proteins, synthetic polymers, and dehydrating solvents are excellent promoters of DNA condensation and aggregation.[1-3] In dilute solutions, these agents collapse DNA to nanoparticles of finite size and ordered morphology.[4-6] Toroidal structures have been observed for these nanoparticles by several investigators, although spherical and rod-like structures have also been found using electron and atomic force microscopy. A hexagonal, liquid crystalline packaging arrangement has been observed for cation condensed DNA.[7,8]

The interaction of oligopeptides, including oligolysines with DNA was studied earlier by several investigators as a model system for evaluating the thermodynamic parameters of protein-DNA interactions.[9,10] In recent years, poly-L-lysine (PLL)-mediated DNA condensation has been studied as a model for DNA compaction to nanoparticles, and for the use of DNA nanoparticles for gene delivery applications.[11-14] Oligolysine-DNA interaction has been modeled on the basis of the counterion condensation theory developed by Manning[15] and Record et al.[16] However, there has not been much attempt to examine the mechanism of the interaction of poly-L-lysine with DNA, especially the effect of ionic conditions of the medium and temperature. Comparative studies on the interaction of oligolysines and PLL with DNA are also scant. We, therefore, undertook the present study to examine the effects of monovalent ion (Na^+) concentration and temperature on the ability of trilysine (Lys_3), tetralysine (Lys_4), pentalysine (Lys_5), and PLL to condense λ-DNA using static and dynamic light scattering techniques, and electron microscopy.

Among the cationic biopolymers with gene therapy applications, PLL has received much attention because it is amenable to chemical modifications and can be conjugated to a variety of ligands to achieve receptor-mediated uptake for gene delivery applications.[17-20] DNA collapse by PLL leads to structures of various shapes (i.e. toroids, spheroids or rods) and sizes, depending on its ratio to DNA and the conditions of the medium.[21-25] PLL can bind DNA cooperatively or non-cooperatively, producing unimolecular complexes or multimolecular aggregates, respectively. In

addition to condensation, polypeptides confer marked stabilization to DNA against thermal denaturation, and the magnitude of stabilization and specificity of the interaction depends on the nature of the polypeptide chain.[17,18]

Our present results indicate that the efficacy of lysines to condense DNA increased with the number of positive charges on the molecules, with PLL being a better condensing agent than oligolysines. Temperature-dependent measurements of hydrodynamic radii of DNA nanoparticles showed that the presence of Lys_5 caused aggregation as the temperature increased > 40 °C, whereas PLL did not have such an effect. Oligolysines increased the T_m of DNA in a concentration-dependent manner, at concentrations used to condense the DNA. Complexes formed with PLL and DNA did not melt at temperatures up to 95 °C. These results provide new insights into the mode of interaction of DNA with oligolysines and PLL.

MATERIALS AND METHODS

λ-DNA. Lyophilized λ phage DNA (MW: 31.5×10^6 Da; 48,502 base pairs) was purchased from Sigma Chemical Co. (St. Louis, MO). It was dissolved in 10 mM Na cacodylate buffer (10 mM Na cacodylate, 0.5 mM EDTA, pH 7.4), and dialyzed against the same buffer for 3 hours. The absorbance ratio (A_{260}/A_{280}) of the DNA solution was 1.9, indicating that the DNA was free from protein contamination.

Lysines and Reagents. Trilysine, tetralysine, pentalysine, and poly-L-lysine (MW range: 30,000-70,000), were purchased from Sigma Chemical Co. (St. Louis, MO). We determined the purity of the oligolysines from Sigma by thin layer chromatography, using silica gel plates with matrix polyester support to run the samples. The mobile phase consisted of 60% butanol, 25% double distilled (dd) deionized water, and 15% glacial acetic acid. The samples were spotted on the plates (at concentrations of 20 and 100 μmoles/liter), and the mobile phase was allowed to run for 5 hours. The plates were dried and sprayed with ninhydrin reagent solution (0.2% ninhydrin in ethanol), and then heated to 50 °C for 3 minutes to visualize the peptides. Lys_3 and Lys_4 migrated as single spots, indicating the homogeneity of the peptides. In the case of Lys_5, we observed 2 minor spots, which co-migrated with a major spot of Lys_5. The minor spots could be due to the presence of Lys_3 and Lys_4. However, the intensity of the major spot indicated that the material was > 95% Lys_5. Average MW of PLL (50,000) was used to calculate the molar concentration in solution. Stock solutions of Lys_3, Lys_4, Lys_5 (10 mM each) and PLL (1 mg/ml) were prepared in 10 mM Na cacodylate buffer. Subsequent dilutions were made with the same buffer. Buffers of increasing ionic strength (25 mM, 50 mM, 75 mM, 100 mM and 150 mM Na^+) were prepared by adding appropriate amounts of 1 M NaCl solution to the 10 mM Na cacodylate buffer.

Total Intensity Light Scattering. Static light scattering experiments were performed using a Fluoromax-2 spectrofluorometer (Jobin Yvon-Spex Instruments S. A., Inc., Edison, NJ).[26] The excitation and emission monochromators were both set to a wavelength of 305 nm with 5 nm band pass. The scattered light intensity was collected at a 90° angle with respect to the incident beam. Small quantities of stock oligolysine or PLL solutions were added to DNA/buffer solutions (0.5 μg/ml DNA) in 2 ml borosilicate glass tubes to achieve the desired concentration of the

condensing agent. The solutions were vortexed gently and allowed to equilibrate for 30 minutes at 22 °C. They were then centrifuged in a Beckman GS 6KR centrifuge for 10 minutes at 500 x g to avoid light scattering from aggregated particles. Centrifugation at 500 x g did not result in phase separation or a reduction in DNA concentration in solution. Therefore, the light scattering measurements are representative of the DNA concentrations used.

Dynamic Laser Light Scattering. Dynamic light scattering experiments were performed using DynaPro model MSX equipment (Protein Solutions, Inc., Charlottesville, VA).[27,28] Lysine solutions were added to DNA solutions (0.5 μg/ml) to achieve the desired condensing agent concentrations. The samples were mixed and allowed to attain equilibrium for 30 minutes at 22 °C, and centrifuged for 10 minutes at 500 x g and 4 °C to remove aggregate particles. Hydrodynamic radii were measured by transferring 45 μl of sample solution to a standard quartz cuvette, and the scattered light was detected at a 90° angle to the incident beam. All measurements were performed in the same cuvette to avoid variations introduced by minor differences between cuvettes. The cuvette was washed with double distilled water and vacuum-dried before each measurement. The measurements were performed at different temperatures, ranging from 20 °C to 80 °C, after equilibrating the sample at the indicated temperatures for 10 min.

A laser beam from a 2W laser (800 nm wavelength) was passed through a quartz cell holding the sample (lysine/DNA mixture), and the scattered light was detected at a 90° angle with respect to the incident beam. The scattered light was analyzed with an autocorrelator in order to generate the first-order autocorrelation function. The following equation describes the autocorrelation function, $g^{(l)}(\tau)$, for monodisperse particles that are much smaller than the incident beam:

$$g^{(l)}(\tau)=\exp[-Dq^2(\tau)]$$

In this equation, τ is the decay time, q (= $4\pi n/[\lambda_o \sin(\theta/2)]$) is the scattering vector which is a function of the incident beam wavelength λ_o, the scattering angle θ, the refractive index of the solvent n, and the diffusion coefficient D. The hydrodynamic radius (R_h) is calculated from the diffusion coefficient using the Stokes-Einstein equation:

$$R_h = kT/6\pi\eta D,$$

where T is the absolute temperature, η is solvent viscosity, and k is the Boltzmann constant. Data were analyzed by a Dynamics Version 6 software package obtained from Protein Solutions, Inc.

Electron Microscopy. Lysine-DNA condensates were visualized using a JEOL 1200EX electron microscope.[27] Briefly, the samples were prepared by combining lysine solutions with DNA solutions (0.5 μg/ml) in order to achieve the desired cationic agent concentrations. The solutions were mixed and allowed to equilibrate for approximately 30 minutes. Formvar-coated copper grids (Electron Microscopy Sciences) were glow discharged for 60 seconds. Samples were placed on the grids for 10 minutes. The grids were then washed with water for 1-2 minutes and excess solution removed using a filter paper. The grids were stained with 1% uranyl acetate solution (1-2 minutes) and allowed to dry in air.

Centrifugation Assay for DNA Precipitation. In order to examine the ability of different lysines to precipitate DNA, we conducted the centrifugation assay.[29] In brief, aliquots of DNA solution (DNA in100 mM Na^+ cacodylate buffer) were mixed with lysine solution to achieve the desired condensing agent concentration in a final volume of 400 μL. The samples were vortexed for 5 seconds, incubated either at 22, 50, or 70 °C for 30 minutes, and centrifuged for 10 minutes at 11000 x g using a microcentrifuge. The supernatant was withdrawn for analysis and placed in a 350 μL quartz microcuvette (path length = 1 cm). Sample absorbance was measured using a Beckman DU 460 spectrophotometer at 260 nm. λ-DNA concentration used in centrifugation experiments was 0.1 A_{260nm} units. The amount of DNA present in solution was calculated using the following equation: percent DNA in solution = $(A_s/A_o) \times 100$; where A_s and A_o are the absorbance of the supernatant and control (DNA in the absence of lysine reagent), respectively, at 260 nm.

Melting Temperature (T_m) Measurements. T_m experiments were performed using a Beckman DU640 spectrophotometer.[30] T_m cell block contained six cells, one of which was filled with buffer (used as a blank). Melting temperature was obtained by increasing the temperature of the sample at a rate of 0.5 °C/min, within a range of 40-95 °C, and monitoring the absorbance (A) every 30

seconds. T_m values were taken as the temperatures at which half of the complex was dissociated. Computer-generated first derivative of the melting curve, dA/dT (where A is absorbance and T is temperature) was also used for determining T_m. T_m measurements obtained by both methods did not deviate by more than 1 °C.

RESULTS

Static Light Scattering. The ability of oligolysines and PLL to condense λ-DNA was studied using static light scattering. Figure 19 shows the relative intensity of scattered light versus concentration of Lys_4, Lys_5, and PLL. In each case, a sharp rise (> 4-fold) occurred in the intensity of scattered light at a critical lysine concentration, which plateaued on further addition of lysine. A plateau in the light scattering profile indicates complete condensation of λ-DNA at high peptide concentrations. Among the oligolysines, Lys_3 did not provoke DNA condensation even up to a concentration of 1 mM.

To compare the relative effectiveness of Lys_4, Lys_5, and PLL in condensing DNA, we calculated the EC_{50} values, which corresponded to lysine concentrations at which half of the DNA was in the compacted form. Our results are presented in Table 6. The effective concentration of PLL in inducing DNA condensation was much lower than that of Lys_5. In the presence of 10 mM Na^+, there was a 10-fold decrease in the EC_{50} value (from 20 to 2 μM) when Lys_4 was replaced by Lys_5, suggesting that Lys_5 was more efficacious in condensing DNA than Lys_4. We also compared the DNA condensing abilities of lysines by calculating the molar ratios of nitrogen to phosphate (N/P values) at the EC_{50} value. PLL demonstrated the greatest DNA condensation efficiency (N/P ~ 1.8), followed by Lys_5 (N/P ~ 13), and Lys_4 (N/P ~ 106). Our results indicate that DNA condensation by lysines is a sensitive function of the cationicity of the condensing agent.

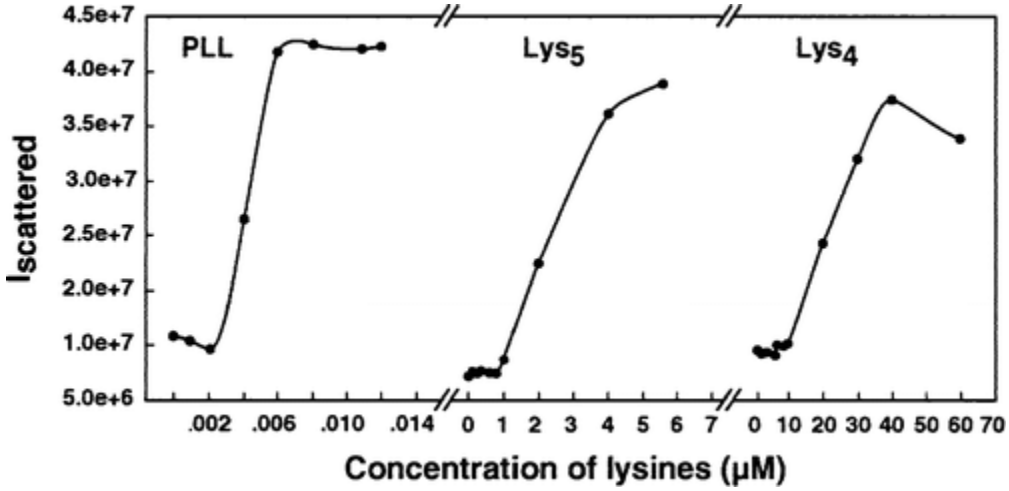

Figure 19. Typical plots of relative intensity of scattered light at 90° against concentrations of Lys_4, Lys_5, and PLL. The λ-DNA solution had a concentration of 1.5 μM DNA phosphate, dissolved in 10 mM Na cacodylate buffer, pH 7.4. Lysine concentrations are in terms of the whole molecules, μmoles/liter.

Table 6. Effects of Na^+ concentration on EC_{50} values and hydrodynamic radius (R_h) of λ-DNA condensates formed in the presence of Lys_4, Lys_5, and poly-L-lysine.

Na^+ (mM)	Tetralysine (Lys_4)		Pentalysine (Lys_5)		Poly-L-lysine (PLL)	
	EC_{50}	R_h (nm)	EC_{50}	R_h	EC_{50}	R_h
10	20	66.3±6.8	2	48±1.8	0.0036	60.9±3
25	32	71.9±4.4	3.4	99.1±6	0.0029	70.6±3
50	75	125.9±3.2	16.7	113±2.6	0.0031	77.1±4
75	138	168.9±2.9	45	144.5±2.6	0.0027	74.7±4
100	257	172.6±1	90	151.5±5	0.0027	84.4±4
150	--	--	148	155.9±5	0.0028	87.0±3

R_h measurements were done with the dynamic laser light scattering equipment in10 mM Na cacodylate buffer (pH 7.4), containing 0, 15, 40, 65, 90, and 140 mM NaCl to make up the Na^+ concentration. ± indicates SD from 4-6 experiments. Standard deviations in EC_{50} values were less than 10%.

Effect of Salt Concentration. We next examined the effect of increasing ionic strength of the medium on the ability of Lys_4, Lys_5, and PLL to condense λ-DNA. The $[Na^+]$ of 10 mM Na cacodylate buffer was increased in stages up to 150 mM by the addition of predetermined aliquots of 1 M NaCl that took into account the original 10 mM $[Na^+]$ in the buffer. At each ionic concentration, plots of total intensity of scattered light against lysine concentrations were generated, similar to Figure 19. From these plots, EC_{50} values were determined. Figure 20 shows the influence of $[Na^+]$ on the effectiveness of lysines in condensing λ-DNA. In these plots of $\log[EC_{50}]$ against $\log[Na^+]$, the critical concentrations of Lys_4 and Lys_5 increased linearly with $[Na^+]$. The slope of the plot, $(d\log[EC_{50}]/d\log[Na^+])$ is a quantitative measure of the concentration dependence between multivalent and monovalent cations during λ-DNA condensation. The slopes obtained from the plot were 1.09 and 1.7 for Lys_4 and Lys_5, respectively. In contrast, a slightly negative slope (- 0.1) was obtained for PLL, pointing to a minimal of change in EC_{50} values with increasing $[Na^+]$.

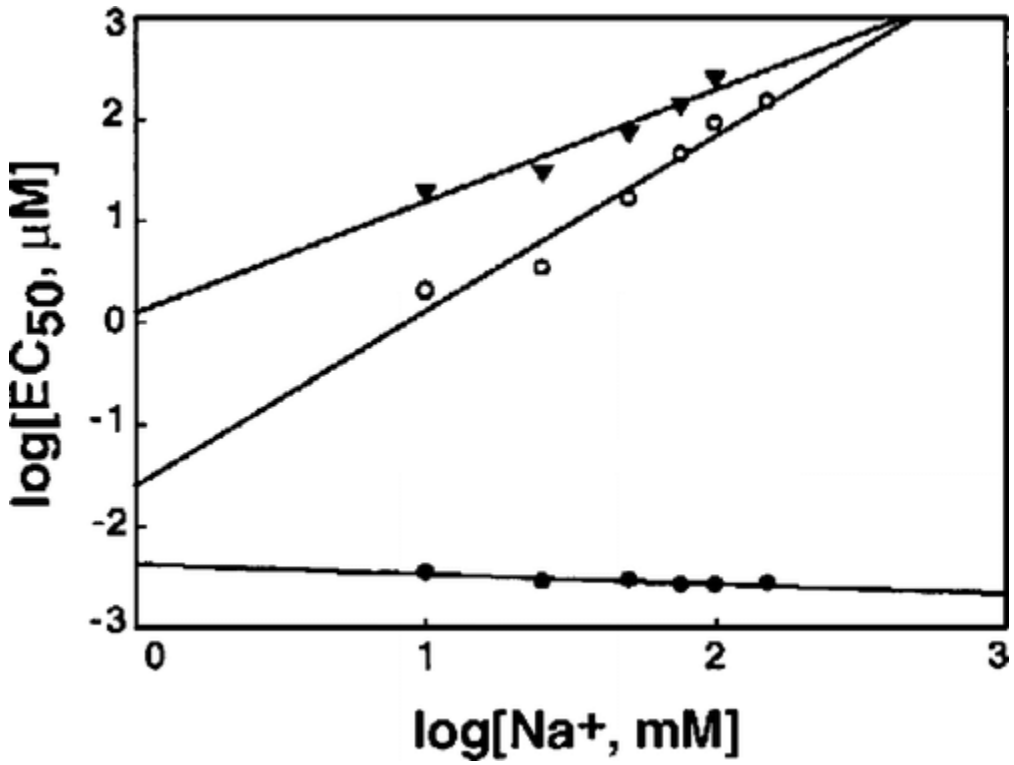

Figure 20. Effect of Na^+ concentration on the midpoint condensing concentration (EC_{50}) of Lys_4, Lys_5 and poly-L-lysine. The log of EC_{50} (μmoles/liter) is plotted against log of [Na^+] (mM). The symbols represent EC_{50} values of Lys_4 (▼), Lys_5 (○), and poly-L-lysine (●). Error bars are of a magnitude to be contained within the symbols, and indicate standard deviation from 3 separate experiments.

Measurement of Hydrodynamic Radius of Condensed Particles. In the next series of experiments, we determined the hydrodynamic radius (R_h) of λ-DNA nanoparticles formed in the presence of oligolysines and PLL, using dynamic laser light scattering equipment. Lysine concentrations at which λ-DNA achieved complete condensation, as established by the plateau region in the light scattering profile, were used in these experiments. R_h values were initially determined using 10 mM Na cacodylate buffer. The size of the DNA nanoparticles was 66.3 ± 6.8 nm, 48.0 ± 1.8 nm, and 60.9 ± 2.7 nm, respectively, in the presence of Lys_4, Lys_5, and PLL (Table 6).

To determine the effect of increasing monovalent ion concentration on particle size, [Na^+] of the buffer was gradually increased from 10 to 150 mM by the addition of required volumes of 1 M NaCl. Table 1 shows the change in R_h values of nanoparticles formed with oligolysines and

PLL in the presence of increasing concentrations of [Na^+]. DNA nanoparticles formed with Lys_4 increased in size from 66.3 nm to 173 nm, as the monovalent ion concentration increased from 10 to 100 mM. At 150 mM Na^+, Lys_4 was unable to condense λ-DNA, as evidenced by its failure to increase the scattered light intensity even up to a concentration of 1 mM. The R_h value of DNA nanoparticles condensed with Lys_5 increased from 48 nm to 156 nm, when [Na^+] was increased from 10 to 150 mM. In the case of PLL, however, the particle size showed only a modest increase, from 61 to 87 nm when [Na^+] increased from 10 mM to 150 mM. Overall, Lys_4 produced larger particles than those produced by Lys_5 at ≥ 50 mM Na^+. Lys_5 and PLL produced the smallest nanoparticles, indicating that the particle size decreased with increasing number of positive charges on the oligo-/polylysines.

Temperature Effect on Particle Size. We next studied the effect of increasing temperature (20 - 80 °C) on the size of DNA nanoparticles formed in the presence of Lys_4, Lys_5 and PLL in cacodylate buffer containing 100 mM Na^+. The results are shown in Figure 21. The average size of nanoparticles formed with PLL increased slightly around 30 °C (R_h ~ 98 nm) and remained almost constant from 30 – 60 °C. Starting at 70 °C, we observed a small decrease (~15-25 nm) in the R_h of these particles. In contrast, a sharp increase in the size of Lys_5 nanoparticles was observed at 50 °C, with R_h value almost tripling in magnitude (R_h ~ 436 nm). The Rh values of Lys_4 condensed particles remained the same from 20 to 37 °C. However, they became unstable at higher temperatures (≥ 40 °C), precluding any further measurement of R_h.

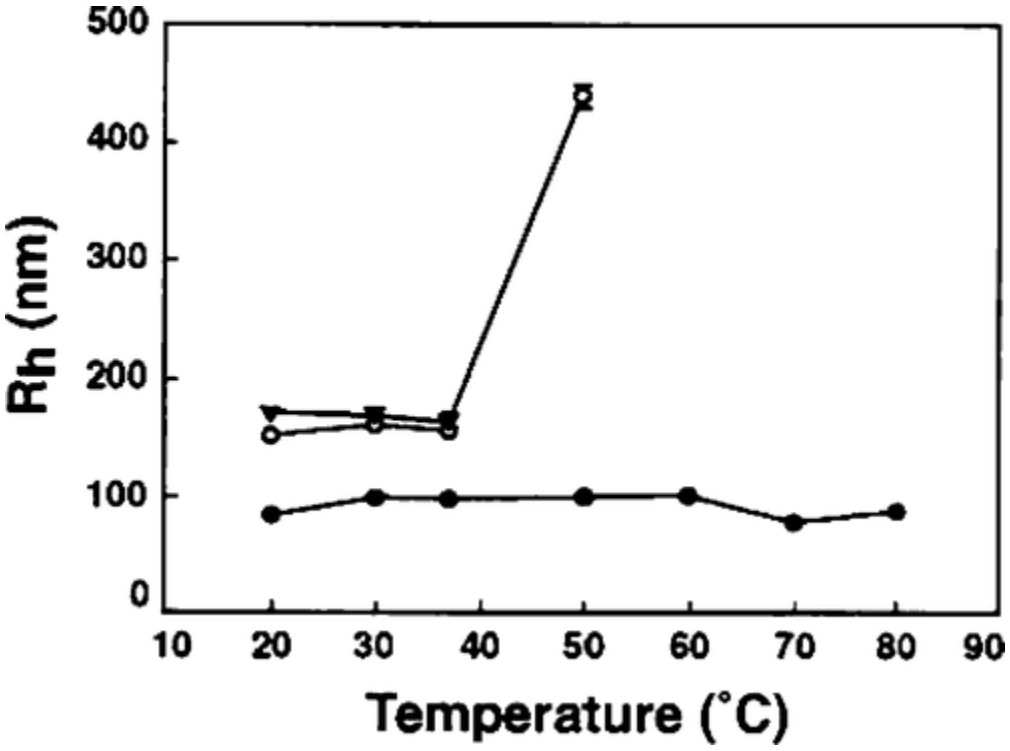

Figure 21. Effect of temperature on hydrodynamic radius (R_h) of λ-DNA nanoparticles. The symbols represent mean R_h values of nanoparticles produced in 100 mM Na cacodylate buffer in the presence of Lys_4 (▼), Lys_5 (○), and poly-L-lysine (●). Error bars indicate standard deviation from 4-6 separate experiments and are generally of a magnitude to be contained within the symbol.

Determination of Nanoparticle Size and Shape by Electron Microscopy (EM). In the next set of experiments, we examined the shape of the nanoparticles formed by the interaction of oligolysines and PLL with λ-DNA. Electron microscopic examination of Lys_5 and PLL condensed DNA complexes at different salt concentrations (10, 50 and 100 mM) revealed the presence of nanoparticles of different sizes and shapes. The structures of DNA nanoparticles formed by the binding of Lys_5 are shown in Figure 22 (A-E), whereas PLL-containing particles are depicted in panels (F-I). DNA condensates appeared predominantly as toroids and spheroids, but occasionally rods were also observed. In some cases, particle sizes determined by EM were smaller than those obtained by dynamic light scattering method. The smaller sizes can be attributed to drying artifacts during the deposition of the condensates on the EM grid.

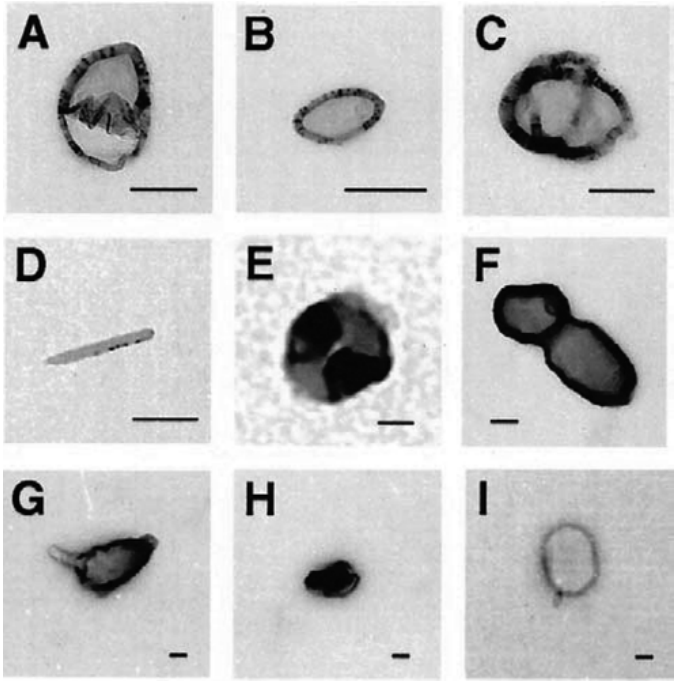

Figure 22. Representative electron micrographs of λ-DNA nanoparticles produced by Lys_5, and poly-L-lysine. Experiments were conducted in Na cacodylate buffer, containing different concentrations of NaCl. A and B, Lys_5 induced particles in 50 mM [Na^+]; C, Lys_5 in 10 mM [Na^+]; D and E, Lys_5 in 100 mM [Na^+]; F, poly-L-lysine in 10 mM [Na^+]; G and H, poly-L-lysine in 50 mM [Na^+]; and I, poly-L-lysine in 100 mM [Na^+]. It should be noted that the intense darkness of the micrographs is due to uranyl acetate staining. The bars in all panels (A-I) represent 100 nm.

Precipitation Studies of λ-DNA in the Presence of Oligo- and Poly-L-lysine. This set of experiments was designed to determine and compare the effect of Lys_4, Lys_5, and PLL on the precipitation of λ-DNA. In agreement with experiments conducted to determine the effect of temperature on particle size, the present experiments were also performed in 100 mM Na

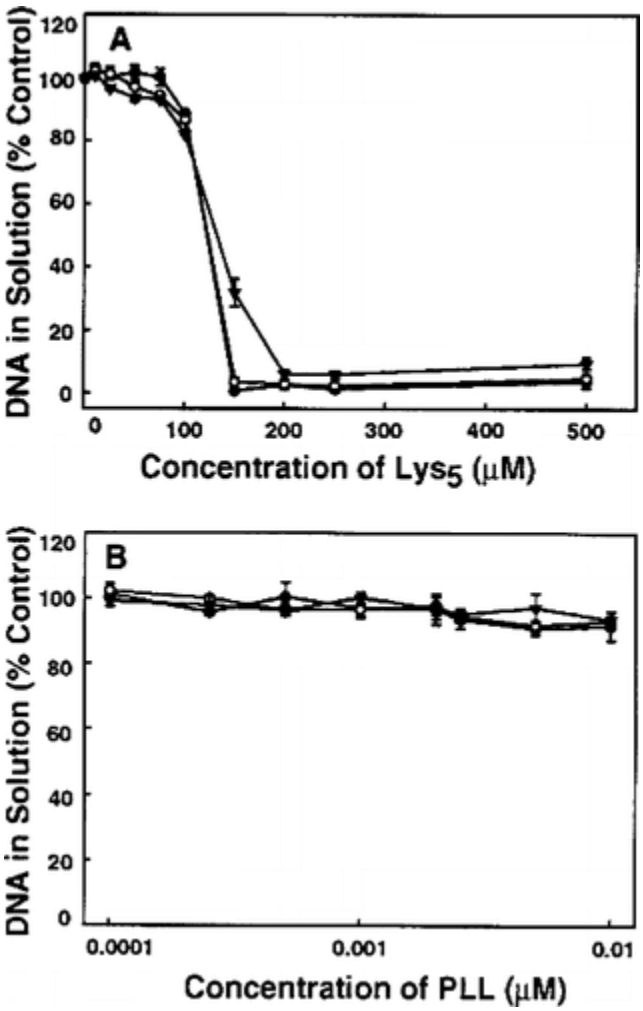

Figure 23. Precipitation/aggregation of λ-DNA in the presence of (A) Lys_5 and (B) PLL, observed at room temperature (●), 50 °C (○), and 70 °C (▼). All experiments were conducted in 100 mM Na cacodylate buffer (pH 7.4). A logarithmic scale is used for PLL concentrations in panel B. Error bars represent standard deviation from 3 separate experiments. The DNA concentration used in these experiments was 0.1 A_{260nm} units.

cacodylate buffer. We conducted the precipitation experiments using samples incubated for 30 minutes at 22, 50, and 70 °C.

Lys_5 caused significant aggregation of λ-DNA, as shown in the Figure 23A. At low Lys_5 concentration (0-100 μM), the precipitation curve showed only a small decrease, with > 88% of DNA remaining in solution at 100 μM. At 150 μM, Lys_5 caused DNA precipitation at all temperatures, as evidenced by a sharp decline of the precipitation curves. Over 90% of DNA was in aggregated form at Lys_5 concentrations ranging from 200 - 500 μM. In contrast, Lys_4 failed to

induce λ-DNA precipitation at either 22, 50, or 70 °C. Reducing DNA concentration from 0.1 to 0.05 A_{260nm} units did not have any noticeable effect on Lys_4's inability to stimulate DNA aggregation.

PLL induced minimal DNA precipitation (≤ 9%) across a wide range of concentrations employed in this study at all experimental temperatures (Figure 23B). A slight trend towards increased precipitation with greater PLL concentration can be observed at concentrations > 0.001 μM.

T_m measurements of DNA complexed with Oligo- and Poly-L-lysine. In order to examine whether the ability of oligo-/poly-L-lysines to condense λ-DNA correlated with their ability to increase the stability of DNA duplex, we determined T_m values of λ-DNA in the presence of increasing concentrations of Lys_3, Lys_4, Lys_5 and PLL. Figure 24 shows representative absorbance-temperature profiles of λ-DNA in the presence of different concentrations of Lys_5. The dissociation of the duplex to single strands was seen as an increase in the absorbance at 260 nm, as the temperature increased from 40 to 95 °C. In the absence of lysines, λ-DNA melted at 71 °C in a buffer containing 10 mM Na cacodylate. The presence of Lys_5 shifted the melting profile to the right, indicating an increase in the T_m in a concentration-dependent manner.

The results of our T_m measurements with all 3 oligolysines and PLL are presented in Table 7. A concentration-dependent increase in T_m was observed for all 3 oligolysines. For the same concentration, Lys_5 had a much higher duplex stabilizing effect than Lys_4 and Lys_3. For example, ΔT_m ($T_{m(\text{in the presence of lysine})}$-$T_{m(\text{in the absence of lysine})}$) with 10 μM Lys_5 was 18.1 °C, compared to that of 12.8 °C and 12.7 °C, respectively, for Lys_3 and Lys_4. The T_m of DNA showed a minor transition at ~ 71°C in the presence of different concentrations of PLL up to 0.02 μM. This is the same T_m as that of λ-DNA in buffer, and may represent the melting of uncomplexed DNA. This result suggests that λ-DNA-PLL complexes do not melt up to 95 °C, the upper limit of our temperature program.

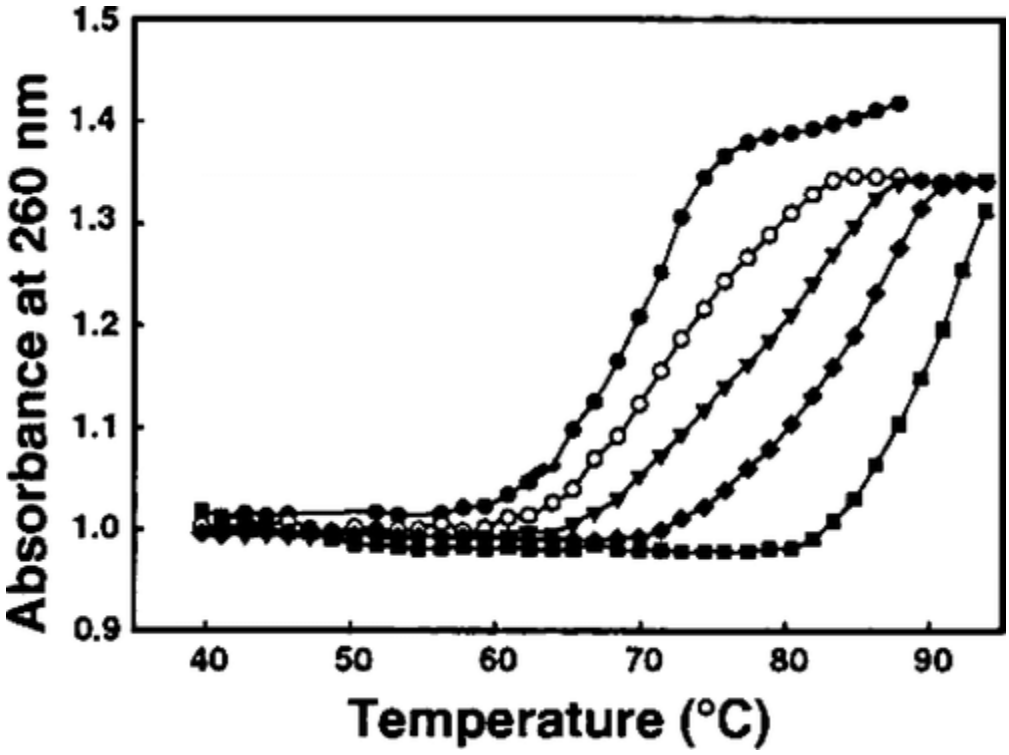

Figure 24. Typical melting profiles of λ-DNA in the presence of Lys_5. The concentrations of Lys_5 were: 0 (●), 1 (○), 2.5 (▼), 5 (♦), and 10 (■) μM. The Tm measurements were conducted in 10 mM Na cacodylate buffer at a heating rate of 0.5 °C/minute.

Table 7. Effects of Lys_3, Lys_4, Lys_5, and poly-L-lysine on the melting T_m of λ-DNA

Trilysine (Lys_3)		Tetralysine (Lys_4)		Pentalysine (Lys_5)	
Conc., μM	T_m,°C	Conc., μM	T_m, °C	Conc., μM	T_m, °C
0	70.9	0	71.2	0	71.1
1	72.7	1	73.4	1	72.5
2.5	78.2	2.5	77.1	2.5	82.3
5.0	81.2	5.0	79.7	5.0	86.9
10	83.6	10	84.0	10	89.2

T_m measurements were done in 3 separate experiments. The values given are the mean values. The SD in T_m measurements was <1 °C. The molar concentration of poly-L-lysine was calculated, using the average molecular weight of 50,000. At concentrations higher than 0.02 μM, DNA precipitated in the presence of poly-L-lysine.

DISCUSSION

Results presented in this report show significant differences in the mechanism(s) by which oligolysines and PLL condense λ-DNA to nanoparticles. Lys_4, Lys_5 and PLL condensed λ-DNA to nanoparticles at very low concentrations, and the critical concentrations required to condense half the DNA in a sample decreased with increasing lysine chain length. In a plot of log[EC_{50}] against log [Na^+], EC_{50} values of Lys_4 and Lys_5 increased linearly with Na^+ concentration with a positive slope. In contrast, such a plot yielded a negative slope (- 0.1) for PLL, indicating that the predominant mode of interaction of PLL with DNA might be different from that of oligolysine-DNA interactions. The hydrodynamic radii of the nanoparticles formed with oligolysines increased with [Na^+] in the medium, whereas no such effect was found for nanoparticles provoked by PLL. While increasing temperature had a large effect on the size and stability of DNA nanoparticles formed in the presence of Lys_4 and Lys_5, temperature had only a modest effect on nanoparticles formed with PLL. In addition, Lys_5 induced DNA aggregation, whereas PLL did not initiate aggregation of the condensates (Figure 5).

As can be seen from Table 1, DNA condensation by lysines is dependent on the nature of the lysine molecule. Decrease in EC_{50} values with increasing lysine chain length indicates that the cationicity of the condensing agent plays an important role in DNA condensation. According to the counterion condensation theory developed by Manning[15] and Record et al,[16] and as applied to the condensation of DNA by multivalent cations,[26,31] approximately 89-90% phosphate charge neutralization is required for DNA condensation. The trend of decreasing EC_{50} values with increasing lysine chain length can be explained in terms of binding affinity. Generally, higher charge of a cation leads to a higher binding affinity than that of lower charge cations, thereby causing DNA to collapse at lower counterion concentrations. Therefore, PLL's ability to condense λ-DNA at significantly lower concentration than that of Lys_4 or Lys_5 can be attributed to its high affinity binding to DNA. However, Lys_3 was incapable of mediating DNA condensation under different conditions tested by us. The lack of Lys_3-mediated λ-DNA condensation in our study is consistent with earlier observations by Wadhwa,[18] who demonstrated that alkylated Lys_3 could not bind to and condense DNA.

Previous studies on DNA condensation by multivalent cations have shown that trivalent cations are excellent promoters of nanoparticle formation in aqueous solution. For example, cobalt hexamine $Co(NH_3)_6^{3+}$ and spermidine^{3+} provoked DNA condensation, with EC_{50} values of 15 and 35 μM, respectively, in 1 mM Na cacodylate buffer, and the resultant nanoparticles had hydrodynamic radius of ~ 50 nm.[27,31] In contrast to these trivalent cations, trilysine could not condense DNA up to 1 mM concentration. Trilysine has three ε amino groups, and an α amino group. When pH is = 7.0, the amino acid groups of lysine are considered to be 99% protonated. At our experimental pH of 7.4, each amino group of the peptide may be partially protonated, making the molecule less than tripositive, thereby contributing to its inability to condense DNA. Trilysine's inability to promote DNA compaction may also be attributed to low charge density of the molecule resulting from the chain separation between positive charges on the ε-terminals of the lysine side-chains. However, tetralysine appears to provide the threshold for sufficient postive charges and charge density for DNA condensation. Although multivalent cation-mediated condensation of DNA has been modeled on the basis of the counterion condensation theory, ion-specific effects have been found in the case of tetravalent polyamines.[26]

There is no consensus regarding the size of DNA nanoparticles produced by PLL or oligolysines. Particle size often depends on the starting reactant concentrations, size of the DNA, ionic environment, mixing conditions, as well as the method of measurement. Hydrodynamic diameters of PLL-DNA condensates (λ-DNA size: ~ 48.5 kb, MW: $31.5x10^6$ Da) in our study varied from approximately 120 to 180 nm, with salt concentration ranging from 0.01 to 0.15 M. Significantly larger particles (diameter: ~ 340 nm) were obtained by Shapiro et al.[32] in the course of light scattering experiments, using sonicated calf thymus DNA (MW: $5x10^5$ Da), which is smaller than the DNA used in our studies. Liu et al.[33] demonstrated the formation of complexes of a significantly lower size than that obtained in our study (diameter: 15-30 nm) between PLL and plasmid DNA of a much smaller size (~5 kb) than that of λ-DNA. These complexes were formed under high salt conditions, and thought to contain 1-3 molecules of DNA. Perales et al.[34] also observed the formation of very small unimolecular particles (diameter: 17 nm) composed of PLL and homogeneous plasmid DNA, under similar ionic conditions. Lower Na^+ concentrations tended

to produce aggregates of unimolecular condensates. Using plasmid DNA, Kwoh et al.[35] found that 10 kDa and 26 kDa PLL produced similar-sized polyplexes , ~255 nm and ~238 nm in diameter, respectively, at physiological Na^+, suggesting that particle size does not vary with increasing PLL chain length. However, using AFM, Wolfert et al.[12] observed a clear trend toward increasing particle diameter with increasing molecular weight of PLL in the presence of plasmid DNA (approximate size 6 kb). These differences may be attributed to differences in ionic conditions and/or kinetic changes occurring after the formation of the particles.

Our T_m experiments demonstrate that λ-DNA undergoes monophasic melting transitions in the presence of Lys_3, Lys_4 and Lys_5, and that greater duplex stabilization is achieved with increasing oligolysine chain length. Dependence of T_m with increasing cation concentration indicates that DNA stabilization is achieved by the reversible binding of these cations to DNA. Our results with oligolysines are in agreement with those of Olins et al.[36] who observed similar monophasic melting of DNA in the presence of Lys_4. Our inability to observe biphasic melting in the presence of PLL may be attributed to the fact that the second melting transition occurs at a temperature above 100 °C, and, therefore, cannot be measured by the instrument used in our melting studies.[37] The T_m of ~71 °C might be that of uncomplexed λ-DNA. Interestingly, Lys_3 stabilizes duplex DNA, but is unable to condense the same.

A novel aspect of our study is the observation that increasing salt concentration has no major effect on the ability of PLL to condense DNA, and on the size of the resultant nanoparticles. We found that increasing salt concentration (0.010 to 0.15 M Na^+) caused significant increase in the amount of Lys_4 and Lys_5 required for λ-DNA condensation, but had a minimal impact on the critical condensing concentration of PLL. Similarly, increase in Na^+ caused only a small increase in the size of PLL nanoparticles, while producing a large increase in the size of DNA condensates produced in the presence of oligolysines. Na^+ concentration was not raised above 0.15 M as our aim was to compare PLL and oligolysines at physiologically compatible salt conditions.

The linear positive slope obtained with oligolysines suggests that electrostatic interactions are the main force involved in oligopeptide-mediated DNA condensation.[15,16,26] The driving force for oligolysine binding to DNA results from a net gain in entropy that occurs when

DNA-bound Na^+ are released into solution. When Na^+ concentration of the medium is increased, the net gain in entropy from the release of Na^+ decreases, and, therefore, a higher concentration of oligolysines is required to compete with Na^+ and induce DNA condensation.[3] Since a positive slope was not observed, which would be expected in the case of electrostatic mode of interaction between multivalent ions and DNA, we believe that PLL-DNA interaction is complicated by other factors.

Significant differences were also observed on the effect of temperature on hydrodynamic radius of DNA nanoparticles. While an increase in temperature favored the assembly of oligolysine condensed particles, with sizes tripling in magnitude at ≥ 50°C, size of PLL condensed particles remained relatively similar, suggesting that temperature-induced aggregation of DNA is prevented by PLL. These results can be attributed to the irreversible binding of PLL to DNA, in contrast to the reversibly bound oligolysines, which are easily replaced by increasing salt concentration.

Our precipitation/aggregation studies demonstrate Lys_5's ability to induce almost complete λ-DNA precipitation (≥ 91%) at 22, 50, and 70°C, at oligolysine concentrations higher than those required for condensation. The shape of the aggregation curve obtained with Lys_5 is similar to those obtained with polyamines and polyamine analogs used by Saminathan et.al.[29] This result is in agreement with our temperature studies, where a large increase in the size of Lys_5-containing particles at ≥ 50 °C suggests a tendency toward aggregation of the nanoparticles. Lys_4's failure to stimulate DNA aggregation at high temperatures is also consistent with the results of our temperature studies that show this oligolysine's inability to form discrete particles at temperatures > 37 °C. Lys_4's behavior may be attributed to its relatively low DNA binding affinity, which can lead to easy displacement of the oligolysine from its complexes with DNA by monovalent ions at high temperatures. We also demonstrated that PLL causes very little λ-DNA aggregation (≤ 9%) at temperatures up to 70 °C. Our results agree with the findings of other studies that demonstrated that PLL-DNA particles are resistant to precipitation at low DNA concentration in aqueous solutions in the presence of little or no salt.[38-40] However, these and

other studies reported that at high salt and DNA concentrations, PLL-containing particles tended to aggregate.

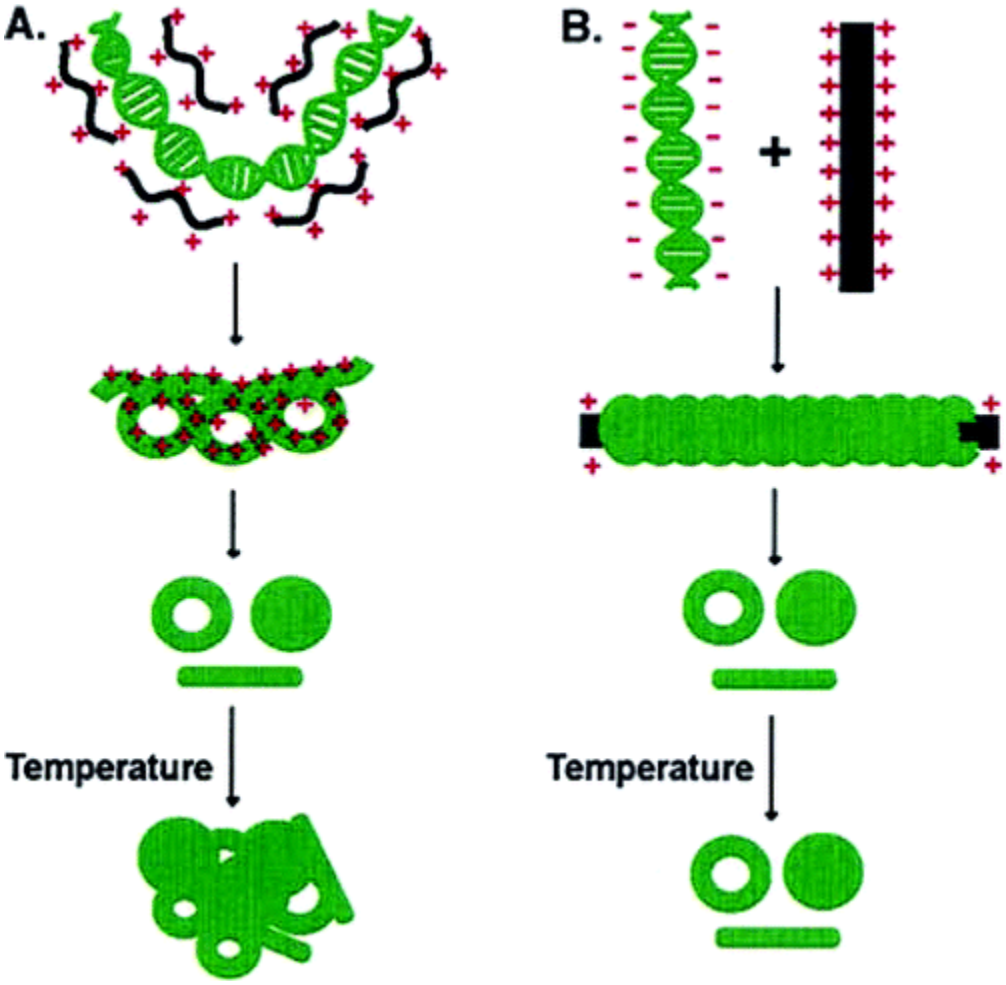

Figure 25. Schematic representation of 2 different mechanisms in the condensation of λ-DNA by: (A) oligolysines and (B) poly-L-lysine. In A, oligolysines are assumed to bind with DNA by electrostatic forces, leading to the collapse of DNA to nanoparticles. When these particles are heated, oligolysines partially dissociate from DNA, leading to partial melting of DNA and cross-linking of different DNA molecules to aggregates. In B, DNA is modeled to wrap around poly-L-lysine. The wrapped particles are protected from heat-induced denaturation and cross-linking.

Taken together, our results indicate that the mode of binding of PLL to DNA is different from that of the binding of oligolysines and other small multivalent cations, such as polyamines and cobalt hexamine.[1,26-28,31,41-45] Studies on DNA interactions of polyamines and H1 histone proteins suggest their preferential binding to the minor groove, the area of highest charge density

in DNA.[46-50] We, therefore, suggest that while the oligolysine molecule can wrap and bind DNA through its minor groove, DNA may wrap around the PLL as a string around a spool. The latter mode of binding is similar to that of DNA–dendronized polymer interaction, in which DNA wraps around the polymer and the calculated pitch decreases with increase in charge density of the polymer.[51] Alternatively, it is conceivable that PLL and DNA undergoes coacervation, so that in the coacervation region, precipitation is prevented.[52-54] Coacervation is a spontaneous process that occurs in aqueous solutions of oppositely charged polyelectolytes and involves a spontaneous liquid-liquid phase separation. Coacervation region is centered around the charge neutrality, dependent on charge neutrality and complex size. However, smaller complexes cannot coacervate even if their charges are neutralized. Therefore, PLL/DNA complexes have greater chances of forming coacervate regions. Molecular mechanical calculation suggests that DNA undergoes different modes of binding, depending on the nature of the multivalent cations.[50,55] Based on our results and the above considerations, we propose a schematic model for the binding of oligolysines and PLL to DNA (Figure 25). This model is supported by our results on temperature effects on nanoparticles as well as our DNA precipitation/aggregation experiments (Figures 21 and 23).

In summary, our results show that both oligolysines and PLL are good DNA condensing agents, and that condensation efficiency increases with greater lysine chain length. The ability of PLL to condense DNA and the size of the resulting nanoparticles are relatively insensitive to salt concentration and increase in temperature. In contrast, oligolysines' ability to condense DNA and the size of the polyplex shows a strong dependence on monovalent ion concentration of the medium. These results might contribute to the development of nonviral gene delivery vehicles because characterization of nanoparticle formation, their stability, and other properties are important in gene therapy.

Acknowledgments

We wish to express our sincere thanks to Dr. Veena Vijayanathan for her help in different stages of conducting the experiments and in preparing this manuscript.

REFERENCES

(1) Vijayanathan, V.; Thomas, T.; Thomas, T. J. DNA Nanoparticles and development of DNA delivery vehicles for gene therapy. Biochemistry **2002,** 41,14085.

(2) Bloomfield, V. A. DNA Condensation. Curr. Opin. Struct. Biol. **1996**, 6, 334.

(3) Hud, N. V.; Vilfan, I. D. Toroidal DNA condensates: unraveling the fine structure and the role of nucleation in determining size. Annu. Rev. Biophys. Biomol. Struct. **2005**, 34, 295.

(4) Gosule, L. C.; Schellman, J. A. DNA condensation with polyamines I. Spectroscopic studies. J. Mol. Biol. **1978**, 121, 311.

(5) Widom, J.; Baldwin, R. L. Cation-induced toroidal condensation of DNA studies with Co3+(NH3)6. J. Mol. Biol. **1980**, 144, 431.

(6) Thomas, T. J.; Bloomfield, V. A. Toroidal condensation of Z DNA and identification of an intermediate in the B to Z transition of poly(dG-m5dC) X poly(dG-m5dC). Biochemistry **1985**, 24, 713.

(7) Hud, N. V.; Downing, K. H. Cryelectron Microscopy of λ Phage DNA Condensates in Vitreous Ice: The Fine Structure of DNA Toroids. Proc. Natl. Acad. Sci. U S A. **2001,** 98, 14925.

(8) Saminathan, M.; Thomas, T.; Shirahata, A.; Pillai, C. K. S.; Thomas, T. J. Polyamine structural effects on the induction and stabilization of liquid crystalline DNA: potential applications to DNA packaging, gene therapy and polyamine therapeutics. Nucleic Acids Res. **2002**, 30, 3722.

(9) Lohman, T. M.; deHaseth P. L.; Record M. T. Pentalysine-deoxyribonucleic acid interactions: a model for the general effects of ion concentrations on the interactions of proteins with nucleic acids. Biochemistry **1980**, 19, 3522.

(10) Leng, M.; Felsenfeld, G. The preferential interactions of polylysine and polyarginine with specific base sequences in DNA. Proc. Natl. Acad. Sci. U S A. **1966**, 56, 1325.

(11) Tang, M. X.; Li, W.; Szoka, F. C., Jr. Toroid formation in charge neutralized flexible or semi-flexible biopolymers: potential pathway for assembly of DNA carriers. J. Gene Med. **2005**, 7, 334.

(12) Wolfert, M. A.; Seymour, L. W. Atomic force microscopic analysis of the influence of the molecular weight of poly(L)lysine on the size of polyelectrolyte complexes formed with DNA. Gene Ther. **1996**, 3, 269.

(13) Guping, Y.; Guping, T.; Yanjie. A new biodegradable poly-amino acid: alpha,beta-poly[(N-hydroxypropyl/aminoethyl)-DL-aspartamide-co-L-lysine], a potential nonviral vector for gene delivery. Drug Deliv. **2005**, 12, 89.

(14) Matthews, C.; Jenkins, G.; Hilfinger, J.; Davidson, B. Poly-L-lysine improves gene transfer with adenovirus formulated in PLGA microspheres. Gene Ther. **1999**, 6, 1558.

(15) Manning, G. S. The Molecular Theory of Polyelectrolyte Solutions with Applications to the Electrostatic Properties of Polynucleotides. Q. Rev. Biophys. **1978**, 11, 179.

(16) Record, M. T., Jr.; Anderson, C. F.; Lohman, T. M. Thermodynamic analysis of ion effects on the binding and conformational equilibria of proteins and nucleic acids: the roles of ion

association or release, screening, and ion effects on water activity. Q. Rev. Biophys. **1978**, 11, 103.

(17) Pannier, A. K.; Shea, L. D. Controlled release systems for DNA delivery. Mol. Ther. **2004**, 10, 19.

(18) Wadhwa, M. S.; Collard, W. T.; Adami, R. C.; McKenzie, D. L.; Rice, K. G. Peptide-mediated gene delivery: influence of peptide structure on gene expression. Bioconjug. Chem. 1997, 8, 81.

(19) Kim, S. W. Terplex gene delivery system. Adv. Genet. 2005, 53PA, 263.

(20) Park, S.; Healy, K. E. Compositional regulation of poly(lysine-g-(lactide-b-ethylene glycol))-DNA complexation and stability. J. Control. Release 2004, 95, 639.

(21) Arscott, P. G.; Li, A. Z.; Bloomfield, V. A. Condensation of DNA by trivalent cations. 1. Effects of DNA length and topology on the size and shape of condensed particles. Biopolymers 1990, 30, 619.

(22) Petersen, H.; Kunath, K.; Martin, A.L.; Stolnik, S.; Roberts, C.J.; Davies, M.C.; Kissel, T. Star-shaped poly(ethylene glycol)-block-polyethylenimine copolymers enhance DNA condensation of low molecular weight polyethylenimines. Biomacromolecules 2002, 3, 926.

(23) Vijayanathan, V.; Thomas, T.; Antony, T.; Shirahata, A.; Thomas, T. J. Formation of DNA Nanoparticles in the Presence of Novel Polyamine Analogues: A Laser Light Scattering and Atomic Force Microscopic Study. Nucleic Acids Res. 2004, 32, 127.

(24) Hansma, H. G. Surface biology of DNA by atomic force microscopy. Annu. Rev. Phys. Chem. 2001, 52, 71.

(25) Molas, M.; Bartrons, R.; Perales, J. C. Single-stranded DNA condensed with poly-L-lysine results in nanometric particles that are significantly smaller, more stable in physiological ionic strength fluids and afford higher efficiency of gene delivery than their double-stranded counterparts. Biochim. Biophys. Acta. 2002, 1572, 37.

(26) Vijayanathan, V.; Thomas, T.; Shirahata, A.; Thomas, T. J. DNA condensation by polyamines: a laser light scattering study of structural effects. Biochemistry **2001**, 40, 13644.

(27) Thomas, T. J.; Bloomfield, V. A. Differential effects on the B-to-Z transition of poly(dG-me5dC).poly(dG-me5dC) produced by N1- and N8-acetyl spermidine. Biopolymers **1985**, 24, 725.

(28) Vijayanathan, V.; Lyall, J.; Thomas, T.; Shirahata, A.; Thomas, T. J. Ionic, structural, and temperature effects on DNA nanoparticles formed by natural and synthetic polyamines. Biomacromolecules **2005**, 6, 1097.

(29) Saminathan, M.; Antony, T.; Shirahata, A.; Sigal, L. H.; Thomas, T.; Thomas, T. J. Ionic and structural specificity effects of natural and synthetic polyamines on the aggregation and resolubilization of single-, double-, and triple-straded DNA. Biochemistry **1999**, 38, 3821.

(30) Thomas, T.; Thomas, T. J. Selectivity of polyamines in triplex DNA stabilization. Biochemistry **1993**, 32, 14068.

(31) Thomas, T. J.; Bloomfield, V. A. Collapse of DNA caused by trivalent cations: pH and ionic specificity effects. Biopolymers **1983**, 22, 1097.

(32) Shapiro, J. T.; Leng, M.; Felsenfeld, G. Deoxyribonucleic acid-polylysine complexes. Structure and nucleotide specificity. Biochemistry **1969**, 8, 3119.

(33) Liu, G.; Molas, M.; Grossmann, G. A.; Pasumarthy, M.; Perales, J. C.; Cooper, M. J.; Hanson, R. W. Biological properties of poly-L-lysine-DNA complexes generated by cooperative binding of the polycation. Biol. Chem. **2001**, 276, 34379.

(34) Perales, J. C.; Grossmann, G. A.; Molas, M.; Liu, G.; Ferkol, T.; Harpst, J.; Oda, H.; Hanson, R. W. Biochemical and functional characterization of DNA complexes capable of targeting genes to hepatocytes via the asialoglycoprotein receptor. J. Biol. Chem. **1997**, 272, 7398.

(35) Kwoh, D. Y.; Coffin, C. C.; Lollo, C. P.; Jovenal, J.; Banaszczyk, M. G.; Mullen, P.; Phillips, A.; Amini, A.; Fabrycki, J.; Bartholomew, R. M.; Brostoff, S. W.; Carlo, D. J. Stabilization of poly-L-lysine/DNA polyplexes for in vivo gene delivery to the liver. Biochim. Biophys. Acta **1999**, 1444, 171.

(36) Olins, D. E.; Olins, A. L.; von Hippel, P. H. On the structure and stability of DNA-protamine and DNA-polypeptide complexes. J. Mol. Biol. **1968**, 33, 265.

(37) Liquier, J.; Pinot-Lafaix, M.; Taillandier, E.; Brahms, J. Infrared linear dichroism investigations of deoxyribonucleic acid complexes with poly(L-arginine) and poly(L-lysine). Biochemistry **1975,** 14, 4191.

(38) Tang, M. X.; Szoka, F.C. The influence of polymer structure on the interactions of cationic polymers with DNA and morphology of the resulting complexes. Gene Ther. **1997**, 4, 823.

(39) Wolfert, M. A.; Seymour L.W. Polyelectrolyte vectors for gene delivery: influence of cationic polymer on biophysical properties of complexes formed with DNA. Gene Ther. **1996**, 3, 269.

(40) Plank, C.; Tang, M. X.; Wolfe, A. R.; Szoka, F. C. Branched cationic peptides for gene delivery: role of type and number of cationic residues in formation and in vitro activity of DNA polyplexes. Hum. Gene Ther. **1999**, 10, 319.

(41) Schurr, J. M.; Fujimoto, B. S. Extensions of counterion condensation theory. I. Alternative geometries and finite salt concentration. Biophys. Chem. **2002**, 101-102, 425.

(42) Bai, Y.; Das, R.; Millett, I. S.; Herschlag, D.; Doniach, S. Probing counterion modulated repulsion and attraction between nucleic acid duplexes in solution. Proc. Natl. Acad. Sci. U S A. **2005,** 102, 1035.

(43) Matulis, D.; Rouzina, I.; Bloomfield, V. A. Thermodynamics of cationic lipid binding to DNA and DNA condensation: roles of electrostatics and hydrophobicity. J. Am. Chem. Soc. **2002**, 124, 7331.

(44) Saminathan, M.; Antony, T.; Shirahata, A.; Sigal, L. H.; Thomas, T.; Thomas, T. J. Ionic and Structural Specificity Effects of Natural and Synthetic Polyamines on the Aggregation and Resolubilization of Single-, Double-, and Triple-Straded DNA. Biochemistry **1999**, 38, 3821.

(45) Bloomfield, V. A. Condensation of DNA by multivalent cations: considerations on mechanism. Biopolymers **1991**, 31, 1471.

(46) Roque, A.; Orrego, M.; Ponte, I.; Suau, P. The prefential binding of histone H1 to DNA scaffold-associated regions is determined by its C-terminal domain. Nucleic Acids Res. **2004**, 32, 6111.

(47) Hendrickson, F. M.; Cole, R. D. Selectivity in the interaction of various DNA sequences with H1 histone. Biochemistry **1994**, 33, 2997.

(48) Sponar, J.; Votavova, H. J. Selective binding of synthetic polypeptides to DNA of varying composition and sequence: effect of minor groove binding drugs. Biomol. Struct. Dyn. **1996**, 13, 979.

(49) Schmid, N.; Behr, J.P. Location of spermine and other polyamines on DNA as revealed by photoaffinity cleavage with polyaminobenzenediazonium salts. Biochemistry **1991**, 30, 4357.

(50) Korolev, N., Lyubartsev, A. P.; Laaksonen, A.; Nordenskiold, L. A Molecular dynamics simulation study of oriented DNA with polyamine and sodium counterions: diffusion and averaged binding of water and cations. Nucleic Acids Res. **2003**, 31, 5971.

(51) Gossl, I.; Shu, L.; Schluter, A. D.; Rabe, J. P. Molecular structure of single DNA complexes with positively charged dendronized polymers. J. Am. Chem. Soc. **2002**, 124, 6860.

(52) Kaibara, K.; Okazaki, T; Bohidar, H. B.; Dubin, P. L. pH-induced coacervation in complexes of bovine serum albumin and cationic polyelectrolytes. Biomacromolecules **2000**, 1, 100.

(53) Seyrek, E.; Dubin, P. L.; Tribet, C.; Gamble, E. A. Ionic strength dependence of protein-polyelectrolyte interactions. Biomacromolecules **2003**, 4, 273.

(54) Yoshida, K.; Sokhakian, S.; Dubin, P. L. Binding of Polycarboxylic Acids to Cationic Mixed Micelles: Effects of Polymer Counterion Binding and Polyion Charge Distribution. J. Colloid Interface Sci. **1998**, 205, 257.

(55) Feuerstein, B. G.; Pattabiraman, N.; Marton, L. J. Molecular mechanics of the interactions of spermine with DNA: DNA bending as a result of ligand binding. Nucleic Acids Res. **1990**, 18, 1271.

GENERAL DISCUSSION

In Chapter 1 of this thesis, we investigated autophagy as a mechanism of antiestrogen resistance. To that end, we examined the role of the autophagy mediator, Beclin 1, in estrogenic signaling and antiestrogen resistance in Beclin 1 overexpressing, ER-positive MCF-7 cells.

Beclin 1 overexpressing cells had reduced proliferative response to E_2, and the expression of E_2-responsive genes was also down-regulated. Akt phosphorylation was also downregulated in the presence of E_2, in Beclin 1-overexpressing cells. One of the mechanisms involved in acquired tamoxifen resistance is that ERα becomes insensitive, as the cell regulatory circuits are taken over by growth factor receptors, including members of the HER-2 family of receptors, or G-protein coupled receptors (Massarweh et al. 2007, Milano et al. 2006, Riggins et al. 2007). Our finding of decreased Akt phosphorylation shows that overexpression of Beclin 1 interferes with E_2-stimulated ERα signaling responses. Down-regulation of E_2-responsive genes, such as c-fos, Erg-1 and Nur77, is indicative of an altered molecular environment for estrogenic function.

It is interesting to note that, unlike Akt, ERK1/2 activation by E_2 was not impaired in Beclin 1-overexpressing cells. ERK1/2 activation may be attributable to non-genomic signaling pathways that bypass the need for functionally available ERα, such as growth receptor or G-protein receptor signaling (Massarweh et al. 2007, Riggins et al. 2007). Thus, certain components of the E_2 signaling pathway seem to be functioning in the presence of Beclin 1 overexpression.

Beclin 1-overexressing cells showed insensitivity to anti-estrogenic effects of raloxifene and 4-hydroxytamoxifen, as demonstrated by the CellTiterGlo assay. Since the function of these antiestrogens is mediated by ERα (Pearce et al., 2004), we hypothesized that an interaction between Beclin 1 and ERα may lead to the sequestration of the receptor, thus limiting its availability to antiestrogens. In addition, ChIP assay results showed that antiestrogen-treatment of Beclin1-overexpressing cells decreased the occupancy of the pS2 promoter by ERα compared to control cells. These results point to the existence of direct interactions between Beclin 1 and ERα, which may affect the actions of these proteins during cellular response to antiestrogens.

To support our hypothesis of an interaction between ERα and Beclin 1, we performed confocal microscopy and co-immunoprecipitation experiments. Confocal microscopic visualization revealed co-localization of ERα and Beclin 1, and the immunoprecipitation assay further demonstrated association between these proteins. Liang et al. showed that Beclin 1 distribution centered in the endoplasmic reticulum, mitochondria, perinuclear membrane, and the nucleus (Liang et al., 2001). Coincidentally, ERα also shuttles between nucleus, cytoplasm and peripheral membrane, where it interacts with multiple proteins in order to exert its effects (Levin et al. 2008, Song et al. 2004). Thus, direct association between ERα and Beclin 1 is clearly possible, and may modulate the function of both proteins.

In summary, our results reveal an interaction between ERα and Beclin 1 in ER-positive breast cancer cells. This interaction may modulate the function of ERα and Beclin 1. In the context of ERα function, we found that Beclin 1 transfected cells were less sensitive to E_2-induced growth stimulation and to the growth inhibitory effects of antiestrogens. Thus, a novel function for Beclin 1 might involve down-regulation of the action of ERα, contributing to resistance of breast cancer cells to antiestrogens.

In Chapter 2 of this thesis, we examined the effect of BE-3-3-3-3 on ERα-positive breast cancer cell growth in the presence and absence of E_2, and found that this polyamine analogue exerts differential effects under these two sets of conditions. In the presence of E_2, there was a concentration-dependent decrease of cell growth, as measured by [^{3}H]-thymidine incorporation. These results are supported by previous work in our laboratory, which showed that BE-3-3-3-3 promoted cell growth inhibition, induced apoptosis, and stimulated SSAT activity (Faaland et al., 2000). In the absence of E_2, low concentrations (1.25 to 10 μM) of BE-3-3-3-3 caused an increase in [^{3}H]-thymidine incorporation (3-5-fold) at 24 and 48 h of treatment. However, growth inhibition was observed by 96 h of treatment. Our results are supported by the report from Minchin et al., who observed a growth-stimulatory effect of low concentration of BE-3-3-3 (up to 10 μM) on melanoma cells (Minchin et al., 2006). However, melanoma cell proliferation was observed even at 4 days after treatment with BE-3-3-3, and may depend on the cell type or conditions of the study.

Our studies of BE-3-3-3-3 in the absence of E_2 are physiologically relevant since ovariectomized breast cancer patients and post-menopausal women are in a state of estrogen deprivation. Dose- and time-dependent differential effects on cell growth are exerted by other antiproliferative agents as well. Differential effects on breast cancer cells, depending on the presence of absence of E_2, were recently demonstrated in our laboratory in the case of 2-methoxyestradiol (2 ME) (Vijayanathan et al., 2006). In the absence of E_2, 2 ME enhanced MCF-7 and T-47D cell growth and Akt phosphorylation at concentrations of 10 to 50 nmol/L. In contrast, in the presence of E_2, 2 ME inhibited E_2–induced cell proliferation and Akt phosphorylation.

BE-3-3-3-3-induced changes in the expression of E_2-modulated genes were determined by real time PCR. Gene regulation by this polyamine analogue was similar to that of E_2 in some cases, and different in others. The early response genes, c-myc and c-jun were significantly upregulated by BE-3-3-3-3, similar to the action of E_2. However, another early response gene, c-fos, was inhibited by 10 μM BE-3-3-3-3. Cyclin B1 mRNA levels were significantly downregulated by BE-3-3-3-3, consistent with E_2's degradative/downregulatory effect on cyclin B1 mRNA during G1 phase (Thomas and Thomas, 1994). In contrast to E_2, PTEN transcription was downregulated by BE-3-3-3-3. In contrast, E_2 increased PTEN protein expression in human endometrial stromal cells at 15 minutes after treatment (Guzeloglu-Kayisli et al. 2003). The expression of the proto-oncogene, c-myb, was downregulated by BE-3-3-3-3 at all time points. This action of the polyamine analogue contradicts the effect of E_2 in ER-positive breast cancer cells, which increased c-myb mRNA levels 20-fold (Gudas et al., 1995). The differences in effects of E_2 and BE-3-3-3-3 on gene expression indicate that the E_2 signaling pathway is not fully activated by BE-3-3-3-3. As genomic and non-genomic signaling is involved in the action of E_2, it is possible that only a part of this signaling pathway is activated by the polyamine analogue.

Another estrogen-mimetic action of BE-3-3-3-3 was increased Akt phosphorylation at the 48 h time point. The proliferative effect of E_2 includes the stimulation of Akt phosphorylation as part of the non-genomic cell signaling of ERα within minutes of the addition of the hormone (Levin et al., 2008). Akt serine/threonine kinase is a key mediator of cell survival, resistance to

apoptosis and sensitivity to chemotherapeutic agents (Cicenas, 2008). At present, it is not clear how BE-3-3-3-3 affects non-genomic signaling through ERα. Nevertheless, it is clear that BE-3-3-3-3-induced cell growth includes elevated levels of Akt phosphorylation at 48 h after treatment. Thus, elements of breast cancer cell growth stimulatory pathway are activated by BE-3-3-3-3 in a manner similar to that of E_2.

We also discovered that autophagy plays a role in the delayed cell growth inhibition by BE-3-3-3-3, in the absence of E_2. Our EM analysis demonstrated the presence of autophagosomes, indicators of autophagy, after treatment with 10 μM BE-3-3-3-3. Previous studies have reported that certain polyamine analogues induced the formation of large lysosomal vacuoles in treated cells (Dai et al. 1999, Porter et al. 1990, Kramer et al. 1998). The appearance and growth of these vacuoles could be reversed by the removal of polyamine treatment. In hematopoietic cells, vacuoles grew in size over time, eventually engulfing key cytoplasmic organelles such as mitochondria (Dai et al. 1999). The characteristic morphology and the reversible growth and appearance of these vacuoles, indicated to us that autophagy was stimulated by these polyamine analogues.

Additional evidence for the stimulation of autophagy in our study comes from the polyamine analogue-mediated increase in the expression of autophagy-related proteins, Beclin 1 and MAP LC3 II. Beclin 1 protein mediates autophagy by forming a complex with class III PI3 kinase (vps34) and several other proteins (i.e. Atg14L), and initiating autophagosome formation (Zhong et al. 2009). MAP LC3 II is found on the pre-autophagic membranes and autophagosomes, and is a widely accepted marker of the detection of autophagy (Klionsky et al., 2008).

Confocal microscopic investigation showed higher levels of Beclin 1 in the presence of BE-3-3-3-3, supporting our data on Beclin 1 protein expression. In addition, BE-3-3-3-3 caused the accumulation of the protein around the nucleus, similar to the effect observed in the presence of E_2. In a previous study, we demonstrated E_2–stimulated Beclin 1 re-localization to the perinuclear area in Beclin 1-overexpressing, MCF-7 cells (John et al., 2008). These results once

again show that BE-3-3-3-3 behaves in an estrogen-mimetic manner during the initial, growth-stimulatory phase.

In summary, our results demonstrate the differential behavior of BE-3-3-3-3 in the presence and absence of E_2. It stimulated cell growth in the absence of E_2, although this effect disappeared by 96 h after treatment. In contrast, BE-3-3-3-3 inhibited cell growth in the presence of E_2. We also showed the involvement of autophagy in the growth-stimulatory phase of BE-3-3-3-3, promoting cell survival and delaying growth inhibition in response to this polyamine analogue.

In the second part of the thesis, Chapters 3 and 4, we explored the use of cationic polymers as gene delivery vehicles in breast cancer therapy by investigating the physico-chemical properties of these polymers in complexes with DNA. In Chapter 3, we examined the characteristics of α,α'-methylated spermine stereoisomers (R,R-Me_2Spm, S,S- Me_2Spm, R,S-Me_2Spm, and racemic (Rac R,R-Me_2Spm, S,S- Me_2Spm, R,S- Me_2Spm, and racemic (R,R; R,S; S,S)- Me_2Spm)- Me_2Spm) and compared them with those of a widely studied polyamine, spermine. Three out of four stereoisomers (RR-, RS-, and Rac- Me_2Spm) were significantly more effective as DNA condensing agents than spermine, demonstrating that spatial geometry plays a role in DNA condensation, in addition to non-specific ionic interactions.

Nanoparticle sizes ranged between 39.6 – 48.4 nm (hydrodynamic radius), and did not follow the same pattern as condensation efficiency. R,R- and S,S- Me_2Spm isomers demonstrated significantly larger condensates than spermine, while the sizes of RS- and Rac-Me_2Spm nanoparticles were comparable to that of spermine. These findings demonstrate that polyamine structure also has an impact on the biophysical properties of polyamine-DNA condensates.

Other studies have demonstrated that stereoisomer structure can influence the physico-chemical properties of its nanoparticles as well as its biological function. Vijayanathan et al. demonstrated that structural arrangements of spermine homologues, such as the number of methylene spacings between the secondary amine groups, play an important role in their DNA condensing abilities and the sizes of resultant nanoparticles (Vijayanathan et al., 2001). Gao et

al. showed that among salicyl diamines of different conformations, the R,R stereoisomer was the most effective cytotoxic agent in MCF-7 cells (Gao et al., 2007). The isomer also had the greatest effect on cyclin D1 mRNA expression, downregulating it to 40% of control, compared to other isomers that were able to lower mRNA expression only to 68-71% of control.

Particle sizes obtained in this study are in overall agreement with the sizes of polyamine-DNA condensates reported previously (Thomas and Bloomfield 1983, Vijayanathan et al. 2001). Size measurements can be influenced by many variables, including the size of the DNA, starting reactant concentrations, ionic environment, mixing protocol, as well as the method of measurement (Vijayanathan et al., 2002).

Electron microscopic visualization revealed the presence of spheroids and toroids, with overall sizes similar to those observed during hydrodynamic radius measurements. We did not observe the formation of rods, although they have been reported in the presence of other multivalent cations, such as cobalt hexamine and PLL (Vilfan et al. 2006, Liu et al. 2001). Particle morphology is influenced by kinetics factors, and toroidal shapes predominate at equilibrium (Vilfan et al., 2006).

Melting temperature analysis demonstrated that spermine and its stereoisomers stabilized CT-DNA in a concentration-dependent manner. This effect has been demonstrated in other melting studies (Thomas and Bloomfield 1984, Saminathan et al., 1999). However, no significant differences in degree of stabilization (i.e. Tm values) were observed between the various cations. The differences in the condensing efficiencies of the spermine analogues, and the lack of differences in the degree of stabilization suggest the involvement of different mechanisms in DNA condensation and stabilization by methylated polyamines.

In the Chapter 4, we continued our investigation of possible gene delivery vehicles for breast cancer therapy. With that purpose, we compared the DNA condensing abilities of PLL and oligolysines, trilysine (Lys_3), tetralysine (Lys_4), pentalysine (Lys_5), and characterized the size, shape and stability of nanoparticles. PLL was a much more effective condensing agent than either oligolysine, and condensing ability correlated with increasing positive charge of the cations. PLL's superior DNA condensing ability can be attributed to its higher binding affinity than that of

oligolysines. Generally, higher charge of a cation leads to a higher binding affinity than that of lower charge cations, thereby causing DNA to collapse at lower counterion concentrations.

Trilysine's inability to provoke DNA condensation in our study has also been reported by other investigators (Wadhwa et al., 1997). Since the amino acid groups of lysine are considered to be 99% protonated at pH of 7.0, the peptide's amino groups may be partially protonated at our experimental pH of 7.4. This would result in an actual charge of less than 3+, thereby contributing to Lys_3 inability to condense DNA. Another reason for Lys_3's inability to induce DNA compaction may result from the low charge density of the molecule because of the chain separation between positive charges.

Nanoparticles produced in the presence of tetra- and penta-lysines were easily destabilized by increasing ionic strength of the medium, as demonstrated by their larger particle size at higher salt concentrations. The linear positive slope obtained in the graph of $\log[EC_{50}]$ against $\log [Na^+]$ shows the purely electrostatic nature of oligolysine-DNA binding. This binding is driven by a net gain in entropy that occurs when DNA-bound Na^+ are released into solution, and is readily reversible at higher $[Na^+]$ when the entropy gain from the release of Na^+ is negligible (Bloomfield, 1991). On the other hand, PLL-containing nanoparticles are relatively stable at higher ionic concentrations. The lack of a positive slope in the graph of $\log[EC_{50}]$ against $\log [Na^+]$ indicates that forces other than electrostatic interaction may be behind PLL-mediated DNA condensation.

PLL also stabilized nanoparticles against thermal denaturation and aggregation up to 70°C, whereas oligolysines were unable to stabilize nanoparticles at higher temperatures. Thermal destabilization of Lys_5-codensates resulted in aggregation at temperatures $\geq$ 50 °C. In addition, Lys_4-containing nanoparticle became unstable at temperatures $\geq$ 40 °C, precluding any further measurement of particle stability and/or aggregation. The observed instability of Lys_4-condensates may result from the relatively low DNA binding affinity of this oligolysine, as well as from the increased entropy of the environment at higher temperatures.

Our melting studies demonstrated that Lys_3, Lys_4 and Lys_5 stabilized λ-DNA in a concentration-dependent manner, and that greater duplex stabilization correlated with increasing

oligolysine chain length. We were unable to detect biphasic melting in the presence of PLL, which may have been due to the fact that the second melting transition occurs at a temperature above 100 °C, and, therefore, cannot be measured by the instrument used in our melting studies. The observation that Lys_3 can confer duplex stability, while, at the same time, is unable to provoke DNA condensation led us to conclude that DNA condensation and stabilization may involve different mechanisms.

Our findings indicate that the mode of binding of PLL to DNA is different from that of the binding of oligolysines, and we propose a model for these divergent binding mechanisms. Studies on DNA interactions of polyamines and H1 histone proteins suggest their preferential binding to the minor groove, the area of highest charge density in DNA (Sponar et al. 1996, Roque et al. 2004, Schmid et al. 1991, Korolev et al. 2003). We, therefore, suggest that while the oligolysine molecule can wrap and bind DNA through its minor groove, DNA may wrap around the PLL as a string around a spool. The latter mode of binding is similar to that of DNA–dendronized polymer interaction, in which DNA wraps around the polymer and the calculated pitch decreases with increase in charge density of the polymer (Gossl et al., 2002).

In conclusion, in Chapters 3 and 4 we investigated DNA condensing abilities of α,α'-methylated spermine stereoisomers, oligolysines, and PLL. In addition, we characterized the size, shape and stability of their nanoparticles. Physico-chemical properties of nanoparticles are important determinants in successful gene delivery. Our research showed that methylated polyamines and lysine polymers have potential as possible gene delivery vehicles and merit further investigation.

Summary and Conclusions

During the course of this study, we investigated the mechanisms of antiestrogen resistance mediated by Beclin 1 in ER-positive breast cancer cells. We concluded that interactions between ERα and Beclin 1 may lead to ERα sequestration, resulting in a diminished response to estrogens and antiestrogens in these cells. In addition, we examined the differential effect of BE-3-3-3-3 on MCF-7 breast cancer cells in the presence and absence of E_2. In the

absence of E_2, this polyamine analogue mimicked estrogenic effects and stimulated autophagy in ER-positive, MCF-7 breast cancer cells. The ability of BE-3-3-3-3 to mimic E_2 might be physiologically relevant during pharmacological drug administration to subsets of patients with low endogenous estrogen levels, such as ovariectomized or postmenopausal women.

We also examined gene therapy approaches to the treatment of breast cancer by studying DNA nanoparticle formation in the presence of α-methyl polyamines, oligolysines, and PLL. α-Methyl polyamines proved to be effective DNA compacting agents, and spatial geometry played an important role in their condensing abilities and particle sizes. PLL was a much more effective DNA condensing agent than the oligolysines, and its nanoparticles were more stable during ionic or thermal challenge. Our results indicate that these cationic polymers have potential as gene delivery vehicles and merit further investigation.

Overall, we investigated estrogenic regulation of the balance of cell growth, autophagy, and cell death. We provide new insights about antiestrogen resistance, development of polyamine analogues for breast cancer therapy, and new gene therapy vehicles with potentially wide applications.

REFERENCES

Bloomfield, V. A. (1991) Condensation of DNA by multivalent cations: considerations on mechanism. *Biopolymers* **31**:1471-1481.

Cicenas, J. (2008) The potential role of Akt phosphorylation in human cancers. *Int. J. Biol*. Markers. **23**:1-9.

Dai, H., Kramer, D. L., Yang, C., Murti, G., Porter, C. W., Cleveland, J. L. (1999) The polyamine oxidase inhibitor MDL-72,527 selectively induces apoptosis of transformed hematopoietic cells through lysosomotropic effects. *Cancer Res*. **59**:4944-4954.

Faaland, C. A., Thomas, T. J., Balabhadrapathruni, S., Langer, T., Mian, S., Shirahata, A., Gallo, M. A., Thomas, T. (2000) Molecular correlates of the action of bis(ethyl)polyamines in breast cancer cell growth inhibition and apoptosis. *Biochem. Cell Biol*. **78**:415-426.

Gao, J., Liu, Y., Zhou, Y., Zingaro, R. A. (2007) Chiral salicyl diamines: potent anticancer molecules. C*hemMedChem* **2**:1723-1729.

Gossl, I., Shu, L., Schluter, A. D., Rabe, J. P. (2002) Molecular structure of single DNA complexes with positively charged dendronized polymers. *J. Am. Chem. Soc*.**124**:6860-6865.

Gudas, J. M., Klein, R. C., Oka, M., Cowan, K. H. (1995) Posttranscriptional regulation of the c-myb proto-oncogene in estrogen receptor-positive breast cancer cells. *Clin. Cancer Res*. **1**:235-243.

Guzeloglu-Kayisli, O., Kayisli, U. A., Al-Rejjal, R., Zheng, W., Luleci, G., Arici, A. (2003) Regulation of PTEN (Phosphatase and tensin Homolog deleted on chromosome 10) expression by estradiol and progesterone in human endometrium. *J. Clin. Endocrinol. Metab*. **88**:5017-5026.

John, S., Nayvelt, I., Hsu, H. C., Yang, P., Liu, W., Das, G. M., Thomas, T., Thomas, T. J. (2008) Regulation of estrogenic effects by Beclin 1 in breast cancer cells. *Cancer Res*. **68**:7855-7863.

Klionsky, D. J., Abeliovich, H., Agostinis, P., Agrawal, D. K., Aliev, G. et al. (2008) Guidelines for the use and interpretation of assays for monitoring autophagy in higher eukaryotes. *Autophagy* **4**:151-175.

Korolev, N., Lyubartsev, A. P., Laaksonen, A., Nordenskiold, L. (2003) A Molecular Dynamics Simulation Study of Oriented DNA with Polyamine and Sodium Counterions: diffusion and averaged binding of water and cations. *Nucleic Acids Res*. **31:**5971-5981.

Kramer, D. L., Black, J. D., Mett, H., Bergeron, R. J., Porter, C. W. (1998) Lysosomal sequestration of polyamine analogues in Chinese hamster ovary cells resistant to the s-adenosylmethionine decarboxylase inhibitor, CGP-48664. *Cancer Res*. **58**:3883-3890.

Levin, E. R., Pietras, R. J. (2008) Estrogen receptors outside the nucleus in breast cancer. Breast *Cancer Res. Treat.***108**:351-361.

Liang, X. H., Yu, J., Brown, K., Levine, B. (2001) Beclin 1 contains a leucine-rich nuclear export signal that is required for its autophagy and tumor suppressor function. *Cancer Res*. **61**:3443-49.

Liu, G., Molas, M., Grossmann, G. A., Pasumarthy, M., Perales, J. C., Cooper, M. J., Hanson, R. W. (2001**)** Biological properties of poly-L-lysine-DNA complexes generated by cooperative binding of the polycation. *Biol. Chem.* **276**:34379-34387.

Massarweh, S., Schiff, R. (2007) Unraveling the mechanisms of endocrine resistance in breast cancer: new therapeutic opportunities. *Clin. Cancer Res*. **13**:1950-1954.

Milano, A., Lago, L. D., Sotiriou, C., Piccart, M., Cardoso, F. (2006) What clinicians need to know about antiestrogen resistance in breast cancer therapy. *Eur. J. Cancer* **42**:2692-2705.

Minchin, R. F., Knight, S., Arulpragasam, A., Fogel-Petrovic, M. (2006) Concentration-dependent effects of N^1, N^{11}-diethylnorspermine on melanoma cell proliferation. *Int. J. Cancer* **118**:509-512.

Pearce, S. T., Jordan, V. C. (2004) The biological role of estrogen receptors α and β in cancer. *Crit. Rev. Oncol. Hematol*. **50**:3-22.

Porter, C. W., Stanek, J., Black, J., Vaughan, M., Ganis, B., Pleshkewych, A. (1990) Morphological evidence for an apparent lysosomotropic activity by unsaturated putrescine analogues. *Cancer Res*. **50**:1929-1935.

Riggins, R., Schrecengost, R. S., Guerrero, M. S., Bouton, A. H. (2007) Pathways to tamoxifen resistance. *Cancer Lett*. **256**:1-24.

Roque, A., Orrego, M., Ponte, I., Suau, P. (2004) The Prefential Binding of Histone H1 to DNA Scaffold-Associated Regions is determined by its C-Terminal Domain. *Nucleic Acids Res*. **32**:6111-6119.

Saminathan, M.; Antony, T.; Shirahata, A.; Sigal, L. H.; Thomas, T.; Thomas, T. J. (1999) Ionic and structural specificity effects of natural and synthetic polyamines on the aggregation and resolubilization of single-, double-, and triple-stranded DNA. *Biochemistry* 38:3821-3830.

Schmid, N., Behr, J. P. (1991) Location of spermine and other polyamines on DNA as revealed by photoaffinity cleavage with polyaminobenzenediazonium salts. *Biochemistry* **30**:4357-4361.

Song, R. X, Barnes, C. J., Zhang, Z., Bao, Y., Kumar, R., Santen, R. J. (2004) The role of Shc and insulin-like growth factor 1 receptor in mediating the translocation of estrogen receptor alpha to the plasma membrane. *Proc. Natl. Acad. Sci. U S A* **101**:2076-2081.

Sponar, J., Votavova, H. J. (1996) Selective binding of synthetic polypeptides to DNA of varying composition and sequence: effect of minor groove binding drugs. *Biomol. Struct. Dyn.* **13:**979-987.

Thomas, T.J., Bloomfield, V. A. (1983) Collapse of DNA caused by trivalent cations:pH and ionic specificity effects. *Biopolymers* **22**:1097-1106.

Thomas, T. J.; Bloomfield, V. A. (1984) Ionic and structural effects on the thermal helix-coil transition of DNA complexed with natural and synthetic polyamines. *Biopolymers* **23:**1295-1306.

Thomas, T., Thomas, T. J. (1994) Regulation of cyclin B1 by estradiol and polyamines in MCF-7 breast cancer cells. *Cancer Res*. **54**:1077-1084.

Vijayanathan, V., Thomas, T., Shirahata, A., Thomas, T. J. (2001) DNA condensation by polyamines: a laser light scattering study of structural effects. *Biochemistry* **40**:13644-13651.

Vijayanathan, V., Thomas, T., Thomas, T.J. (2002) DNA nanoparticles and development of DNA delivery vehicles for gene therapy. *Biochemistry* **41**:4085-14094.

Vijayanathan, V., Venkiteswaran, S., Nair, S. K., Verma, A., Thomas, T. J., Zhu, B. T., Thomas, T. (2006) Physiologic levels of 2-methoxyestradiol interfere with nongenomic signaling of 17beta-estradiol in human breast cancer cells. *Clin. Cancer Res*. **12**:2038-48.

Vilfan, I. D., Conwell, C. C., Sarkar, T., Hud, N. V. (2006) Time study of DNA condensate morphology: implications regarding the nucleation, growth, and equilibrium populations of toroids and rods. *Biochemistry* **2006**:8174-8183.

Wadhwa, M. S., Collard, W. T., Adami, R. C., McKenzie, D. L., Rice, K. G. (1997) Peptide-mediated gene delivery: influence of peptide structure on gene expression. *Bioconjug. Chem.* **8**:81-88.

Zhong, Y., Wang, Q. J., Li, X., Yan, Y., Backer, J. M., Chait, B. T., Heintz, N., Yue, Z. (2009) Distinct regulation of autophagic activity by Atg14L and Rubicon associated with Beclin 1-phoshatidylinositol 3-kinase complex. *Nat. Cell Biol*. Epub ahead of print.

Irina Nayvelt
220 Silver Lane
Old Bridge, NJ08857
Phone: (732) 360-0285
e-mail: iridium8888@gmail.com

Education

2000–present **Rutgers University,** Graduate School of New Brunswick
Ph.D. in Nutritional Sciences, May 2009
Molecular Aspects of Antiestrogen Resistance and Autophagy in Breast Cancer Cells

1997–2000 **Rutgers University, Rutgers College,** New Brunswick, NJ
B.A., Biological Sciences

1995–1997 **New York University,** New York, NY
Major: Biological Sciences

Experience

2000–present Graduate Assistant, University of Medicine and Dentistry of New Jersey, Department of Medicine, NJ

Publications

Nayvelt, I., Vijayanathan, V., Thomas T., and Thomas T.J. (2002). Condensation of λ-DNA by oligo- and poly-L-lysines. Biophys. J., 82: 128a.

Nayvelt, I., Vijayanathan, V., Thomas T., and Thomas T.J. (2007). Mechanistic Differences in DNA Nanoparticle Formation in the Presence of Oligolysines and Poly-L-lysine. Biomacromolecules, 8, 477-484.

John, S., **Nayvelt, I.*,** Hsu, H., Yang, P., Liu, W., Das, G., Thomas, T., Thomas, T. J. (2008) Regulation of Estrogenic Effects by Beclin 1 in Breast Cancer Cells. Cancer Research, 68, 7855-7863.

***Joint First Author**